JOSHUA

The Journal of Science and Health at the University of Alabama

2020 Volume 17

About the Cover:
Dr. Jeff Lozier in the Department of Biological Sciences at The University of Alabama focuses his research on native bees. Most of his work involves genetics of bumble bees, but he also has an interest in the thousands of other native bee species in North America. The cover photos represent several native bees from Alabama, including species in the genus *Nomada* (left) and *Augochloropsis* (lower right) collected in Tuscaloosa at the UA Arboretum, and an interesting rare species of *Hesperapis* photographed down at the Gulf Coast (upper right).

Questions should be directed to joshua.alabama@gmail.com, and more information and all archived volumes are available at https://joshua.ua.edu/archive.html

Table of Contents

Characterization of Fuel Properties Relevant to Low-Emission Diesel Engines Using OH* Chemiluminescence Analysis

Anna Stevenson[1], Shawn Reggeti[2], Ajay K Agrawal[3], Joshua Bittle[4]

Faculty Advisor(s): Ajay K Agrawal, Joshua Bittle
Department of Mechanical Engineering, The University of Alabama, Tuscaloosa, AL 35487

In this study, OH chemiluminescence was used to image ignition, flame propagation and stabilization, and combustion in a transient diesel-like flame. A constant pressure flow rig was used to conduct multiple injections in quick succession, thus building a statistically significant dataset to study the average behavior and variability. n-heptane, a research grade fuel surrogate for diesel, was injected at a nominal supply pressure of 1000 bar from a single-hole diesel injector into ambient conditions at a pressure of 30 bar and temperature of 800 K. 100 injections were performed and analyzed. Quantitative results of ignition delay and lift-off length are presented. The average ignition delay for n-heptane fuel at ambient conditions of 30 bar and 800 K was experimentally determined to be 1.7 ms, with a standard deviation of 0.102 ms. The average initial lift-off length was determined to be 58.5 mm with a standard deviation of 2.5 mm, and the average stable lift-off length was determined to be 43.8 mm with a standard deviation of 3.7 mm, indicating that after ignition the reactions race upstream to consume fresh reactants. Being able to accurately quantify ignition delay and lift-off length for different fuels in different test conditions allows for better control over advanced combustion strategies, as well as prediction of which fuels will produce the least amount of soot downstream.*

Keywords: *spray diagnostics, chemiluminescence imaging, diesel spray flames, constant pressure flow rig*

Introduction

Traditional diesel engines require expensive after-treatment strategies in order to meet strict emissions regulations [10]. In recent years, low temperature combustion (LTC) strategies have received attention for their potential to achieve high levels of fuel efficiency without producing harmful emissions [19]. LTC strategies refer to the combustion of lean fuel-air mixtures that result in low nitrogen oxide (NOx) and particulate matter (PM, or soot) emissions [1]. The fuel-air equivalence ratio is maintained below 2 and combustion temperatures are maintained below 2200 K in order to by-pass NOx and soot formation zones [19]. Figure 1 displays the soot and NOx formation zones as they relate to flame temperature and equivalence ratio for traditional diesel and LTC strategies [13]. LTC strategies have the potential to achieve higher levels of fuel efficiency than traditional diesel strategies because the fuel-air mixture is lean and homogeneous, resulting in lower, more uniform temperature distribution with less heat loss [1].

The success of LTC depend on several factors. Combustion and emissions behaviors are de- pendent on the phenomena that occur in the region upstream of the combustion zone, such as liquid length, fuel vaporization, and fuel/air

liquid length, fuel vaporization, and fuel/air mixing [2]. Such behaviors all consolidate to impact the lift-off length. Initial lift-off length is the distance be- tween the injector nozzle and the first downstream location of the flame. Stable lift-off length is the distance between the injector nozzle and the most upstream edge of the stabilized flame. The location of the lift-off length and the fuel-air ratio at the lift- off length profoundly impact the subsequent soot formation at locations further downstream [9]. The mechanism of lift-off stabilization is currently under scientific debate. Some studies have suggested that lift-off stabilization is determined by auto-ignition due to mixing with ambient air, while others have suggested that lift-off length stabilization is determined by ignition delay and mixing with hot combustion products at the spray edges [16]. It has also been proposed that lift-off length may be influenced by the cetane number of the fuel [8]. In general, there is still much unknown about the causation and stabilization of lift-off length, making it hard to predict. Being able to accurately quantify lift-off length for different fuels and test conditions can aid in the understanding of general trends relating fuel type and conditions, lift-off length, and subsequent soot formation [9].

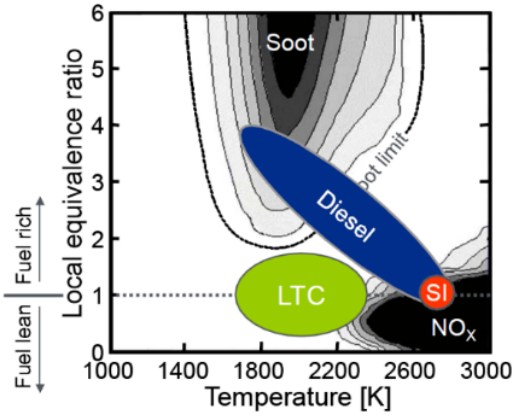

Figure 1. Soot and NOx formation zones for traditional diesel and low temperature combustion strategies [13]

Additionally, LTC engines require precise and accurate control over fuel injection timing [1]. Slightly early injection could result in pre-ignition and slightly late injection could result in unburned fuel [3]. The non-premixed fuel air mixture results in a time lapse between the start of fuel injection and the start of combustion [5], defined as ignition delay in this study. Ignition delay is associated with both the physical and chemical effects of the interaction of the fuel with the nozzle and gas in the combustion chamber [5]. A physical ignition delay occurs as the fuel and ambient air achieve reactive conditions at the boundaries of the fuel spray. The physical impact of ignition delay is predominately affected by the viscosity of the fuel, whereas the duration is shorter for low viscosity fuels [5, 18]. A chemical ignition delay occurs as the population of reactive radicals increases, which eventually leads to an exothermic reaction of the fuel-air mixture [5, 11]. Thus, the chemical contribution to ignition delay depends mainly on the fuel chemical composition [5,11,18]. As a result, ignition delay is affected by many factors including fuel type and quality, fuel-air ratio, injection pressure, injection timing, and ambient conditions in the CPFR [11, 18]. Understanding ignition delay allows for more control over fuel injection timing in engines, hopefully improving fuel efficiency. Being able to accurately quantify ignition delay for different fuels in different test conditions would allow for better control over advanced combustion strategies.

This study focused on the spray combustion of n-heptane fuel in ambient conditions of 800 K and 30 bar. A diesel spray flame is investigated with the purpose of quantifying lift-off length and ignition delay using high-speed diagnostic techniques. An in-house developed constant pressure flow rig (CPFR) is used for experimentation and OH* chemiluminescence diagnostics is used for data

analysis.

OH* chemiluminescence imaging has traditionally been used to determine the location of flame fronts and heat release [20, 6, 12], but it has also been used to quantitatively describe lift-off length and ignition delay [2]. The production of OH* in typical combustion processes is generally recognized as occurring through the recombination reaction, R1, shown below, where H collides with O and a third body. The primary pathways for OH* formation and depletion are commonly proposed as a set of elementary reactions,

$$H + O + M \rightleftharpoons OH^* + M \quad (R1)$$
$$OH^* \rightarrow OH + h\nu \quad (R2)$$
$$OH^* + M \rightleftharpoons OH + M \quad (R3)$$

Studies have revealed that OH* is predominantly formed by reaction R1 at temperatures below 2800 K, whereas at temperatures above 2800 K, the production of OH* is mainly via the reverse reaction R3 [20]. The OH* imaging technique captures the signals (~ 310 nm) from the excited OH* radicals as they return to the ground state [7]. In this study, OH* imaging will be used specifically to quantify lift-off length and ignition delay for n-heptane fuel at the specific ambient conditions of 800 K and 30 bar. However, the methods used to analyze these properties for n-heptane can be easily adapted to analyze these same properties for other fuels and/or conditions tested in the combustion chamber.

Experimental Set-Up

Constant Pressure Flow Rig (CPFR)

Figure 2a illustrates the CPFR used in this study. The vertical continuous flow system is designed to provide line-of-sight optical access of fuel injection into a nearly quiescent environment to generate large datasets (~ 500 injections) in about an hour. The chamber is supplied with pressurized, electrically preheated air at an average speed of about 0.5 m/s, nearly three orders of magnitude less than the fuel injection velocity, in a counter flow arrangement. The air enters through a flow conditioner consisting of six 0.5 mm thick, 100-micron mesh elements followed by a diffuser section to uniformly distribute the flow across the CPFR. The air exits at the top of the rig through four 3 mm diameter holes placed symmetrically around the injector tip. The air supply pressure is controlled by an upstream dome regulator and the air flow rate is regulated by a downstream control valve. Fuel is injected by a Bosch CRIN3-18 injector modified to have a single 100 μm hole at the tip to create a spray along the axis of the rig. The fuel temperature is maintained at 90 °C by a surrounding cooling jacket that circulates coolant around the injector tip. Table 1 shows the test conditions recorded during a typical experiment [15, 17].

Table 1. Operating Conditions

Amb. Temp. (K)	Amb. Pres. (bar)	Fuel Temp (K)	Fuel Pres. (bar)
803 ± 10	30.1 ± 0.3	89 ± 6	990 ± 8

(a)

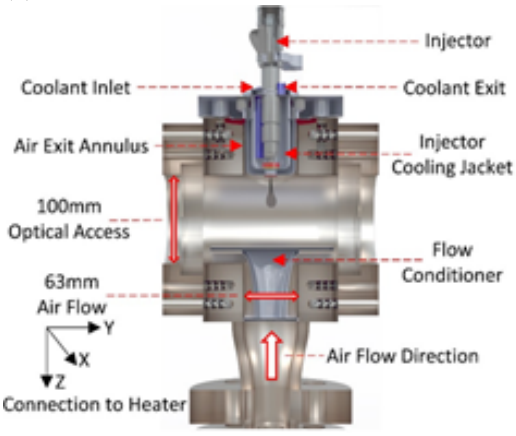

(b)

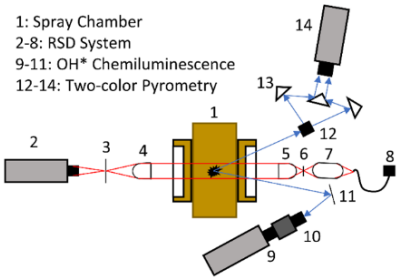

Figure 2. (a, top) Constant pressure flow rig CPFR) illustration; (b, bottom) Schematic of simultaneous diagnostics where each component is labelled as: CPFR (1), RSD Camera (2), rainbow filter (3), de-collimating lenses (4), focusing aperture (5), laser light source (6), collimating lenses (7), white light source (8), chemiluminescence camera (9), intensifier (10), mirror (11), beam splitter (12), mirrors (13), 2CP camera (14) [15,17]

Optical Diagnostics

Figure 2b shows the layout of the three simultaneous optical diagnostics used for data acquisition, though only OH* chemiluminescence (OH*) was used in this study. OH* is viewed at an angle relative to the chamber [9-11 in Figure 2b]. The OH* chemiluminescence emitted in the reacting spray is reflected by a mirror towards the Invisible Vision UV intensifier with a gate time of 70 µs outfitted with a 310 nm band pass filter. The OH* images are acquired by a monochromatic Photron SA5 camera with a pixel resolution of 896 x 848. The maximum framing rate and spatial resolution of the camera are 20 kHz and 160 m/pixel, respectively. A framing rate of 10 kHz was used in this study.

Data Processing

Frame Intensity Analysis

The monochrome images recorded by the Photron SA5 camera indicate the presence of OH* radicals in the flame based on the level of intensity. The intensity of a pixel is a unit-less measurement, expressed within a given range from 0 (total absence, black) to 255 (total presence, white), including the intermediate values corresponding to varying brightness levels and OH* presence. The camera records 60 images, or frames, per injection and the bright region of each frame corresponds to the reaction zones and tracks flame propagation inside the CPFR. The average intensity of a frame is the average of the intensities of all the individual pixels in that frame. The OH* imaging technique captures signals from excited OH* radicals as they return to the ground state. Before the flame ignites, no OH* has been emitted so the image is black, corresponding to an average intensity of 0 (Figure 3a). Once the flame ignites and begins to propagate, the average intensity ranges from 20 to 50 and is characterized by a somewhat circular ignition spot (Figure 3b). Then the reaction zone grows by consuming fresh reactants upstream, continues to move downward due to the spray velocity, and expands radially downstream, eventually reaching a maximum intensity of ~120 (Figure 3c). Figures 3a-c show the sequence of combustion, as detected by the OH* chemiluminescence diagnostic, for a single, typical injection.

Figure 4 shows the average intensity profile for 40 different injections. The average intensity profile is the average of all frame intensities at a given time step for 40 injections, with error bars indicating the standard deviation in average intensity for each time step. Figure 4 shows that the minimum intensity is 0 before the fuel ignites. When the flame ignites at approximately 2 ms, the average intensity increases and reaches a maximum when the flame begins to stabilize, before decreasing again as the combustion reactants are used up. The maximum intensity is approximately 120 and the average intensity when ignition begins is between 20 and 50.

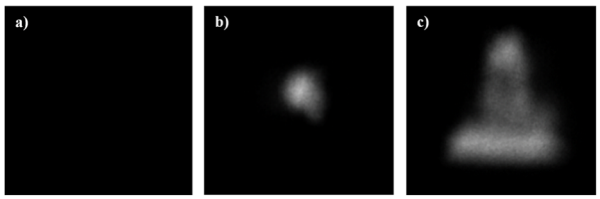

Figure 3. (a, left) Photron SA5 OH* Chemiluminescence image before ignition, frame 0; (b, center) Photron SA5 OH* Chemiluminescence image during initial stages of flame ignition and propagation, frame 25; (c, right) Photron SA5 OH* Chemiluminescence image during flame radial expansion and stabilization, frame 45

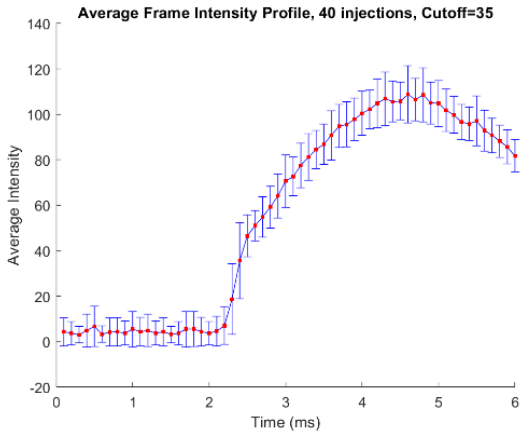

Figure 4. Average Ignition Profile for 40 Injections

Ignition Delay Analysis

Ignition delay (ID) is the time between when the fuel is injected into the CPFR and when the fuel begins to ignite [5]. Figure 3b is a SA5 OH* image showing the initial stage of flame ignition and propagation. The Photron SA5 begins recording images approximately 1 ms before the fuel is injected. Total time to combustion (TTC) is the time between when the SA5 begins recording and when the flame ignites. In order to determine the ignition delay, the combustion start time must first be identified. Frame rate is used to convert frame to time using the following conversion factor:

$$\text{Time} = \frac{1}{FrameRate} = \frac{1}{10{,}000s}$$

The frame rate of the Photron SA5 used in this analysis is 10 kHz, therefore each frame time step is equivalent to 1e-5 s, or 0.1 ms. Each injection includes 60 frames; therefore, each injection lasts 6 ms. The Photron SA5 stops recording after flame stabilization has occurred but before all of the reactants have been exhausted. TTC and ignition delay are both quantified by identifying the first frame where OH* is visible, indicating that combustion has begun. The fuel is injected 0.725 ms after the camera starts recording, which is determined by injection system measurements. Once TTC is calculated, this constant fuel injection time delay can be subtracted to calculate ignition delay. The average intensity of this first frame where OH* is present varies from injection to injection, with average intensities ranging from 20 to 50.

Figure 4 shows the average intensity profile for 40 injections. On average, total time to combustion is around 2 ms. The data changes from an average intensity of approximately 0 to an average intensity of approximately 25 when the fuel initially ignites. However, the error bars are quite large, indicating a large standard deviation in the average intensity of the first frame where OH* is present. The average intensity of the frame must be greater than a certain threshold in order for combustion to have begun. This threshold is referred to as the cut-off intensity. The cut-off intensity affects ID because this threshold influences which frame is identified as the first frame where OH* is present. The data is analyzed using a wide variety of cutoff intensities in order to accurately analyze the data and account for the large standard deviation in intensity shown in Figure 4.

Lift-off Length Analysis

Another important property for fuel analysis is the lift-off length. Flame lift-off length is the distance between the injector nozzle and the first downstream location of the flame [10]. Figure 5 shows liftoff-length for a general, quasi-steady diesel flame [4].

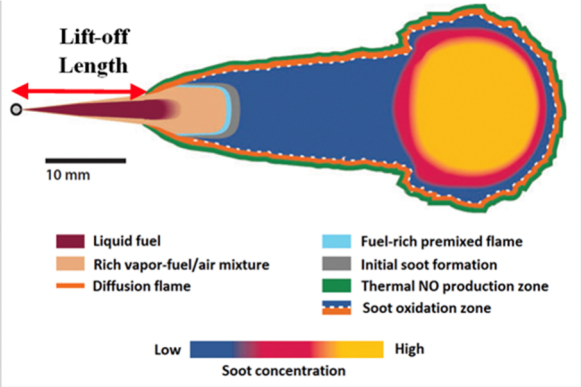

Figure 5. Dec schematic of the conceptual diesel spray model; arrow indicates lift-off length [4]

Lift-off length is analyzed using the axial location of the flame. Axial location is the location of the flame in the CPFR relative to the fuel injector. Figures 6a-c shows plots of axial location versus time for a typical injection. Lift-off length changes as the flame propagates. In order to accurately quantify lift-off length, the initial and stable lift-off lengths are both determined. Initial lift-off length (ILOL) is the distance between the fuel injector, located at a pixel height of 0, and the initial location of fuel ignition, shown by the arrow in Figure 6a. Stable lift-off length (SLOL) is the distance from the fuel injector to the maximum point on the contour curve once the flame has begun to stabilize, shown by the arrow in Figure 6b. SLOL is measured for each frame after ignition has begun. The average stable lift-off length (ASLOL) is the average of the middle third of these stable lift-off lengths. A box indicating the approximate range of SLOLs averaged together for the ASLOL calculation is shown in Figure 6c.

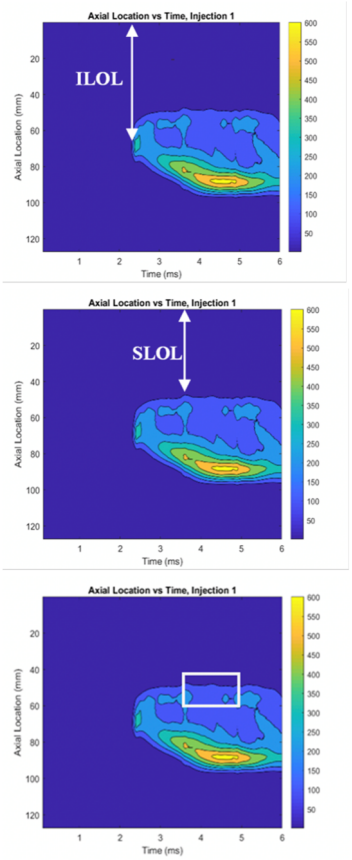

Figure 6. (all) Axial location versus time plot for a standard injection; (a, top) arrow indicates initial lift-off length (ILOL); (b, middle) arrow indicates stable lift-off length (SLOL) for one frame; (c, bottom) box indicates approximate range of SLOLs that are averaged together for average SLOL calculation

Results

Ignition Delay

Figure 7 shows the TTC and ID for 100 injections of n-heptane at ambient conditions of 800 K and 30 bar, and a cut-off value of 350. Similar plots were produced for all cut-off values tested. Table 2 shows a sensitivity analysis performed for ignition delay data. As discussed in section 3.2, the ignition delay

changes slightly based on the cutoff value assigned. Four different cutoff values were tested in the sensitivity analysis. Results from the sensitivity test are shown in Table 2.

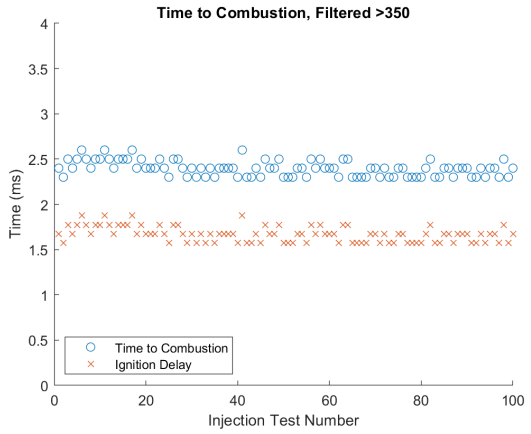

Figure 7. TTC and ID for 100 injections of n-heptane at ambient conditions of 800 K and 30 bar filtered at a cut-off value of 350. Typical plots produced for all cut-off values tested in Table 2.

Table 2. Sensitivity Analysis of n-heptane at ambient conditions of 800 K and 30 bar

Cut-off*	Average TTC (ms)	Average ID (ms)	ID Standard Deviation (ms)
30	2.372	1.647	0.0867
35	2.395	1.670	0.0840
40	2.434	1.709	0.1056
45	2.502	1.777	0.1303

* Cut-off is the value the average intensity must be greater than in order for fuel ignition to have begun

The overall average ignition delay and standard deviation is calculated by averaging together the individual averages and standard deviations from the sensitivity analysis. From this analysis, the average ignition delay for n-heptane fuel under the ambient conditions 800 K and 30 bar was determined to be 1.70 ms with a standard deviation of 0.102 ms. This standard deviation is small, indicating low variability in the data.

Lift-off Length

Figure 8a shows a plot of axial location versus time, in milliseconds, for one typical injection. Figure 8b shows the average axial location versus time for 100 injections. The contour curve is smooth, indicating that the data is repeatable and the variability from injection to injection is cancelled out. The data from this analysis is summarized in Table 3.

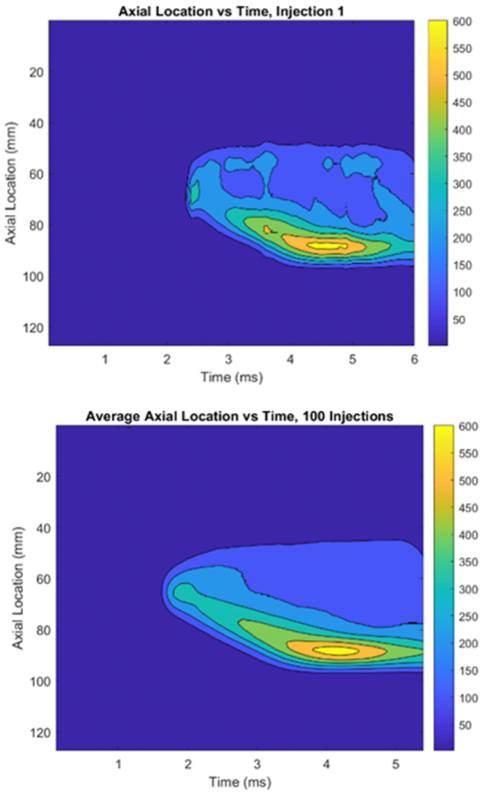

Figure 8. (a, top) Axial location versus time for a typical injection; (b, bottom) Average Axial Location for 100 injections

Table 3: Lift-off Length Data for n-heptane fuel ignition delay at 800 K and 30 bar

Average Initial Lift-off Length (mm)	STD Initial Lift-off Length (mm)	Average Stable Lift-off Length (mm)	STD Stable Lift-Off Length (mm)
58.5197	2.4592	43.7671	3.7236

Initial lift-off length and average stable lift-off length were experimentally determined to

be an average of 58.5 mm with a standard deviation of 2.5 mm and 43.8 mm with a standard deviation of 3.7 mm, respectively. Again, the standard deviation is small, indicating low variability in the data. The ASLOL is greater than the ILOL, suggesting that after ignition the reactions race upstream to consume fresh reactants. The MATLAB program used to analyze these properties produces one instantaneous and one average axial location plot, and saves relevant variables to a data file. The program also produces plots of initial lift-off length and average stable lift-off length versus injection number, shown in Figure 9 and 10, respectively.

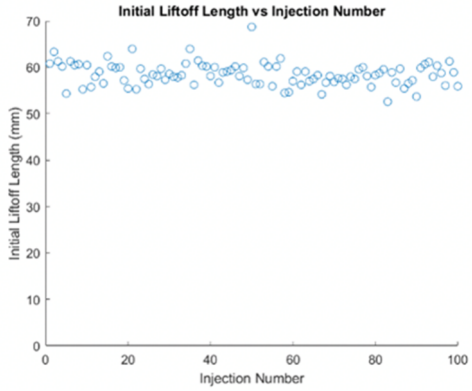

Figure 9. Initial liftoff length versus injection number for 100 injections of n-heptane fuel at ambient conditions of 800 K and 30 bar

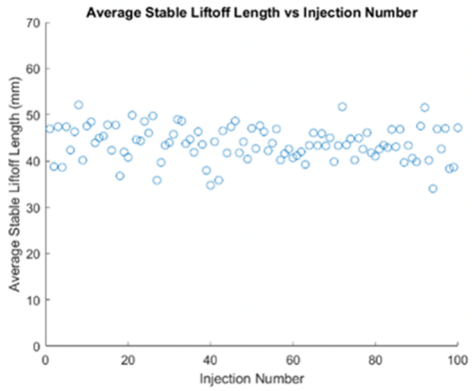

Figure 10. Average stable liftoff length versus injection number for 100 injections of n-heptane fuel at ambient conditions of 800 K and 30 bar

This method of analysis can also be used to calculate ignition delay. TTC is the time when initial lift-off length occurs, shown by the arrow in Figure 11. By subtracting the constant 0.725 ms fuel injection time, ignition delay can be determined and used to verify the results of section 4.1. Figure 12 shows the plot of ignition delay versus injection number for 100 injections of n-heptane fuel at ambient conditions of 800 K and 30 bar. The average ignition delay was determined to be 1.80 ms with a standard deviation of 0.09 ms. This ID falls within the standard deviation of the ID determined in the earlier section. The values are close enough to be confident that the average ID is approximately 1.7 ms. More data should be collected in order to determine exactly when the ID determined from these two methods converge.

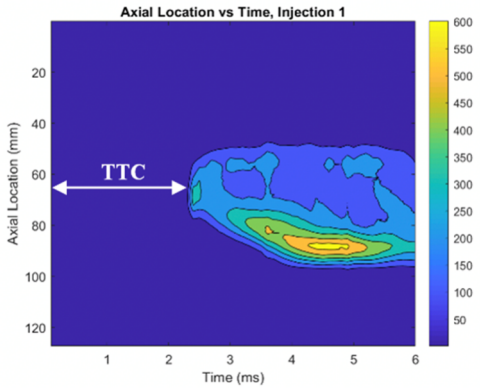

Figure 11. Axial location versus time plot for a typical injection. Arrow indicates total time to combustion (TTC).

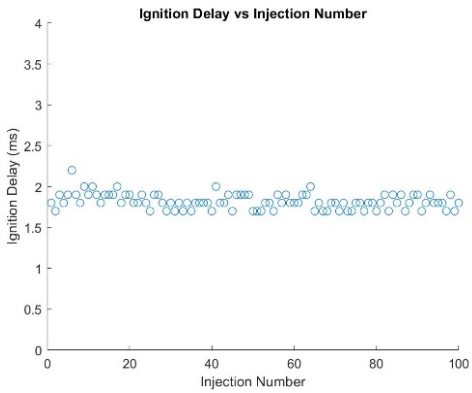

Figure 12. Ignition Delay versus Injection Number for 100 injections of n-heptane fuel at ambient conditions of 800 K and 30 bar using the axial location method of analysis

Conclusion and Summary

This study provides unique insight into the use of OH* chemiluminescence imaging to quantitatively describe properties relevant to the combustion of a n-heptane spray at diesel-like conditions. In this study, OH* chemiluminescence was used to image ignition, flame propagation and stabilization, and combustion in a transient diesel-like flame. OH* images were used to determine ignition delay by identifying the first frame where OH* is visible, indicating that flame ignition had begun. Using this method, the average ignition delay for n-heptane fuel under the ambient conditions 800 K and 30 bar was determined to be 1.70 ms with a standard deviation of 0.102 ms. OH* images were also used to produce a plot of axial location versus time. This plot was analyzed to quantify initial lift-off length and average stable lift-off length, which were determined to be an average of 58.5 mm with a standard deviation of 2.5 mm and 43.8 mm with a standard deviation of 3.7 mm, respectively. The average stable lift-off length is greater than the average initial lift-off length. This difference indicates that after ignition, the reactions race upstream to consume fresh reactants. This method was also used to verify the ignition delay results. Using the axial location method, the average ignition delay was determined to be 1.80 ms with a standard deviation of 0.09 ms, which fits into the range of ignition delay determined using the previous method. Understanding parameters such as ignition delay and lift-off length can help ensure the success of LTC modes. Better understanding of ignition delay and lift-off length parameters can allow for more control over fuel injection timing and more accurate predictions of the combustion profile, resulting in improved fuel efficiency and a reduction in pollutant emissions. Being able to accurately quantify ignition delay and lift-off length for different fuels in different test conditions allows for better control over advanced combustion strategies, as well as prediction of which fuels will produce the least amount of soot downstream.

Acknowledgements

Funding for this work was provided by award from US Department of Energy, Office of Energy Efficiency and Renewable Energy (EERE) DE-EE0007980. Mr. Allen Parker and Mr. C. Taber Wanstall are thanked for their roles in supporting experimental setup, data collection, and data processing efforts.

References

[1] “Advanced Combustion Strategies”. (n.d.). Advanced Combustion Strategies. Office of Energy Efficiency Renewable Energy. Retrieved from “https://www.energy.gov/eere/vehicles/advanced- combustion-strategies”.

[2] Benajes J, Payri R, Bardi M & Mart´ı-Aldarav´ı P. (2013). Experimental Characterization of Diesel Ignition and Lift-Off Length Using a Single-Hole ECN Injector. Applied Thermal Engineering, 58:554-563.

[3] de Oliveria PM & Mastorakos E. (2019). Mechanisms Of Flame Propagation In Jet Fuel Sprays as Revealed by OH/Fuel Planar Lase-Induced Fluorescence and OH* Chemiluminescence. The Journal of the Combustion Institute - Combustion and Flame, 206:308-321.

[4] Dec JE. (1997). A Conceptual Model of Diesel combustion based on laser-sheet imaging. SAE Transactions - Journal of Engines, 106: 1319-1348.

[5] Garz´on NN, Oliveira AA & Bazzo E. (2019). An Ignition Delay Correlation for Compression Ignition Engines Fueled with

Straight Soybean Oil and Diesel Oil Blends. The Science and Technology of Fuel and Energy, 257:1-8.
[6] Hall JM & Petersen EL. (2005). An optimized kinetics model for OH* chemiluminescence at high temperatures and atmospheric pressures. International Journal of Chemical Kinetics, 38:714-724.
[7] He L, Guo Q, Gong Y & Wang Fu. (2017). Investigation of OH* Chemiluminescence and Heat Release in Laminar Methane-Oxygen Co-Flow Diffusion Flames. The Journal of the Combustion Institute - Combustion and Flame, 201:12-22.
[8] Hottenbach P, Brands T, Gru¨nefeld G, Janssen A, Muther M, & Pischinger S. (2010). Optical and thermodynamics investigations of reference fuels for future combustion systems. SAE Transactions – Journal of Fuels and Lubricants, 3:819-838.
[9] Jakob M, Hu¨lser T, Janssen A, Adomeit P, Pischinger S & Grunfeld G. (2011). Simultaneous High-Speed Visualization of Soot Luminosity and OH* Chemiluminescence of Alternative-Fuel Combustion in a HSDI Diesel Engine Under Realistic Operating Conditions. The Journal of the Combustion Institute - Combustion and Flame, 159:2516-2529.
[10] Klein-Douwel RJH, Donkerbroek AJ, van Vliet AP, Boot MD, Somers LMT, Baert RSG, Dam NJ & ter Meulen JJ. (2009). Proceedings of the Combustion Institute - 32:2817-2825.
[11] Mollenhauer K, Tschoeke H & Johnson K. (2010). Handbook of diesel engines. Berlin: Springer.
[12] Najm HN, Paul PH, Mueller CJ & Wyckoff PS. (1998). On the adequacy of certain experimental observables as measurements of flame burning rate. The Journal of the Combustion Institute- Combustion and Flame, 113:312-332.
[13] Pal, P. (2015). Computation Modeling and Analysis of Low Temperature Combustion Regimes for Advanced Engine Applications, submitted, The University of Michigan.
[14] Pandian MM & Krishnasamy A. (2017). A Comparison of Different Low Temperature Combustion Strategies in a Small Single Cylinder Diesel Engine under Low Load Conditions. SAE International.
[15] Parker A, Wanstall CT, Reggeti SA, Agrawal AK & Bittle J. (2019). Simultaneous Rainbow Schlieren and OH* Chemiluminescence Imaging of the Dynamics of a Diesel Spray Flame in a Constant Pressure Flow Rig, submitted, Proceedings of the Combustion Symposium.
[16] Pickett LM, Siebers DL & Idicheria CA. (2005). Relationship between ignition processes and the lift-off length of diesel fuel jets. SAE Transactions, 114:1714–1731.
[17] Reggeti SA, Agrawal AK & Bittle J. (2019) A Two-Color Pyrometry System to Eliminate Optical Errors for Spatially Resolved Measurements in Flames. Applied Optics, 58:8905-8913.
[18] Shahabuddin M, Liaquat AM, Masjuki HH, Kalam MA & Mofijur M. (2013). Ignition delay, combustion and emission characteristics of diesel engine fueled with biodiesel. Renewable and Sustainable Energy Reviews, 21:623-632.
[19] Zhang J, Jing W & Fang T. (2012). High Speed Imaging of OH* Chemiluminescence and Natural Luminosity of Low Temperature Diesel Spray Combustion. The Science and Technology of Fuel and Energy, 99:226-234.
[20] Zhao M, Buttsworth D & Choudhury R. (2018). Experimental and Numerical Stud of OH* Chemiluminescence in Hydrogen Diffusion Flames. The Journal of the Combustion Institute - Combustion and Flame, 197:369-377.

Photoactive Nanoparticles-Loaded Bio-Nanofibers for Photothermal Conversion

Nicole Angel[1], S. N. Vijayaraghavan[2], Feng Yan[2], Lingyan Kong[3,*]

Faculty mentors: Feng Yan, Lingyan Kong
[1]*Department of Mechanical Engineering, The University of Alabama, Tuscaloosa, AL 35487*
[2]*Department of Metallurgical and Materials Engineering, The University of Alabama, Tuscaloosa, AL 35487*
[3]*Department of Human Nutrition and Hospitality Management, The University of Alabama, Tuscaloosa, AL 35487*
** Corresponding author*

Recently, implementation of solar-driven vaporization for the production of clean water has gained interest. Benefits of this technique include that it does not require water to reach its boiling temperature, can potentially be employed by both developed and undeveloped nations, and proposes a sustainable solution for overcoming water scarcity. However, low utilization efficiency of solar energy is currently a significant roadblock when it comes to the successful implementation of this technique. Photoactive nanoparticles used as solar absorbers have the potential to overcome this obstacle because of their demonstrated ability to increase solar evaporation efficiency. This study aims to develop cellulose acetate (CA) nanofibers doped with cadmium selenide (CdSe) nanoparticles as a solar energy conversion device and evaluate its performance in solar vapor generation. Preliminary experiments were conducted in order to determine the optimum electrospinning parameters, including CA solution concentration (12 wt%), flow rate (3 mL/h), voltage (12 kV), and spinning distance (8 cm), at which to fabricate the CA nanofibers. CdSe-loaded CA nanofibers, with varying CA:CdSe ratios, were fabricated in order to determine the optimal CA:CdSe ratio for solar conversion efficiency. The fibers were characterized by scanning electron microscopy (SEM) for their morphology and X-ray diffraction (XRD) for their microstructural and phase properties. UV-visible spectrophotoscopy and Fourier-transform infrared spectroscopy (FTIR) were conducted to determine the transmittance and thus the sunlight absorption range. The nanofibers were further tested for photothermal conversion under 1 sun (100 mW/cm^2) using an infrared (IR) camera. The CdSe-loaded CA nanofibers were shown as a feasible and promising hybrid material to achieve efficient photothermal conversion.

Keywords: *photoactive nanoparticles; nanofibers; biopolymer; cellulose acetate; electrospinning; solar energy*

Introduction

In modern society, water scarcity is a significant issue linked closely with social and economic development [1–3]. Billions of people worldwide lack access to clean water and/or potable water, and millions of people die annually from diseases relating to water-borne illnesses [2,4]. Moreover, it is those with the lowest economic standing who are most significantly affected by water scarcity [4]. As the world's population continues to increase, the Earth's ability to support its population, specifically in reference to clean water access, will become increasingly strained [1,2]. Some proposed solutions for addressing water scarcity come at the expense of aggravating present energy problems or suggest the implementation of large-scale infrastructure [1,4]. Given current large-scale infrastructure management, this solution is likely unsustainable in the long term [4]. Therefore, developing a method to address water scarcity in a clean, affordable, and sustainable manner is of increasing importance. Solar vapor generators demonstrate some of the

greatest potential to provide a sustainable solution to water scarcity [1,3,5,6].

Solar vapor generators work on the basic principle of converting light energy into the necessary heat for water evaporation [3,5]. One of the main disadvantages of this technique is low photothermal conversion efficiency [1]. Both low solar absorption of water and heat loss caused by traditional system bulk heating have significantly contributed to this poor efficiency [1]. However, shifting from a bulk heating system to a nano-scaled solar absorber system, specifically through the implementation of photosensitive nanoparticles (NPs), has demonstrated a noticeable increase in conversion efficiency [1,5,6]. Crystalline NPs are highly efficient at releasing heat when under photoexcitation because the applied light excites the NPs' mobile carriers. The energy from the excited carrier is converted to heat and is diffused into the surrounding substrate, i.e., water [7]. Beneficially, this process does not require the total surrounding liquid volume to reach its boiling point for successful vapor generation [6]. This study investigates the implementation of electrospun cellulose acetate (CA) nanofibers carrying photosensitive cadmium selenide (CdSe) NPs as a nano-scaled solar conversion device for solar vapor generation.

CdSe displays two key characteristics that make it an ideal material to use for this study. One, it is a semiconducting material, and two, due to its band gap (1.74 eV), it is highly photosensitive in the visible light region [8]. CA is a low-cost cellulose derivative produced via the acetylation of cellulose [9,10]. It was chosen as the carrying material for this study because it demonstrates advantageous mechanical properties, good fiber-forming ability, biodegradability, stability in water, and is cost-effective [10,11]. Moreover, nano-scale fibers display a high surface area to volume ratio, good flexibility, high porosity, and superior stiffness and tensile strength [11].

CA nanofibers were fabricated by electrospinning, a simple, scalable, and versatile technique for nanofiber production [12]. Given the potential applications of this study, the ability for the resulting solar vapor generator to be mass scaled is of the utmost importance. The basic lab scale electrospinning setup (Figure 1) only requires a high voltage source, a syringe with a blunt needle tip (i.e., the spinneret), and a grounded collector [11,12]. High voltage is applied to the spinneret, where the spinning dope is pumped via a syringe pump at a constant rate. Once the applied voltage reaches the critical point, a Taylor cone will form at the spinneret tip. A continuous jet flows from the Taylor cone to the grounded collector. During this process, the electric field causes the jet to stretch and elongate as the solvent evaporates. Nanofibers are collected on the grounded collector, e.g., an aluminum foil as used in this study [11,13,14].

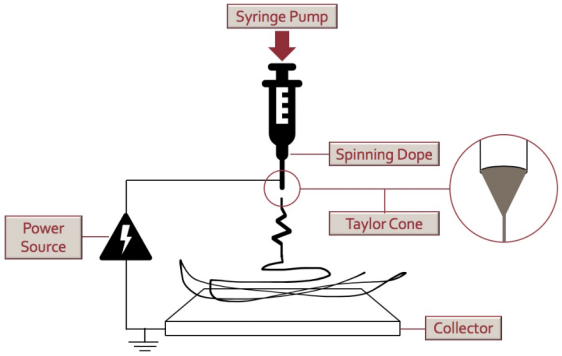

Figure 1. The basic electrospinning setup used in this study

The objectives of this study were to demonstrate the feasibility of fabricating CdSe-loaded CA nanofibers by electrospinning; characterize their morphological, microstructural, and optical properties; and evaluate their performance in solar energy

conversion. The CA nanofibers were loaded with various CdSe contents (CdSe:CA ratio of 1:4 and 1:1, w/w) in order to analyze the successful uptake of CdSe into the CA nanofibers and observe the resulting photosensitive properties of the fibers as provided by the CdSe NPs. This study will present information regarding the ability of CdSe-loaded CA nanofibers to successfully function as independent solar vapor generators.

Materials and Methods

2.1. Materials

Cellulose acetate (MW~100,000 Da; acetyl content ~ 39.7 wt%) and acetone were purchased from VWR International (Radnor, PA, USA).

The CdSe nanoparticles were fabricated using a chemical bath deposition process. The $CdSO_4$ was used as the Cd^{2+} source, and the sodium selenosulfate (Na_2SeSO_3) was used as the Se^{2-} source. A slow reaction occurs between Cd^{2+} and Se^{2-} ions in an aqueous basic bath with pH greater than 10. The Na_2SeSO_3 was prepared by dissolving elemental Se, in the form of a fine powder, into an aqueous solution of sodium sulfate heated to 60°C. The solution was stirred well until Se was fully dissolved. The pH of the solution was adjusted by adding excess NaOH. CdSe formed in two hours at a temperature of 70°C. The obtained CdSe powder was then washed using a centrifuge and deionized water several times and dried in the vacuum oven.

Because CdSe is considered to be toxic to human cells, it was handled with the utmost care during this study [15]. CdSe toxicity has been mainly attributed to the release of Cd^{2+} ions from the CdSe to the affected cells [15]. The method of exposure by which this occurs highly alters how significantly the affected cells react to the CdSe [15]. Consequently, equipment that came in contact with CdSe was cleaned thoroughly, waste was properly disposed of, and the CdSe NPs were properly labeled and stored before use.

2.2. Electrospinning

In this study, CA concentration in the spinning dope was held constant at 12% (w/v). To prepare the spinning solutions, CA and CdSe were mixed in pure acetone by magnetic stirring at room temperature (20°C) and ultrasonication (VWR International, Radnor, PA, USA). The spinning dope was then loaded into a 10 mL syringe (Becton, Dickinson and Company, Franklin Lakes, NJ, USA) with a 22 gauge blunt needle (Hamilton Company, Reno, NV, USA) as the spinneret.

The electrospinning setup was comprised of a high voltage generator (ES30P, Gamma High Voltage Research, Inc., Ormond Beach, FL, USA), a syringe pump (NE-300, New Era Pump Systems, Inc., Farmingdale, NY, USA), and a grounded aluminum foil as the collector. In the present study, the optimal spinning parameters to spin CA nanofibers were determined from our previous study [11]. Specifically, the spinning distance was held at 8 cm, feed rate at 3 mL/h, and voltage at 12 kV. Electrospinning was conducted in a fume hood at 20℃ without airflow. Airflow was removed due to the high evaporation rate of acetone. Eliminating airflow helped to slow the buildup of viscous fluid at the spinneret tip which leads to destabilization of the spinning jet. When this occurs, nanofiber formation is halted because the spinneret is clogged, and the jet is no longer considered continuous. Despite the lack of airflow in this study, the spinneret required constant cleaning during the spinning process in order to successfully obtain nanofibers. Rodríguez et al. experienced this as well in their study [16]. After the spinning process, the formed nanofibers, which had been deposited on the aluminum foil directly beneath the spinneret tip, were collected and stored away from light and moisture for further analysis.

2.3. Scanning Electron Microscopy (SEM)

Observation of the electrospun nanofibers was accomplished using an Apreo FE-SEM (Thermo Fisher Scientific, Waltham, MA), equipped with energy-dispersive X-ray spectroscopy (EDS), at an accelerating voltage of 20 kV. Images were subsequently analyzed using ImageJ software (National Institute of Health, Bethesda, MD, USA). Multiple images were used for each nanofiber sample. Ten random segments on each image were then used to determine the average diameter. Through

visual inspection, nanofiber morphology was visually evaluated as either good, fair, or poor. Good nanofibers are defined as continuous, uniform, smooth, and defect free. Fair nanofibers display the fibrous shape with moderate defects. Poor fibers have significant defects, such as beads or sprayed particles. It is important to note that the CdSe NPs will alter how smooth the nanofibers appear but will not be considered as defects of the nanofibers.

2.4. Wide angle X-ray diffraction (XRD)

Wide angle X-ray diffraction (XRD) patterns were obtained using a Philips X'Pert Materials Research Diffractometer operated at 45 kV, 40 mA Cu Kα radiation (λ = 0.15405 nm).

2.5. Ultraviolet–visible (UV-vis) spectroscopy

Light absorbance of the fiber samples was measured using the EnliTech QE measurement system (Kaohsiung City, Taiwan). The incident wavelength was swept from 300 to 1100 nm, and the absorbance of the fibers was recorded. The optical direct band gap (Eg) of the fibers was determined by using Tauc plot relation to plot $(\alpha h\nu)^{1/r}$ versus energy of the photons, where r represents the nature of transition of the charge carriers, and r = ½ for direct band gap materials.

2.6. Solar energy conversion

Using an infrared (IR) camera, the nanofibers were tested for solar vapor generation under 1 sun (100 mW/cm^2).

Results and Discussion

3.1. Electrospinnability and fiber morphology

The overall electrospinnability of the nanofibers was analyzed through both visual inspection during spinning and the obtained SEM images. All three CdSe-CA compositions were able to successfully produce fibers in a relatively short amount of time. The time needed for the collector to become completely covered in nanofibers was relatively the same in all three runs, leading to the conclusion that CdSe did not have a drastic effect on the electrospinnability of CA in acetone as a single solvent.

The overall fiber quality of the electrospun nanofibers was also relatively independent of the addition of CdSe. As seen in Figure 2, the CdSe-CA nanofibers remain continuous, smooth, and display approximately the same amount of beading as the pure CA nanofibers. It is important to note that the presence of CdSe NPs was disregarded when categorizing the fibers as smooth or unsmooth. Overall, the morphology of the nanofibers was unexpected but promising. As demonstrated by Lee et al., the addition of a non-soluble particle or material into the spinning dope alters the overall viscosity of the spinning dope, which, in their study, led to increased beading and fiber diameter [17].

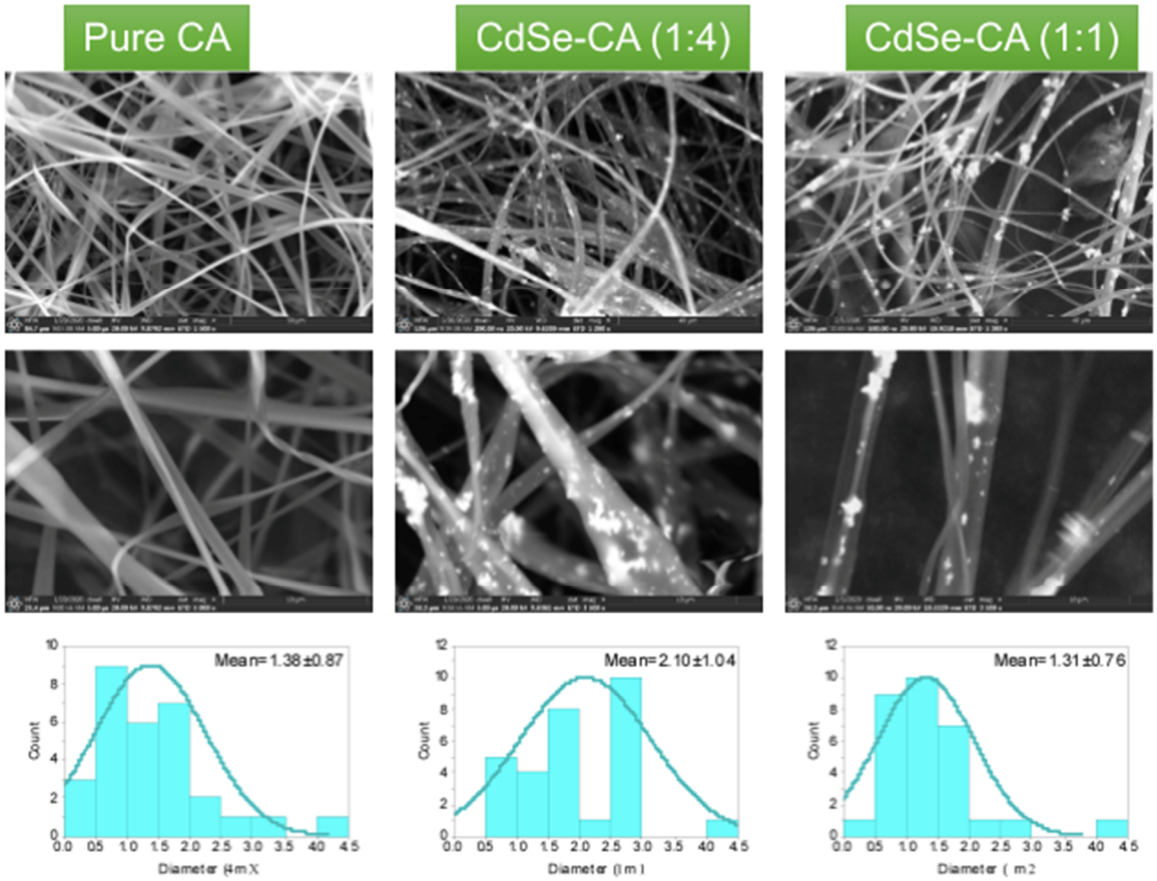

Figure 2. Scanning electron micrographs and fiber diameter distributions of CA, CdSe-CA (1:4), and CdSe-CA (1:1) fibers

The fiber diameters of the three different nanofibers are given in Figure 2. There was no trend in the change in fiber diameter correlating to the addition of CdSe to the solution. Again, this was unexpected. Lee et al. found that adding a non-soluble material into their polymer spinning dope led to an increase in fiber diameter [17]. However, in this study, we see that the fiber diameter for CdSe-CA (1:4) is significantly greater (p<0.05) than the other two runs where the diameters of the other two runs were approximately the same.

3.2. CdSe incorporation

As shown in both Figures 2 and 3, CdSe was successfully incorporated into the nanofibers. The white particles embedded in the fibers were confirmed to comprise the element Cd (Figure 3). As expected, the CdSe-CA (1:1) fibers demonstrated a higher quantity of successful CdSe incorporation than when compared to the CdSe-CA (1:4) fibers. However, the CdSe particles are heterogeneous in their size, which could be due to difficulty in achieving a homogeneous and stable suspension of the CdSe in the spinning dope. Furthermore, visual inspection of the CdSe suspension is difficult and unreliable due to the dark color of the solution. Further research is warranted to create CdSe NPs of uniform size and homogeneous spinning suspension for making nanofibers, which would improve the efficiency and performance of the CdSe-CA fibers.

The presence of CdSe was also evidenced from its diffraction peaks at 2θ =25.3°, 42°, and 50°, as these peaks were not present in the pattern of the pure CA fibers (Figure 4). Similar to most other biopolymers, CA is semi-crystalline yet largely amorphous. The halos

around 2θ ~ 10° and 20° corresponding to (101) and (020) planes confirm the semi-crystalline nature of cellulose acetate. The (002), (110), and (201) peaks of CdSe corresponding to 2θ ~ 25°, 41°, and 50°, respectively, can be indexed to the wurtzite phase. Low intensity of the CdSe peaks suggest that CA was higher in concentration than CdSe.

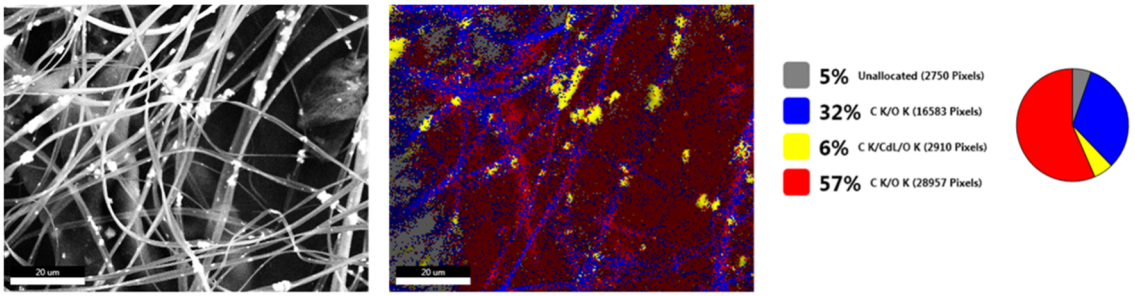

Figure 3. Scanning electron micrograph of CdSe-CA (1:1) fibers with elemental mapping and composition obtained using energy dispersive X-ray spectrometry

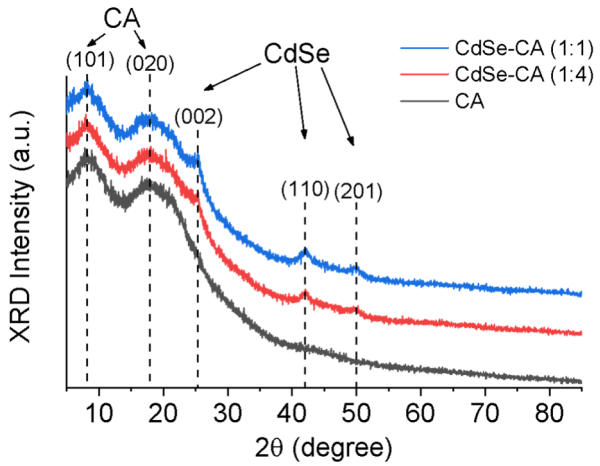

Figure 4. X-ray diffraction patterns of CA, CdSe-CA (1:4), and CdSe-CA (1:1) fibers

3.3. Optical properties

As shown in Figure 5A, the absorbance of the nanofibers, especially in the visible light range from about 300 to 700 nm, increased with increasing CdSe:CA ratios. These nanofibers have the potential to have a superior solar conversion efficiency which is supported by the findings of López-Herraiz et al., who found that an increased absorbance of their system led to an increase in thermal efficiency of their system [18]. From the extrapolation of Tauc plot as shown in Figure 5B, CA was determined to have a wide band gap of ~3.77 eV. Pure CdSe is estimated to have a band gap of 1.74 eV as per previous works [8]. When CdSe was introduced into CA fibers in varying concentrations, the band gap decreased with increasing CdSe concentrations. The CdSe-CA (1:4) fibers were found to have a band gap of ~3.53 eV, but when more CdSe was incorporated into CA in CdSe-CA (1:1), the band gap was further reduced to ~1.84 eV. Bandwidth is the minimum amount of energy required to excite an electron from its ground valence energy band into the empty conduction energy band [19]. Therefore, the lower the bandwidth, the less energy needed to excite the electron from the valence band to the conductive band. This process of exciting certain electrons, as previously stated, is crucial to how NPs transform light energy into heat. The fact that the bandwidth of the CdSe-loaded nanofibers is relatively the same as pure CdSe demonstrates that loading CdSe into CA nanofibers had a relatively insignificant effect on CdSe's ability to act as a light absorber. Therefore, CA nanofibers show potential in their ability to act as a supporting membrane for CdSe NP-based solar vapor generators.

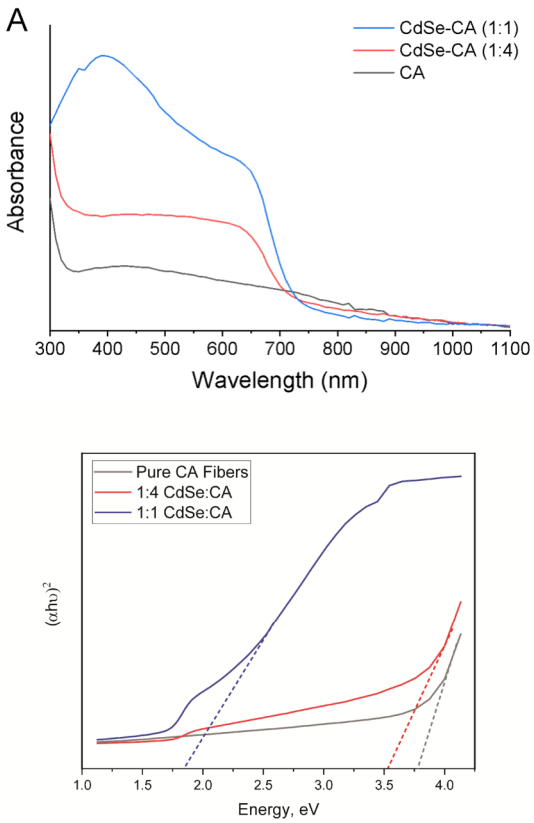

Figure 5. (A) UV-vis absorbance spectra (normalized at 1100 nm) and (B) Tauc plot of CA, CdSe-CA (1:4), and CdSe-CA (1:1) fibers.

3.4. Photothermal conversion

To investigate the photothermal properties of the CA and CA-CdSe nanofibers, both optical and IR thermal images were taken for both pure CA nanofibers and CdSe-CA nanofibers (Figure 6). As seen from the optical image, the CdSe-CA (1:4) nanofibers were dark in color due to the light absorption by CdSe, while the CA nanofibers were white, which is in agreement with the UV-Vis absorbance test shown above. The maximum temperature in the CdSe-CA (1:4) nanofibers can be over 40°C under 1 sun (100 mW/cm^2), while the CA nanofibers stay at a low temperature without photothermal conversion. It is suggested that the CA-CdSe nanofibers could effectively absorb the sunlight and convert it into thermal energy.

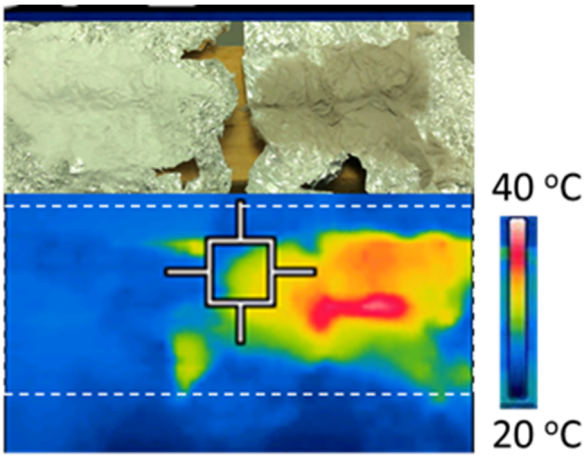

Figure 6. Optical picture (top) and the infrared thermal image (bottom) of the CA and CA-CdSe nanofibers.

Conclusion

In conclusion, the loading of CdSe into CA nanofibers was successful, and CdSe still demonstrated its photosensitive properties even while in the fibers. Overall, fiber morphology, including quality and diameter, was relatively independent of the addition of CdSe, which was surprising because the addition of the CdSe NPs alters the overall viscosity of the spinning dope. CdSe was successfully incorporated into the CA fibers in both runs. However, possibly due to low loading efficiency and the nonhomogeneous suspension of CdSe in the spinning dope, the amount of CdSe observed in the CdSe-CA (1:1) nanofibers did not significantly increase as expected when compared to the CdSe-CA (1:4) nanofibers. Beneficially, the CdSe NPs maintained their photosensitive properties while incorporated into the CA nanofibers. Specifically, they demonstrated the correct bandwidth and were highly absorbent in the visible light spectrum. From here, future work will focus on determining the overall effectiveness of implementing these fibers as solar vapor generators. Once its effectiveness is determined, a method for mass producing these fibers will be necessary.

Acknowledgments

This work was jointly supported by the Alabama Water Institute and the College of

Human Environmental Sciences at the University of Alabama.

References

[1] Gao, M., Zhu, L., Peh, C. K., and Ho, G. W. (2019) Solar absorber material and system designs for photothermal water vaporization towards clean water and energy production. *Energy Environ. Sci. 12*, 841–864.
[2] Shannon, M. A., Bohn, P. W., Elimelech, M., Georgiadis, J. G., Mariñas, B. J., and Mayes, A. M. (2008) Science and technology for water purification in the coming decades. *Nature 452*, 301–310.
[3] Liu, C., Huang, J., Hsiung, C.-E., Tian, Y., Wang, J., Han, Y., and Fratalocchi, A. (2017) High-Performance Large-Scale Solar Steam Generation with Nanolayers of Reusable Biomimetic Nanoparticles. *Advanced Sustainable Systems 1*, 1600013.
[4] Rijsberman, F. R. (2006) Water scarcity: Fact or fiction? *Agricultural Water Management 80*, 5–22.
[5] Zhao, F., Zhou, X., Shi, Y., Qian, X., Alexander, M., Zhao, X., Mendez, S., Yang, R., Qu, L., and Yu, G. (2018) Highly efficient solar vapour generation via hierarchically nanostructured gels. *Nature Nanotech 13*, 489–495.
[6] Neumann, O., Urban, A. S., Day, J., Lal, S., Nordlander, P., and Halas, N. J. (2013) Solar Vapor Generation Enabled by Nanoparticles. *ACS Nano 7*, 42–49.
[7] Govorov, A. O., and Richardson, H. H. (2007) Generating heat with metal nanoparticles. *Nano Today 2*, 30–38.
[8] Mahato, S., and Kar, A. K. (2017) The effect of annealing on structural, optical and photosensitive properties of electrodeposited cadmium selenide thin films. *Journal of Science: Advanced Materials and Devices 2*, 165–171.
[9] Fischer, S., Thümmler, K., Volkert, B., Hettrich, K., Schmidt, I., and Fischer, K. (2008) Properties and Applications of Cellulose Acetate. *Macromolecular Symposia 262*, 89–96.
[10] Nosar, M. N., Salehi, M., Ghorbani, S., Beiranvand, S. P., Goodarzi, A., and Azami, M. (2016) Characterization of wet-electrospun cellulose acetate based 3-dimensional scaffolds for skin tissue engineering applications: influence of cellulose acetate concentration. *Cellulose 23*, 3239–3248.
[11] Angel, N., Guo, L., Yan, F., Wang, H., and Kong, L. (2020) Effect of processing parameters on the electrospinning of cellulose acetate studied by response surface methodology. *Journal of Agriculture and Food Research 2*, 100015.
[12] Teo, W. E., and Ramakrishna, S. (2006) A review on electrospinning design and nanofibre assemblies. *Nanotechnology 17*, R89–R106.
[13] Suwantong, O., Opanasopit, P., Ruktanonchai, U., and Supaphol, P. (2007) Electrospun cellulose acetate fiber mats containing curcumin and release characteristic of the herbal substance. *Polymer 48*, 7546–7557.
[14] Deitzel, J. M., Kleinmeyer, J., Harris, D., and Beck Tan, N. C. (2001) The effect of processing variables on the morphology of electrospun nanofibers and textiles. *Polymer 42*, 261–272.
[15] Wang, L., Nagesha, D. K., Selvarasah, S., Dokmeci, M. R., and Carrier, R. L. (2008) Toxicity of CdSe Nanoparticles in Caco-2 Cell Cultures. *J Nanobiotechnol 6*, 11.
[16] Rodríguez, K., Gatenholm, P., and Renneckar, S. (2012) Electrospinning cellulosic nanofibers for biomedical applications: structure and in vitro biocompatibility. *Cellulose 19*, 1583–1598.
[17] Lee, Y.-F., Sridewi, N., Ramanathan, S., and Sudesh, K. (2017) The Influence of Electrospinning Parameters and Drug Loading on Polyhydroxyalkanoate (PHA) Nanofibers for Drug Delivery. *International Journal of Biotechnology for Wellness Industries 4*, 103-113–113.
[18] López-Herraiz, M., Fernández, A. B., Martinez, N., and Gallas, M. (2017) Effect of the optical properties of the coating of a concentrated solar power central receiver on its thermal efficiency. *Solar Energy Materials and Solar Cells 159*, 66–72.
[19] SMITH, A. M., and NIE, S. (2010) Semiconductor Nanocrystals: Structure, Properties, and Band Gap Engineering. *Acc Chem Res 43*, 190–200.

Enzymatic Digestion of Starch Inclusion Complexes with Alkyl Gallates

Isabella Gladden[1], Yanqi Zhang[2], Jiayue Guo[2], Libo Tan[2], Lingyan Kong[2,*]

Faculty Mentor: Lingyan Kong
[1]*Department of Mechanical Engineering, The University of Alabama, Tuscaloosa 35487, Alabama, United States*
[2]*Department of Human Nutrition & Hospitality Management, The University of Alabama, Tuscaloosa 35487, Alabama, United States*
** Corresponding author*

The interactions between starch and phenolic compounds have a great impact on the physicochemical and nutritional properties of starch-containing foods. One particular form of the interaction is starch-guest inclusion complexation, which is a specific non-covalent interaction formed between starch and guest molecules. This study investigates complexation ability and enzymatic digestibility profiles of amylose inclusion complexes with gallic acid and alkyl gallates of various chain lengths, including butyl (BG), octyl (OG), dodecyl (DG), hexadecyl (HG), and octadecyl (SG) gallates. The formation of the inclusion complex was examined by complementary techniques including differential scanning calorimetry (DSC), X-ray diffraction (XRD), and Fourier transform infrared (FTIR) spectroscopy. The digestibility profiles, represented as rapid digestible starch (RDS), slowly digestible starch (SDS), and resistant starch (RS) contents, were obtained through simulated in vitro enzymatic digestion assays. The results showed that while gallic acid (GA), BG, and OG were not capable of forming an inclusion complex with amylose, gallates with longer alkyl chains were able to form more stable inclusion complexes. Precipitated amylose samples with GA, BG, and OG contained highest RS, probably due to starch retrogradation. Amylose inclusion complexes with long alkyl chains, particularly HG and SG, also possessed low RDS and the highest SDS and RS combined, but higher SDS proportions than the non-complexed amylose samples. This suggested that the inclusion complexes, especially amylose-HG and SG, might have contributed to the increase in SDS content. The water insusceptibility and high thermal stability of these inclusion complexes helped retard the starch digestion. The resistant yet steady digestion behavior of the amylose-gallate inclusion complexes has significant implications in modulating glycemic response, as well as enabling a slow and sustained release of bioactive guest compounds into the gastrointestinal tract.

Keywords: *starch; amylose; gallic acid; alkyl gallates; phenolic compounds; slowly digestible starch*

Introduction

Starch is one of the most prevalent carbohydrates, as an energy source and a staple in many cultures' diets. Based on its digestion and the subsequent release and absorption of glucose, starch can be categorized into three portions, rapidly digestible starch (RDS), slowly digestible starch (SDS), and resistant starch (RS). RDS is digested quickly in the beginning and middle sections of the small intestine, leading to a rapid elevation of blood glucose. On the other hand, SDS provides a steadier rise in the glucose levels due to the longer time needed to fully digest the starch, while RS may not even be digested in the small intestine [6]. In its raw or retrogradated form, some starch has a densely packed molecular order, which leads to less of the starch being fully digested [22]. However, most forms of starch undergo a heating or cooking process which leads to gelatinization and more of the starch is rapidly digested as a result. The rate at which the body digests starch is critical for the prevention and treatment of many chronic diseases. If starch is rapidly

digested, the glucose absorption will also happen rapidly, providing a spike of energy rather than sustained energy over time. Thus, RDS may lead to hyperglycemia, increasing the risk of cardiovascular diseases, obesity, and diabetes [18].

Previous studies suggested that the formation of starch-inclusion complexes reduces the amount of RDS and increases the amount of SDS or RS [19]. Starch-guest inclusion complexes are supramolecular combinations of starch and a guest compound. The starch, especially amylose, acts as a "host", forming a cavity that encapsulates the guest compound [16]. This phenomenon is mainly driven by weak intermolecular hydrophobic interactions between the amylose helical core and the guest compound [4]. The formation of starch-guest inclusion complexes results in the V-type crystalline structure, which leads to decreased solubility, increased gelatinization temperature, and retarded retrogradation, all of which affect the digestion of starch [19]. Some studies have suggested that starch inclusion complexes contribute to slowly digestible starch and resistant starch. Gutierrez et. al. [9] found that when alkyl gallates were added to a solution with amylose, digestion was retarded. It was hypothesized that the alkyl gallates with shorter chain lengths merely inhibited the activity of amylase while those with longer chain lengths were more likely to form inclusion complexes, leading to an increase in slowly digestible starch and resistant starch.

Based on the previous hypothesis proposed by Gutierrez, Guo, Feng, Tan and Kong [9], this study utilizes gallic acid (GA) and alkyl gallates with various chain lengths, including butyl (BG), octyl (OG), dodecyl (DG), hexadecyl (HG), and octadecyl (SG) gallates, as the guest compounds to form inclusion complexes with amylose, and to study the digestibility profiles of the inclusion complexes formed. The retardation on digestion by the starch inclusion complex may be dictated by the guest structure, which was seen to affect the strength of the hydrophobic interaction and thus thermal stability [13]. Therefore, we expected that alkyl gallates with longer alkyl chains would bind stronger with the starch helical interior, and thus result in higher thermal stability and higher resistance to digestion.

Materials and Methods

2.1 Materials

Amylose from potato starch (degree of polymerization ca. 900, A0512), gallic acid (G7384), butyl gallate (S764868), octyl gallate (48700), and dodecyl gallate (48660), amyloglucosidase from *Aspergillus niger* (EC 3.2.1.3, A7095, 300 U/mL), porcine pancreatin (EC 232-468-9, P7545, 8 x USP), invertase from baker's yeast (EC 3.2.1.26, I4504, 300 U/mg), guar gum (G4129), and sodium acetate trihydrate (S7670) were purchased from Sigma-Aldrich Inc. (St. Louis, MO, USA). D-glucose assay kit (GOPOD format, K-GLUC) was obtained from Megazyme (Wicklow, Ireland). Hexadecyl gallate (TCG0013), octadecyl gallate (TCG0019), dimethyl sulfoxide (DMSO), Drierite™ desiccant, and ethanol were purchased from VWR International (Radnor, PA, USA).

2.2. Preparation of amylose inclusion complex

Amylose inclusion complexes were prepared using the previously reported DMSO method with slight modifications [14]. Amylose (500 mg) was dissolved in 10 ml of 95% (v/v) DMSO in a 90 °C water bath with constant stirring for at least 30 min. Guest compound (50 mg) was pre-dissolved in 1 mL of 95% (v/v) DMSO by heating to 90 °C. The guest solution was then added into the amylose dispersion and the mixture was kept at 90 °C for another 15 min. Then, 25 ml of water preheated to 90 °C was rapidly added into the amylose and guest compound mixture with vigorous stirring. This mixture was incubated at 90 °C for 15 min, and then allowed to cool to room temperature (20 °C) and held for at least 24 hrs. The precipitate was recovered by centrifugation (3000 g, 20 min), then washed with 50% (v/v) aqueous ethanol twice, and finally washed with 100% ethanol. The resulting pellet was transferred into an aluminum dish with a small amount of 100% ethanol and allowed to dry at room temperature (20 °C) in a desiccator containing Drierite™ as the desiccant. Dried samples were pulverized into fine powders for further analysis.

2.3. Differential scanning calorimeter (DSC)

Approximately 5-6 mg of dry sample was weighed using a Mettler-Toledo XP2U ultra-microbalance (Mettler-Toledo International Inc., Columbus, OH, USA) into a large-volume stainless steel DSC pan (Perkin-Elmer Instruments, Norwalk, CT, USA). Deionized water was added to obtain a 10% (w/v) dispersion. The DSC Pan was hermetically sealed. Using an empty pan as the reference, the pans were equilibrated to 10 °C, and then heated to 150 °C at 10 °C/min in a Discovery DSC 250 DSC (TA Instruments, New Castle, DE, USA).

2.4. Wide angle X-ray diffraction (XRD)

Wide angle X-ray diffraction patterns were obtained with a Philips X'PERT MPD X-ray diffractometer (Philips, now Malvern Panalytical Inc., Westborough, MA, USA). The ground samples were exposed to Cu Ka radiation (1.5405 Å) and scanned between 2θ = 5° and 30° at 40 mA current. Data were analyzed using the HighScore software (Malvern Panalytical Inc.)

2.5. Fourier transform infrared spectroscopy (FTIR) analysis

Fourier transform infrared (FTIR) spectra of inclusion complex samples were obtained using a PerkinElmer Spectrum 100 FTIR spectrometer (PerkinElmer Inc., Waltham, MA, USA), with an attenuated total reflection (ATR) accessory. The spectra were recorded in the wavelength region of 650 to 4000 cm^{-1}, with an average of 32 scans at a resolution of 4 cm^{-1}.

2.6. Simulated in vitro digestion

The starch inclusion complex samples were subjected to simulated *in vitro* digestion based on the method outlined by Englyst and Hudson [6], with slight modifications. Specifically, the enzyme solution comprised of pancreatin (46.8 mg/mL prior to centrifugation), amyloglucosidase (13 U/mL), and invertase (187.5 U/mL) was prepared immediately before use. Starch inclusion complex sample (80 mg) was mixed into 4 mL of an acetate buffer and incubated in a water bath for 5 min at 37 °C. Then, 1 mL of the enzyme solution was added to each sample and placed in a shaking water bath at 37° C and 150 strokes per min. After incubating for 20 and 120 min, aliquots of 200 µL were mixed into 900 µL of 66% (v/v) ethanol and mixed vigorously to denature the enzymes and stop the reaction. Then, the samples were centrifuged (2700 g, 3 min) and the glucose concentrations in the supernatant were measured using the glucose oxidase-peroxidase (GOPOD) method. Starch contents at 20 and 120 min corresponded to the proportion of rapidly digestible starch (RDS) and slowly digestible starch (SDS), respectively. The amount of RS was determined as the amount remaining after 120 min.

2.7. Statistical analysis

Results are recorded as the means ± standard deviation, and significant differences between groups were tested using one-way analysis of variance (ANOVA) and Fisher's Least Significant Difference (LSD) test at $p < 0.05$. Statistical analysis was conducted using SPSS version 19.0 software (SPSS, Inc., Chicago, IL, USA). The letters a, b, and c indicate statistically significant differences, $p < 0.05$ (a > b > c).

Results and Discussions

3.1. Inclusion complex formation

Complementary techniques including DSC, XRD, and FTIR were used to confirm the formation of inclusion complexes. On the DSC thermogram, the inclusion complex, if formed, would show an endothermic peak during heating and an exothermic peak during cooling, indicating the dissociation and reassociation of the inclusion complexes formed [2]. Among the prepared samples in this study, no visible endothermic peak was found on the DSC thermograms of precipitated amylose with GA, BG, and OG (Figure 1a, 1b, & 1c), and hence, the inclusion complex might not have formed between amylose and these guests. In contrast, samples added with DG, HG, and SG showed endotherms with peak temperatures at around 83 °C, 100 °C, and 105 °C, respectively, indicating the formation of inclusion complexes (Fig. 1d, 1e, & 1f). The endothermic peaks around 80-110 °C are consistent with previous research studying the amylose inclusion complexes with

long-chain fatty acids [8, 21]. In addition, the peak temperature increased as the alkyl chain length increased. This trend has been reported in many studies on starch inclusion complexes with lipids [1, 11, 13, 20]. The phenomenon could be explained by the fact that guest compounds with longer alkyl chains present greater hydrophobicity, so that they tend to stay inside of the helix and yield stronger intermolecular hydrophobic interactions. Therefore, a higher energy is needed to break the association between the amylose and the guest molecules [13, 17].

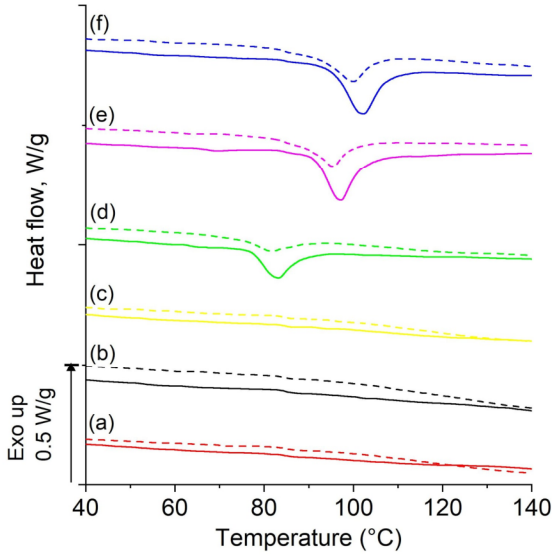

Figure. 1. DSC thermograms of precipitated amylose samples with (a) gallic acid (GA), (b) butyl gallate (BG), (c) octyl gallate (OG), (d) dodecyl gallate (DG), (e) hexadecyl gallate (HG), and (f) octadecyl gallate (SG).

XRD provides the crystalline structural evidence of amylose/starch inclusion complexes, i.e., the characteristic V-type diffraction peaks. The XRD patterns of amylose-gallates inclusion complexes are shown in Fig 2. Amylose-OG, DG, HG, and SG samples showed characteristic V_6-type peaks at 13° and 20°, indicating the formation of amylose-gallates inclusion complex in a V_6-type [12]. In contrast, precipitated amylose samples with GA and BG were essentially amorphous with no characteristic V-type diffraction peaks observed. A very small peak of 17° suggests that small B-type crystals might have formed. Inclusion complexation stems from the diffusion of guest molecules from the solvent into the hydrophobic core of amylose helices. If the guests do not favor the amylose helical cavity over the solvent, a competing crystallization process, also known as retrogradation, would proceed to form double helices and precipitate as the diffuse B-type. Overall, the XRD results are consistent with the speculation of DSC thermograms, confirming the formation of amylose inclusion complexes with long chain alkyl gallates. However, while there were V-type diffraction peaks identified in the amylose-OG sample, no endothermic peak was observed during heating this sample (Fig. 1c). A possible explanation is that the formed amylose-OG inclusion complex was not stable, and was destroyed in water before heating in DSC.

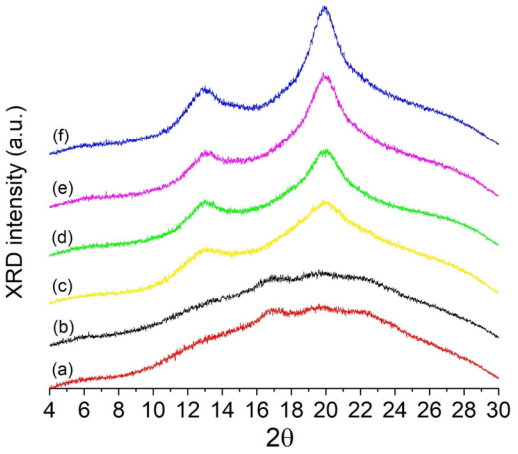

Figure 2. XRD patterns of precipitated amylose samples with (a) gallic acid (GA), (b) butyl gallate (BG), (c) octyl gallate (OG), (d) dodecyl gallate (DG), (e) hexadecyl gallate (HG), and (f) octadecyl gallate (SG).

FTIR helps identify the functional groups and thus the presence of guest molecules in the samples (Fig 3). The amylose-DG, HG, and SG inclusion complexes showed the presence of characteristic phenol deformation bands at around 1500, 1600, and 1670 cm^{-1} [21]. Also, as alkyl chain length increased, especially in amylose-DG, HG, and SG samples, bands at 2850 cm^{-1} and 2920 cm^{-1} appeared and became sharper. These two bands correspond to the

stretching vibration of CH_2 on the alkyl chain [15]. The increase in intensity with alkyl chain length could result from either more guest encapsulated or more CH_2 on the alkyl chain. The absence of characteristic bands for phenol group and alkyl chains in the amylose-GA, BG, and OG samples suggests little guest was captured inside the amylose helices. Overall, the three complementary techniques provided evidence for inclusion complex formation between amylose and gallates with long alkyl chain lengths (DG, HG, and SG).

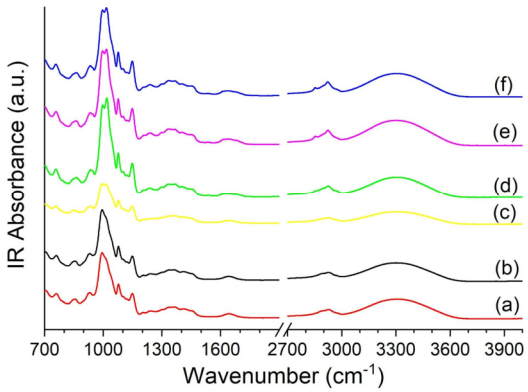

Figure 3. FTIR spectra of precipitated amylose samples with (a) gallic acid (GA), (b) butyl gallate (BG), (c) octyl gallate (OG), (d) dodecyl gallate (DG), (e) hexadecyl gallate (HG), and (f) octadecyl gallate (SG).

3.2. Simulated in vitro digestion

The digestibility profiles of amylose-gallates samples were obtained using simulated *in vitro* enzymatic digestion and are shown in Fig. 4. The amylose-GA, BG, and OG samples demonstrated similar digestibility profiles with the highest RS (57% – 64%) and relatively low SDS contents. Starting from the amylose-DG sample, RS contents remain at around 29% – 34%, while SDS contents increased steadily. The RDS contents in these samples range from 26% to 37%, except for amylose-DG with 58% RDS content. Amylose inclusion complexes are all semi-crystalline materials consisting of amorphous and crystalline regions. Similar to native starch granules, it was suggested that enzymatic digestion would initially take place in the amorphous regions and then proceed to the crystalized amylose-guest helices [10]. It is worth noting that the amorphous regions subject to fast digestion are not identical to the amorphous component on the XRD patterns, because molecules will rearrange when in contact with water in the digestion mixture. Hence, the hypothesis was that the amorphous regions formed upon contact with water should account for most of the RDS contents, whereas amylose-guest inclusion complexes contribute to the SDS and RS contents determined during enzymatic digestion.

The SDS contents in the amylose-DG, HG, and SG inclusion complex samples were 13%, 34%, and 42%, as compared to 3%, 6%, and 16% in amylose-GA, BG, and OG samples, respectively, indicating that inclusion complexes contributed to the increase in SDS content. The inclusion complexes formed by OG and DG with amylose seem unstable in the digestion mixture but were disrupted in different ways. The amylose-OG was transformed to a more resistant structure similar to amylose-GA and BG samples, because fewer guests were precipitated with amylose and OG has higher solubility to escape the amylose matrix. On the other hand, amylose-DG was not dissociated at the digestion temperature but was more susceptible to enzymatic digestion than amylose inclusion complexes with longer alkyl chains. Thus, unlike amylose-HG and SG inclusion complexes, it resulted in less SDS content and more RDS content. The fact that SDS content increased with alkyl chain length could be explained by the increasing quantity and stability of the inclusion complex formed as the alkyl chain became longer, which was evidenced by the increasing trend in crystallinity and endothermic peak temperature shown in the XRD patterns and DSC thermograms. Such a trend suggested a stronger hydrophobic interaction between the amylose helix and alkyl gallates with longer chain lengths, contributing to a more stable structure, and thus a higher resistance of dissolution and enzymatic hydrolysis [9]. Overall, the trend in SDS contents agrees with previous research findings that inclusion complex formation between amylose and some lipid molecules could slow down the digestion rate of amylose [5].

In addition, the sum of RS and SDS portions is higher in the amylose inclusion

complexes than that found in our previous study which assayed a mixture of cooked high amylose maize starch with alkyl gallates [9]. Although cooking and digesting starch with lipid guest molecules could both facilitate inclusion complex formation [5, 19], its efficiency is still limited, as compared to the DMSO method that intentionally produces inclusion complex. The amylose-HG and SG inclusion complexes formed using the DMSO method showed higher resistance against enzymatic digestion.

Despite the low possibility of inclusion complex formation in amylose-GA, BG, and OG samples, their RS contents were higher than those in amylose-DG, HG, and SG inclusion complexes. This was mainly due to the precipitation and retrogradation of the amylose, leading to the formation of a compact retrograded starch structure, also referred to as the type 3 resistant starch (RS3) [3]. In addition, raw amylose serves as an excellent source of type 2 resistant starch (RS2), which also has a high resistance to enzymatic digestion [3, 7]. Compared with RS2 and RS3 formed in amylose-GA, BG, and OG samples, although the inclusion complexes had lower RS contents, their SDS and RS contents are comparable. Digestion of the inclusion complex proceeds at a steady rate, leading to additional benefits beyond the inhibition of starch digestion. The amylose inclusion complex could enable the delivery and slow release of bioactive food components (e.g., alkyl gallates) in the gastrointestinal tract as it is digested. In addition, as the RS, SDS, and RDS contents were very close, especially in amylose-HG and SG inclusion complexes, their digestion could occur more gradually, allowing the modulation of the glycemic response.

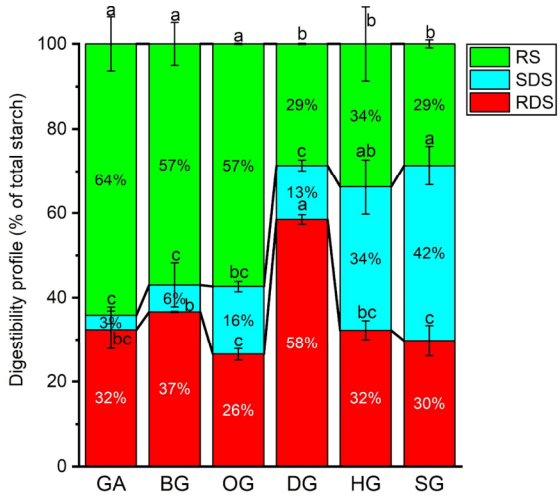

Figure 4. Starch digestibility profiles, presented as rapid digestible starch (RDS), slowly digestible starch (SDS), and resistant starch (RS) contents in precipitated amylose samples with gallic acid (GA), butyl gallate (BG), octyl gallate (OG), dodecyl gallate (DG), hexadecyl gallate (HG), and octadecyl gallate (SG). Error bars show standard deviation; n=2. Significant differences among samples within each starch digestion fraction are indicated by difference letters (a > b > c, $p < 0.05$).

Conclusion

This study investigated the formation of amylose inclusion complexes with various alkyl gallates, and the digestibility profiles of these samples. Gallic acid and gallates with short alkyl chains were not able to form an inclusion complex with amylose, therefore, amylose was precipitated and retrograded to a resistant form known as the type 3 resistant starch. Guests with longer alkyl chains can be more easily wrapped into the helical cavity of amylose, creating inclusion complexes of higher thermal stability and resistance to enzymatic digestion. Specifically, amylose-HG and SG inclusion complexes mainly contributed to the increase in SDS content. Such digestion behavior has significant implications for starch inclusion complex in modulating glycemic response and maintaining a steadier digestion process, making it a potentially valuable prevention strategy for diabetic patients. Meanwhile, the steady rate of digestion implies that starch inclusion complexes can be used as a delivery formulation

enabling slow and sustained release of bioactive guest compounds.

Acknowledgments

This project is funded by the USDA National Institute for Food and Agriculture, Agriculture and Food Research Initiative Program, Competitive Grants Program award from the Improving Food Quality (A1361) program FY 2018 as grant # 2018-67017-27558.

References

[1] Biliaderis CG, Page CM & Maurice TJ, (1986). Non-equilibrium melting of amylose-V complexes. 6: 269-288.
[2] Biliaderis CG, Page CM, Slade L & Sirett RR, (1985). Thermal behavior of amylose-lipid complexes. 5: 367-389.
[3] Birt DF, Boylston T, Hendrich S, Jane J-L, Hollis J, Li L, McClelland J, Moore S, Phillips GJ, Rowling M, Schalinske K, Scott MP & Whitley EM, (2013). Resistant starch: promise for improving human health. 4: 587-601.
[4] Chi C, Li X, Zhang Y, Chen L, Li L & Wang Z, (2017). Digestibility and supramolecular structural changes of maize starch by non-covalent interactions with gallic acid. 8: 720-730.
[5] Crowe TC, Seligman SA & Copeland L, (2000). Inhibition of enzymic digestion of amylose by free fatty acids in vitro contributes to resistant starch formation. 130: 2006-8.
[6] Englyst HN & Hudson GJ, (1996). The classification and measurement of dietary carbohydrates. 57: 15-21.
[7] Englyst HN, Kingman SM & Cummings JH, (1992). Classification and measurement of nutritionally important starch fractions. 46 Suppl 2: S33-50.
[8] Felker FC, Kenar JA, Fanta GF & Biswas A, (2013). Comparison of microwave processing and excess steam jet cooking for spherulite production from amylose–fatty acid inclusion complexes. 65: 864-874.
[9] Gutierrez ASA, Guo J, Feng J, Tan L & Kong L, (2020). Inhibition of starch digestion by gallic acid and alkyl gallates. 102: 105603.
[10] Jane J-L & Robyt JF, (1984). Structure studies of amylose-V complexes and retro-graded amylose by action of alpha amylases, and a new method for preparing amylodextrins. 132: 105-118.
[11] Karkalas J, Ma S, Morrison WR & Pethrick RA, (1995). Some factors determining the thermal properties of amylose inclusion complexes with fatty acids. 268: 233-247.
[12] Kong L, Bhosale R & Ziegler GR, (2018). Encapsulation and stabilization of β-carotene by amylose inclusion complexes. 105: 446-452.
[13] Kong L, Perez-Santos DM & Ziegler GR, (2019). Effect of guest structure on amylose-guest inclusion complexation. 97: 105188.
[14] Kong L, Yucel U, Yoksan R, Elias RJ & Ziegler GR, (2018). Characterization of amylose inclusion complexes using electron paramagnetic resonance spectroscopy. 82: 82-88.
[15] Kong L & Ziegler GR, (2014). Formation of starch-guest inclusion complexes in electrospun starch fibers. 38: 211-219.
[16] Manca M, Woortman AJJ, Loos K & Loi MA, (2015). Imaging inclusion complex formation in starch granules using confocal laser scanning microscopy. 67: 132-138.
[17] Putseys JA, Lamberts L & Delcour JA, (2010). Amylose-inclusion complexes: Formation, identity and physico-chemical properties. 51: 238-247.
[18] Svihus B & Hervik AK, (2016). Digestion and metabolic fates of starch, and its relation to major nutrition-related health problems: A review. 68: 302-313.
[19] Tan L & Kong L, (2019). Starch-guest inclusion complexes: Formation, structure, and enzymatic digestion. 1-11.
[20] Tufvesson F, Wahlgren M & Eliasson A-C, (2003). Formation of Amylose-Lipid Complexes and Effects of Temperature Treatment. Part 2. Fatty Acids. 55: 138-149.
[21] Wang S, Kong L, Zhao Y, Tan L, Zhang J, Du Z & Zhang H, (2019). Lipophilization and molecular encapsulation of p-coumaric acid by amylose inclusion complex. 93: 270-275.
[22] Zhang B, Dhital S & Gidley MJ, (2015). Densely packed matrices as rate determining features in starch hydrolysis. 43: 18-31.

Memories of Adult Survivors of Childhood Cancer: Parent and Sibling Relationships

Amber Wesoloski[1], Emily Goldstein[2], BS, CCLS, Shannon Anderson[1], Tori Hinton[2], MS, CCLS, Sherwood Burns-Nader[2], PhD, CCLS

Faculty Mentor: Sherwood Burns-Nader, Associate Professor
[1]*Department of Biological Sciences, The University of Alabama, Tuscaloosa, AL 35487*
[2]*Department of Human Development and Family Studies, The University of Alabama, Tuscaloosa, AL 35487*

Pediatric cancer poses challenges for both the patients and their families. The purpose of this study is to examine pediatric cancer survivors' memories of their parents and siblings throughout their diagnosis. Participants (n=22) were recruited via Amazon's Mechanical Turk (MTurk) and answered a demographic questionnaire and a qualitative survey containing questions about their memories of experiencing childhood cancer. The study's research questions were: 1) What are adult survivors' of childhood cancer memories of their parents' experiences with the diagnosis of their cancer? and 2) What are adult survivors' of childhood cancer memories of their siblings' experiences with their cancer diagnosis? Participant responses were analyzed using constant comparative analysis. Survivors remembered their parents being emotionally supportive, showing emotion, giving gifts, spending more quality time with them, performing acts of service, or implementing treatment traditions. During conversations about their cancer experience, they remembered their parents having a positive outlook, explaining the treatments, what to expect from them, or explaining the cancer itself. Survivors remembered their siblings' experience fear, helplessness, grief, sadness, empathy, or a lack of understanding regarding their cancer. Furthermore, survivors recalled being treated by their siblings with more kindness, gentleness, sensitivity, or leniency after their diagnosis. The future implications of these findings may entail the development and provision of appropriate psychosocial support for patients and their families throughout the cancer journey.

Introduction

Cancer is the third leading cause of death in children in the United States, compromising about 9% of all child and adolescent mortalities [4]. However, the rate of death among childhood cancer patients has continuously been on a decline in the past few decades [15]. In fact, the average 5-year survival rate of all cancer types in the year 2019 was 83% for children and 85% for adolescents [15]. Each year, there are approximately 11,060 new cases of childhood cancer, and about 1,190 children died from childhood cancers in 2019 [15]. Of those that successfully beat childhood cancer, many experience long-term effects of their cancer on their physical, mental, and social well-being [5]. For reference, one study found that survivors of childhood cancer had higher chances of being unmarried, not living independently, and using social welfare services than people who did not experience childhood cancer [5].

The detriment of a childhood cancer diagnosis can have negative effects on other members of the family unit, particularly parents and siblings of the child with cancer [12]. After examining the psychological well-being of parents of children with cancer, it was found that more than 50% of parents experienced high levels of distress pertaining to their child's diagnosis [11]. It was also noted that poor family unity was correlated with higher levels of maladaptation in adult survivors of adolescent cancer [11]. However, there is also evidence that the more cohesive and united a family is in helping their child through the illness, the better

both the ill child and the parents cope with cancer [11].

Siblings are impacted by the change in the family dynamic during treatment of childhood cancer [11]. Healthy siblings may experience dramatic changes to their family unit as the child with cancer becomes the focus of the family's attention [11]. Siblings may feel jealous, unnoticed, and isolated from their family due to constant interruptions to their normal routine, as well as uncertainty as to what might happen [11].

When examining the memories of adult survivors of childhood cancer, it was found that most people specifically remembered events that lead to the diagnosis and their peers' misunderstanding and lack of empathy towards their situation [12]. However, it was confirmed that survivors primarily remembered the strength and support that their family provided throughout the treatment and how that was able to overshadow the difficult times [12].

Research findings have shown that children with cancer do not perceive parental care any differently than healthy children [10]. Previous studies have looked at how siblings are impacted by childhood cancer patients and the ways in which the siblings adapt to their sibling's cancer during childhood [10]. However, there is not much research from the perspective of the individual with childhood cancer, especially regarding their specific memories of how or if they were treated differently by their parents and siblings during their treatment. The purpose of this study is to examine the memories that adult survivors of childhood cancer have regarding their parent and sibling relationships. To address this purpose, the following research questions were examined: 1) What are adult survivors' of childhood cancer memories of their parents' experiences with the diagnosis of their cancer? and 2) What are adult survivors' of childhood cancer memories of their siblings' experiences with their cancer diagnosis? Relationships between parents and siblings and childhood cancer patients are examined in order to identify memories that may explain how the parent-child and sibling relationship can be impacted during diagnosis and treatment.

Methods

Participants

Twenty-two childhood cancer survivors were included in the study. Participants were recruited through Amazon Mechanical Turk (MTurk), an online system containing multiple research surveys for people to take. Participant inclusion criteria consisted of 3 self-identified factors: born and raised in the United States, between the ages of 18-40, and cancer free for five or more years from pediatric cancer. Participants were removed from the dataset if they did not meet these criteria, completed the survey in less than two minutes, or only answered no or other variations. This two-minute time limit was established because the survey could not be completed within that amount of time due to the length and types of questions asked. Seventeen of the 125 responses were deleted for being incomplete or being completed in less than two minutes. Not meeting inclusion criteria disqualified 29 surveys, and 35 surveys were removed for nonapplicable answers.

Participants (n=27) included 15 men and 12 women, with ages ranging from 20 to 39 years (m =28.27). Of the participants, the majority were either white (77.8%) or African American (11.1%). Leukemia (59.3%) was the most common form of cancer reported, followed by lymphoma (22.2%), brain/spinal cord (7.4%), Wilm's tumor (3.7%) and others (7.4%). Those who reported "other" classified their cancer as melanoma and heptoblastoma. Treatments reported included chemotherapy (96.3%), radiation (29.6%), surgery (25.9%), bone marrow or stem cell transplant (14.8%), and target therapy (3.7%). One participant was diagnosed with a secondary cancer (3.7%), and three participants experienced relapse (11.1%). See Table 1 for further demographic information.

Table 1. ***Participant Demographic Frequencies and Percentages***		
Variable	**N**	**%**
Age (M, SD)		28.27; 4.88
Gender (%)		
Male	15	55.6
Female	12	44.4
Race (%)		
White	21	77.8
Black or African American	3	11.1
American Indian	1	3.7
Asian	1	3.7
Other	1	3.7
Ethnicity (%)		
Hispanic, Latino, or Spanish origin	2	7.4
Not Hispanic, Latino, or Spanish origin	25	92.6
Education (%)		
Some college	9	33.4
Associate degree	5	18.5
Bachelor's degree	9	33.3
Master's degree	2	7.4
Doctorate degree	2	7.4
Marital Status (%)		
Single, never married	17	63.0
Married	8	29.6
Divorced	1	3.7
Separated	1	3.7
Employment (%)		
Out of work, looking	4	14.8
Student	4	14.8
Working full time	17	63.0
Working part- time	2	7.4
Retired	0	0
Region of US (%)		
Northeast	9	33.3
Midwest	5	18.5
South	7	26.0
West	6	22.2

Procedure

After obtaining Institutional Review Board approval, data was collected through an anonymous Qualtrics survey posted on MTurk. The survey was titled, "Memories of Adult Survivors of Childhood Cancer." Selecting the survey allowed participants to read a detailed description of the study and provide their consent. The length of the survey was approximately 30 minutes, and participants received 50 cents for its completion. To ensure anonymity of the participants, no identifying information was collected. The survey was closed when saturation was achieved (i.e., no new themes emerged from the data).

Materials

Demographic Questionnaire

This questionnaire collected information on the following: the participant's age, race, gender, marital status, education/employment status, and diagnosis information.

Memories of Adult Survivors of Childhood Cancer

This survey was created by two child life specialists, each contributing specific knowledge and experience to the development of the survey. The primary author of the survey is an adult childhood cancer survivor with over 15 years of lived experience with surviving childhood cancer and a year's worth of clinical training in providing psychosocial care to children in the healthcare environment as a child life specialist. The second contributing author is a Certified Child Life Specialist with 16 years of experience and is a preeminent scholar in the field. The survey questions were based on their training in child life and experiences being and working with childhood cancer patients, as well as their empirical based knowledge from the literature in the field. For example, previous research has shown siblings felt a disruption in the routine of family life and felt less noticed by members of the family [11]. Therefore, the question "How do you think your sibling(s) felt about your cancer?" was included to examine the participant's memories of their siblings' feelings.

The survey included 67 questions focusing on the survivors' memories of family factors, peer factors, diagnosis, treatment, survivorship, and important dates. There was a combination of quantitative (e.g. "How long was your entire treatment process?" and "How many

years post treatment are you?"), and qualitative questions. Five qualitative questions were coded and analyzed for this study. The questions analyzed were 1)"Discuss one memory with one or both of your parents during your cancer."; 2) "Please describe what your parents talked to you about in regards to your cancer."; 3) "Discuss one memory with your sibling(s) during your cancer."; 4) "How do you think your sibling(s) felt about your cancer?"; and 5) "How did your sibling(s) treat you differently?"

Data Analysis

Demographic data was analyzed using IMB SPSS version 23, a statistics program that runs descriptive statistical measures. Qualitative data was coded and themes were developed using a constant comparative analysis [6]. To begin, a team of three researchers reviewed the responses to the 5 questions being studied, identifying themes to generalize participant responses. The researchers worked independently to identify themes then collaborated to discuss them and define codes. Once a consensus was reached, the three researchers independently coded the data for each question using the agreed upon codes. Codes were compared across the three researchers and discussed until a consensus was reached. Finally, a fourth researcher, who had not participated in the previous steps in the thematic analysis of this data, coded the answers to the questions being analyzed. Inter-rater reliability was high between the primary investigator and the reliability coder (89% for question one, 85% for question two, 92% for question three, and 88% for question four). Following inter-rater reliability coding, the coders resolved any discrepancies reaching 100% agreement.

Results

What are adult survivors' of childhood cancer memories of their parents' experiences with the diagnosis of their cancer?

Participants were asked to recall a memory with a parent(s) during cancer. Several themes emerged. The most common theme was that participants remembered their parents being emotionally supportive (n=7). For example, one participant said their parents were "very sad and upset about what was happening. They helped [the participant] through it the whole way". Other parents showed emotion (n=6), with many remembering their parents crying and "trying to keep their composure for [the survivor]". Other participants remembered receiving gifts from their parents (n=5), or spending more quality time with parents (n=5), such as when one family watched "Jerry Springer without a care in the world" together. Some parents performed acts of service for their children (n=3); for example, one participant remembers their "dad making high calorie food for [them] in an attempt to keep [them] from losing too much weight". Lastly, one participant reported having a treatment tradition with their parents (n=1). The participant discussed the memory of "going to get ice cream after every doctor's appointment during the summer months".

Parents talking about cancer.

Participants were asked to recall how their parents spoke to them about their cancer. Participants mostly remembered their parents having a positive outlook or coping (n=14), with parents often telling their sick child "that everything would be okay". Other participants remember their parents providing an explanation of treatment or what to expect (n=9), and how their parents would talk "to [them] in terms that [they] would get without babying [them]." Some participants received explanations of cancer from their parents (n=5), but that parents often "held back on the technical details" or were "told all about what happened when [they were] older" (n=1).

What are adult survivors' of childhood cancer memories of their siblings' experiences with their cancer diagnosis?

Participants were asked to describe a memory with their sibling during their cancer. Primarily, participants remember occasions where their siblings provided support/empathy (n=8), such as when one participant recounted their sibling being "very supported, always there to help me during school breaks. Play (n=3) was also a common theme in memories with siblings, as seen by when one participant recalls that their sibling "loved to tell me silly jokes during

radiation, especially [their] little sister." Lastly, some participants focused on special treatment/gifts (n=3), such as their sibling would "always bring [them] stuffed animals". Additionally, participants remembered siblings performing acts of service (n=2); for example, one sibling "had decorated the whole entire inside of our house with signs and presents that people got [them]".

Siblings' feelings about cancer

Participants were also asked to describe how they think their siblings felt about their cancer. Participants mostly recall their siblings feeling fear or helplessness (n=8). One participant explained that they "think [their sibling] felt sad for [them], just because [the sibling] didn't know what they could do to help. Some perceived their siblings to feel primarily grief and sadness (n=5), as explained by one participant that they "could tell [their siblings] were scared but tried not to act like it". Some siblings displayed empathy (n=2) and others showed a lack of understanding (n=2) because the siblings were "too young to remember".

Differential sibling treatment

Participants were asked how they were treated differently by their siblings after being diagnosed with cancer. Most participants reported not remembering being treated differently by their sibling (n=7). Other participants remember their siblings being kinder (n=4), sometimes going "out of their way for [the patient] and [the patient's] needs". Some siblings were gentler or more sensitive with their sick sibling (n=2), and some participants remember their siblings being more lenient and "let me do whatever [the patient] wanted and gave [the patient] whatever [they] wanted" (n=1).

Discussion

The purpose of this study is to examine the memories of adult survivors of childhood cancer in regards to their parents and siblings. Survivors were asked to reflect on memories with their parents and siblings during the cancer, conversations with parents regarding the cancer, how siblings felt about the cancer and the ways siblings behaved differently during the cancer. In summary, it was found that most adult survivors had positive and supportive memories of both their parents and their siblings throughout their cancer experience.

By examining adult survivors' memories of their parent's during their cancer, it was found that survivors primarily remember their parents being both emotionally supportive and willing to express their own emotions. Parents tended to care for their children with cancer by identifying and caring for the child's various needs, particularly their psychosocial reactions to having cancer. This was also found to be true in a meta-analysis that analyzed the responses of parents of children with cancer, in which parents were found to promote social and emotional balance for their child with cancer [1]. There is evidence that children and parents often avoid talking about difficult topics in order to protect one another [16]. However, the current study found that adult survivors of childhood cancer remember their parents talking to them about cancer with a positive outlook. Considering that parent's verbal and nonverbal communication with their child can reduce the child's stress in difficult situations [9], future research would benefit from examining the impact of parent's emotional support, validation, and positive outlook on the children's own perception of their prognosis and resilience.

When adult survivors of childhood cancer were asked about their memories of their siblings during their cancer treatment, they usually remembered a moment in which their sibling showed support and empathy to their situation. This finding is supported by another study where 85.7% of siblings self-reported the following behavioral changes: increased sensitivity to others' needs, becoming more thoughtful, and increased time playing with friends [8]. Additionally, adult survivors recall their siblings feeling helpless and fearful about their cancer. However, previous research found that siblings of children with cancer felt a disruption in family routine and felt unnoticed [11]. The current findings did not reflect adult childhood cancer survivors remembering such feelings. It could be that children with cancer view the siblings' experience differently than the

sibling. Future research should continue to examine this topic to further identify similarities and differences in the experiences of the siblings during the cancer diagnosis.

Implications

The findings of this study have several implications. One major finding is that participants felt well supported by their parents and siblings. Some studies have shown that the burden of being a caregiver or family member of someone with cancer can cause a heavy emotional load [13]. While parents and siblings are often happy to provide this support, this lends to the importance of making sure that parents and siblings are also provided with the proper resources to deal with the difficulty of having a child or sibling with cancer. Another finding is that some participants remember their parents talking to them about cancer, although not always in complete transparency. This could be due to lack of knowledge about the medical parts of cancer, the desire not to "scare" their child, or the simple fear of not knowing exactly what to say. There are psychosocial care providers, such as child life specialists, that can take on this role in explaining cancer to children in developmentally appropriate terms. Child life specialists are specifically trained in helping children cope with illness and hospitalization [2]. Having a child life specialist available to take this burden off of a parent would allow a parent to focus their energy on caring for their child. Furthermore, some participants also reported that their sibling did not understand everything that was going on and were sometimes scared. Child life specialists are also trained in providing sibling preparation and support in order to boost the whole family's ability to cope with the cancer journey [7]. A third finding is that many participants remember their siblings being a large part of their cancer journey and being around for normal experiences like playing and hanging out with their siblings. This emphasizes the importance of the whole family being allowed to visit and be involved with care. Models of care such as the patient and family centered care model encourage whole families to be together in the hospital in order to promote family unity and reduce familial stress [3].

Limitations

One of the limitations of this study is that it is a retrospective study; participants' memories may have deteriorated over time, making it hard to recall such memories. Therefore, results may be impacted by hindsight emotions, and memories of events may not be accurate. Additionally, the analysis was completed using a secondary data set, so the researchers were unable to develop follow-up questions to provide further clarification on the participants' responses. Moreover, this study was conducted via an open online survey in which participants were paid for completing the survey, so the reliability of participants' responses is unknown.

Conclusion

Overall, the study found that most adult survivors of childhood cancer have positive memories of their relationships with their parents and siblings during their cancer experience. Most survivors recall both their parents and siblings being supportive during their cancer treatment. Such findings emphasize the importance of family for childhood cancer patients. Having a strong familial support system may be a cornerstone to how childhood cancer patients perceive and remember treatment and diagnosis experiences.

References

[1] Cerqueira C, Pereira F, & do Céu Barbieri Figueiredo M. (2016). Patterns of response in parents of children with cancer: An integrative review. Oncol Nurs Forum, 43:E43–E55.
[2] Committee on Hospital Care & Child Life Council. (2014). Child life services. Pediatr, 133: e1471-e14.
[3] Committee on Hospital Care & Institute for Patient- and Family-Centered Care. (2012). Patient- and family-centered care and the Pediatricians role. *Pediatr*, *129*: 394–404.
[4] Cunningham RM, Walton MA, & Carter PM. (2018). The major causes of death in children and adolescents in the United States. NEJM, 379: 2468–2475.

[5] Font-Gonzalez A, Feijen E, Sieswerda E, Dulmen-den Broeder E, Grootenhuis M, Maurice-Stam H, Caron H, Essink-Bot M, Pal H, Geskus R, & Kremer L. (2016). Social outcomes in adult survivors of childhood cancer compared to the general population: Linkage of a cohort with population registers. Psy-Onc, 25:933–941.
[6] Glasser BG. (1965). The constant comparative method of qualitative analysis. Soc Probl, 12:436-445.
[7] Gursky B. (2007). The effect of educational interventions with siblings of hospitalized children. *J Dev Behav Pediatr, 28*: 392-398.
[8] Heffernan SM & Zanelli AS. (1997). Behavior changes exhibited by siblings of pediatric oncology patients: A comparison between maternal and sibling descriptions. J Pediatr Oncol Nurs, 14:3–14.
[9] Jinbing Bai, Harper FK, Penner LA, Swanson K, & Santacroce SJ. (2017). Parents' verbal and nonverbal caring behaviors and child distress during cancer-related port access procedures: A time-window sequential analysis. Oncol Nurs Forum, 44:675–687.
[10] Long KA, Lehmann V, Gerhardt CA, Carpenter AL, Marsland AL, & Alderfer MA. (2018). Psychosocial functioning and risk factors among siblings of children with cancer: An updated systematic review. Psycho-Oncol, 27*:*1467–1479.
[11] Mavrides N, & Pao M. (2014). Updates in paediatric psycho-oncology. Int Rev Psychiatry, 26:63.
[12] Molinaro ML, & Fletcher PC. (2017). "It Changed Everything. And Not All in a Bad Way": reflections of pediatric cancer experiences. Compre Child Adolesc Nurs, 40:157–172.
[13] Panganiban-Corales AT & Medina MF (2011). Family resources study: Part 1: Family resources, family function and caregiver strain in childhood cancer. *Asia Pac Fam Med,10*: 14
[14] Samson K, Rourke MT, & Alderfer MA. (2016). A qualitative analysis of the impact of childhood cancer on the lives of siblings at school, in extracurricular activities, and with friends. *Clin Pract Pediatr Psychol*, 4:362–372.
[15] Siegel RL, Miller KD, & Jemal A. (2019). Cancer statistics, 2019. CA, 69:7–34.
[16] Son H, Haase J, & Docherty S. (2019). Parent-child communication in a childhood cancer context: A literature review. Pediatr Nurs, 45*:*129–141.

Parent Perceptions and Influence on Sport Specialization as It Relates to Injury in Youth Baseball

Laura Carrasquilla[1], Elizabeth Hibberd[2,3]

Faculty Mentor: Elizabeth Hibberd, PhD, ATC
[1]*Department of Biological Sciences, The University of Alabama, Tuscaloosa, AL 35487*
[2]*Department of Health Science, The University of Alabama, Tuscaloosa, AL 35487*
[3]*Athletic Training Program, The University of Alabama, Tuscaloosa, AL 35487*

Sport specialization commonly refers to intensive training in one sport year-round at the exclusion of all other sports. While sport specialization is now described on a scale ascending from low to high specialization, recent research has reported a general trend in the increase of sport specialization among youth athletes. This trend has been connected to an increase in injury among youth athletes, particularly upper-extremity injuries related to youth baseball. The objective of this study is to determine the influence of parents on sport specialization and injury rates in youth baseball players through an online questionnaire regarding their child or athlete's injury history, the extent of their participation, and their own demographics and knowledge of current youth baseball guidelines.

Introduction

Organized sports comprise a major pastime for the youth of America, with participation of youth athletes between the ages of 6 to 18 in organized sports totaling nearly 60 million in 2008 [7]. While there is some contention as to whether participation levels have increased or decreased in recent years, most recent data sources show an increase in injury rates among youth athletes, particularly in the shoulders and elbows of youth and adolescent baseball players. In fact, 15- to 19-year-olds make up the largest age group for elbow ulnar collateral ligament (UCL) reconstruction surgeries (56.8%). The incidence of UCL reconstruction is growing at a rate of 9.1% per year among this age group [5]. As sports injuries become increasingly common in youth athletes, there is not only a rise in the number of corrective surgeries performed, such as UCL reconstruction surgeries, but an increase in sport drop-out rates [8]. In one study, 70% of children dropped out of organized sports participation before age 13, and injury was a major contributing cause [4].

One explanation for this observed increase in injury is the simultaneous increase in sports specialization throughout all sports. The most common definition of sport specialization is the year-long, intensive training in one sport at the exclusion of other sports. Still, it may be more accurate to define sport specialization on a spectrum, with some athletes intensely specializing and others only moderately specializing. Questions used to determine an athlete's level of specialization commonly ask if the athlete views their particular sport as more important than other sports, if they have ever quit other sports to pursue their particular sport, and if they play their particular sport more than eight months out of the year. Answering yes to all three of these questions indicates a high level of specialization, while answering yes to only two or one indicates a moderate to low level, respectively. Baseball specialization is occurring despite recommendations from the USA Baseball Medical and Safety Advisory Committee Guidelines, which advise taking time off from the sport, pitch count limits, and recovery recommendations [3]. In a study that analyzed over 1000 athletes between 7 to 18 years of age, more than 60% were at least moderately specialized and, on average, had begun to specialize before age 12 [2]. Sport specialization has repeatedly been associated with an increased risk of physical and emotional harm for youth athletes, especially since children under the age of 18 are still considered skeletally

and mentally immature, which increases their chances for burnout and overuse injuries [8].

There are many factors that may influence this trend towards sport specialization despite suggestions from medical research and official baseball guidelines. It is popularly believed that specializing early increases athletes' chances of continuing into professional leagues, with the 10,000-hour rule (a rule stating that one must practice for 10,000 hours to become an expert at something) acting as an instance where extensive time and devotion to a single activity is accredited with eventual expertise and success in that field. However, countless studies have shown that the majority of professional athletes do not believe specializing early will increase an athlete's chances of competing professionally, and some claim that specializing early may actually be detrimental to a player's athletic ability since it encourages the development of very specific skills rather than general athletic capabilities [6]. In one study, professional players generally opposed specialization in baseball for players ages 10-14 (68.7%) [1]. In another study, 97% of professional athletes stated that multisport participation contributed to their success in their chosen sport [9].

Related studies have examined the influence of parents on a child's decision to specialize. In one study, approximately one-third of young athletes had been explicitly told not to play other sports by parents and coaches [6]. In another study, 22% of players had been told by their parents not to play other sports [6]. Many players have reported that intensive training in their sport has disrupted their academic and social lives, which can lead to burnout and decreased enjoyment of sports [2,6]. Still, there is limited research on parent perception of sport specialization in baseball across the United States. This study aims to survey parents regarding their outlook on youth specialization and participation in baseball and assess their role in the recent increase in sport specialization across the nation.

Methods and Materials

Participant recruitment was completed through Qualtrics Panels, a service that allows researchers to send a survey to a targeted population of respondents from across the United States. Respondents can choose to join a panel through a double opt-in process. Upon registration, participants self-report basic personal data, including demographic information, hobbies, interests, etc. Qualtrics Panels then creates a panel of individuals that meet the inclusion criteria identified by the research team. Participants were identified for this study with the requirement that they had a child that plays baseball on an organized baseball team and that the child was between the ages of 10-18. If a parent met the criteria, they were notified via email and invited to participate in the survey for a given incentive. The email invitation sent was a generic invitation to participate in a study, with no specifics given as to the topic of the survey itself. Potential candidates were informed that they qualified for a survey and given a link to follow if they would like to participate in the study for the given incentive.

The final survey was administered through Qualtrics. The survey consisted of five sections: 1) demographic information, including participant age, sex, average annual income, and highest degree level; 2) information regarding the participant's child's sport and baseball participation, including their sport position, baseball participation volume (hours per week, months per year, innings per year, pitches per game), participation on multiple teams, private coaching, and types of pitches thrown; 3) sport specialization, including a widely-utilized specialization scale and an assessment of attitudes and beliefs; 4) parent knowledge of USA Baseball Medical and Safety Advisory Committee Guidelines; and 5) self-reported injury history of their child from the previous 12 months. The questionnaire was designed to be completed in 15 minutes and was written at a Flesch-Kincaid Grade Level of 5.7.

Over 1500 individuals began the survey. All survey responses were manually filtered, and individuals that did not meet the inclusion criteria verification questions, did not complete all questions on the survey, or completed the survey with answers that did not logically answer the questions being asked were excluded.

After manually filtering the data, 517 complete responses met the inclusion criteria and were included in the analysis. Data were summarized as frequencies and proportions (%) and means and standard deviations (SD).

Results

The mean age of parents was 40.3 ± 7.8 (a range of 35 years). Sixty-nine percent of respondents claimed that one parent had participated in baseball to some extent in their youth. Additionally, responses resulted from diverse regions across the United States, including from 45 states and the District of Columbia, and included players involved in variable levels of baseball participation, giving a more representative sample of baseball participants across the U.S. than many past studies who tended to recruit players at competitive tournaments or baseball symposiums.

Levels of Specialization

The level of specialization for players was determined through three questions directed towards the parents: 1) Does your child consider baseball more important than the other sports they play? 2) Has your child ever quit playing another sport(s) to focus on baseball? 3) In the last 12 months, which months did your child participate in organized baseball activities? Months were tallied, and players participating for more than 8 months out of the year were considered to be specialized. For each question to which the participant responded "yes," 1 point was added to the specialization score, with scores ranging from 0-3. Participants were categorized into a level of specialization based on the sum, with 0 and 1 indicating low specialization, 2 indicating moderate specialization, and 3 indicating high specialization. Data are summarized in **Table 1.** Most athletes were found to have low levels of specialization, with only 18% being moderately specialized and 2% being highly specialized.

Degree of Specialization	Number of Players	Percent of Players
0	217	42%
1	195	38%
2	92	18%
3	13	2%

Table 1. Levels of specialization calculated for youth players based on parental responses (n=517)

Parental Influence on Specialization

In order to determine the influence of parents on their child's specialization habits, parents were asked if they had ever encouraged their child to participate in baseball exclusively. 23% stated that they had encouraged their child to specialize. Additionally, 49% of parents admitted to never having heard of the USA Baseball Medical and Safety Advisory Committee pitching guidelines, the current youth baseball guidelines, set in place to encourage healthy levels of participation and prevent overuse injuries from overexertion.

Parental Perceptions on Sport Specialization

Parents who reported that their child had quit another sport in order to focus primarily on baseball were asked about their child's motivations for specializing **(Figure 1)**. Sixty-four percent of parents (n=91) stated that improving their baseball skills had at least "quite a bit" of influence on their child's specialization. Fifty-seven percent said staying competitive among their division had a similar influence, along with 63% who stated this for the importance of their child improving their chances of receiving a baseball scholarship or contract.

Figure 1. Reasons for specializing among youth baseball athletes as reported by parents

Parents were also asked about their personal beliefs about sport specialization and its effect on both performance and injury rates among youth baseball athletes (Figure 2). Fifty-two percent of parents stated that they believed sport specialization in baseball improved their child's chances at least "quite a bit" of making a high school baseball team. However, only 26% believed that sport specialization increased their child's chances of getting injured by the same amount.

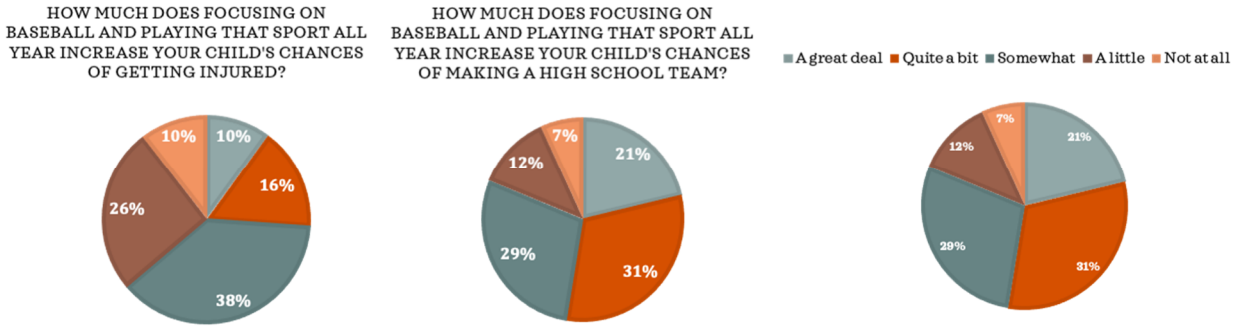

Figure 2. Parental perceptions on effects of sport specialization in youth baseball (n=517)

Player Injury

Twenty-four percent of parents reported that their child had sustained an injury due to baseball. Additionally, 30% stated that their child had complained of pain or fatigue at some point in their time playing baseball, and 19% of parents reported that their child continued playing baseball despite this pain or fatigue.

Discussion

The purpose of this study was to examine parental perceptions of sport specialization, particularly as it pertains to youth baseball, and to investigate if parental influence contributed to the increasing popularity of sport specialization among current youth baseball athletes. While previous research has looked into parental influence on specialization, research is still limited, and few studies delve into parental perceptions of sport specialization and knowledge of current research and youth baseball guidelines. It was hypothesized that similar levels of sport specialization would be seen in this cohort of athletes as compared to previous findings and that parental perceptions of sport specialization would contradict current research findings on the subject.

A small proportion of children included in this research study were found to be moderately or highly specialized in baseball as compared to other research findings. The lower rates may be a result of the diverse population recruited in the current study, as well as the recruiting methods. Previous studies recruited participants at showcase tournaments or training facilities, which may have biased the results

towards higher rates of specialization. The reported rates of specialization from our study may be more representative of baseball specialization rates across all levels of competition and geographical regions of the United States. Though the levels of specialization were low, they closely resembled the reported levels of injury, with 20% of athletes being at least moderately specialized and 24% having sustained an injury. This is in concordance with other studies that tend to find similar rates between the two, with injury rates increasing as specialization rates increase. Injuries were twice as common among those who were specialized, with 42/105 (40%) specialized athletes sustaining injuries compared to 83/412 (20%) non-specialized athletes. Parents were greatly unaware of current guidelines put in place to protect their child throughout their baseball participation. Their ideas about sport specialization contradicted most current research, emphasizing its limited effect on performance and underestimating its major impact on overuse injuries. The findings from this project highlight the importance of developing educational materials for parents, coaches, and recreational leagues to ensure that information regarding the health and safety of their child is reaching the individuals that can impact their participation decisions.

Limitations

Limitations arise from the self-report survey methods utilized in this study, which may allow for potential bias or dishonesty in how questions are answered. Asking parents about their child's motivations or views of baseball may result in inaccurate responses that aren't entirely indicative of their child's true beliefs or sentiments. Finally, the cross-sectional nature of the study does not allow the same benefits a longitudinal study method may have allowed in terms of insight into the long-term effects of sport specialization on injury and competitive performance among this cohort.

Conclusion

The results of this study give insight into how uninformed and unprepared the parents of youth baseball athletes are to ensure safe levels of participation for their children during their baseball careers. This study, in congruence with several others, reveals a relationship between sport specialization and injury. Parents need to be better informed of current guidelines set in place to protect their children, along with current research that highlights some of the disadvantages and dangers of specializing at an early age.

References

[1] Hill GM. (1993). Youth Sport Participation of Professional Baseball Players. Sociology of Sport Journal, 10:107–114.,
[2] Jayanthi NA, LaBella CR, Fischer D, Pasulka J, Dugas LR. (2015). Sports-specialized intensive training and the risk of injury in young athletes: a clinical case-control study. Am J Sports Med, 43:794-801.
[3] Mautner BK & Blazuk J. (2015). Overuse Throwing Injuries in Skeletally Immature Athletes Diagnosis, Treatment, and Prevention. Current Sports Medicine Reports, 14:209–214
[4] Mckay CD, et al. (2019). Youth Sport: Friend or Foe? Best Practice & Research Clinical Rheumatology, 33:141–157
[5] Mehta S. (2019). Relationship between Workload and Throwing Injury in Varsity Baseball Players. Physical Therapy in Sport, 40:66–70
[6] Padaki AS, et al. (2017). Factors That Drive Youth Specialization. Sports Health: A Multidisciplinary Approach, 9:532–536
[7] Popkin CA., et al. (2019). Early Sport Specialization. Journal of the American Academy of Orthopaedic Surgeons, 27:995-1000
[8] Smucny M, et al. (2015). Consequences of Single Sport Specialization in the Pediatric and Adolescent Athlete. Orthopedic Clinics of North America, 46: 249–258
[9] Snyder C. (2014). The Path to Excellence: A View on the Athletic Development of U.S. Olympians Who Competed From 2000-2012. Initial Report of the Results of the Talent Identification and Development Questionnaire to U.S. Olympians

The Effects of Transcranial Direct Current Stimulation on the Dorsolateral Prefrontal Cortex During Language Learning

Bolling AJ, King VL, Welch MM, Schrobilgen AN, Enam T

Faculty Mentor:, & McDonough IM
Department of Psychology, The University of Alabama, Tuscaloosa, AL 35487

The present study aims to use transcranial direct current stimulation (tDCS) to determine if the left dorsolateral prefrontal cortex (DLPFC) is causally involved in foreign-language learning and if tDCS is an effective technique to improve language acquisition in adults. This study includes three sessions that take place 24 hours apart. In the first two sessions, participants were stimulated for 20 minutes, and then learned 72 English-Swahili word pairs. On the third day, participants were tested using cued-recall, where the Swahili word was shown, and participants typed the English equivalent. One week later, the test was retaken for latency effects. It was hypothesized that participants who received tDCS would have higher memory retention for the word pairs than those in the sham condition. It was also hypothesized that participants who received tDCS would forget less between the immediate and delayed tests than those who received the sham treatment. We found that there were no statistically significant effects of tDCS on the level of retention. We did, however, find significant differences in the amount of forgetting between the 1mA and 1.5mA groups such that the 1.5mA group forgot more than the 1mA group. The direction of these effects were in the opposite direction of our predictions. Overall, our findings indicate that tDCS, administered to the left DLPFC before encoding using the parameters in this study, does not have a strong beneficial effect on language learning in young adults. If the findings remain consistent with further research, it could suggest that the left DLPFC is not causally involved in language learning, specifically in the aspect of verbal declarative memory.

Introduction

Learning a new language creates the opportunity for people to gain connections, perspectives, and ideas. One critical aspect of foreign language learning is memory - the ability to encode, store, and retrieve information. While children acquire new languages relatively easily, learning a new language as an adult can be quite difficult [7]. Another critical aspect of learning a new language is the ability to pair words in the native and foreign language. Functional magnetic resonance imaging (fMRI) research on semantic [3] and declarative memory [1] as well as other tDCS research [2] has suggested that the DLPFC is involved in this process. However, because fMRI is correlational, additional research is needed to further investigate the implicated brain region and how it is involved in language learning. tDCS is a non-invasive procedure that uses electrodes to send small electrical currents through the scalp, modulating brain activity. The physiology of tDCS is based on the view that low current stimulation impacts neuron membrane potential [8]. Anodal stimulation (positive electrode) promotes Long Term Potentiation (LTP) which creates strong connections between neurons and increases synaptic plasticity [8]. Cathodal stimulation (negative electrode) promotes Long Term Depression (LTD) which involves slowing the neuronal connections or decreasing neuronal excitability [8]. Nitsche and Paulus (2001) found that the effect of tDCS on neuronal connectivity lasts between 60 and 90 minutes after a single administration [5]. Other researchers have suggested investigation into increasing the impact of low current brain stimulation over a longer period of time with repeated administrations [6]. Through these aspects of previous procedures, the present study aims to use tDCS to determine if the DLPFC is causally involved in foreign-language learning and if tDCS is an effective technique to improve language acquisition in adults. Our main

hypothesis is that participants who receive tDCS have higher memory retention for the word pairs than those in the sham condition. A second hypothesis is that participants who receive tDCS forget less between the immediate and the delayed test.

Materials and Methods

Materials

A 9V-battery-operated tDCS device (Soterix Medical 1x1 tDCS Low-Intensity Stimulator) was used to administer the stimulation. We ensured correct and consistent placement of the electrodes with electrode placement caps based on the International 10-20 system for EEG electrode placement. The electrodes were placed inside Soterix Medical 5 x 7cm EASYpad sponges that were doused in phosphate buffered saline (pH 7.2) using a plastic syringe. Analyses were run using Collector, a program utilizing Excel, written in PHP.

Participants

Sixty-two young adults ages 18-25 were recruited from the UA Psychology Subject Pool. These students received course credit for participating in our study. The participants were randomly assigned to stimulation or sham groups. Eleven subjects were excluded due to "cheating" (determined by having higher delayed scores than immediate scores). Two additional participants were excluded because they did not complete the delayed test.

Methods

The study was conducted in four parts (see Figure 1). During Part 1, participants' contact information was recorded and they were assigned a participant ID. The tDCS apparatus was placed on their head with the anode at the F3 placement site according to the International 10-20 system for EEG electrode placement and the cathode on the contralateral supraorbital position (F4) on the same system in order to stimulate the left DLPFC. Either the sham, 1mA, or 1.5mA current was administered for twenty minutes while they completed a series of questionnaires. Sham was a brief 30 second stimulation at the beginning and end of the 20 minute period. This gave participants a tingling sensation to mimic the feeling of tDCS ramping up and down. If the participant finished the questionnaires before the 20 minutes were up, they were instructed to wait for the remainder of the 20 minutes. After the tDCS administration, participants were presented with Swahili-English word pairs (Table 1). In order to control for levels of prior knowledge between participants, Swahili was chosen as the foreign language because it is not a commonly known language. Participants were instructed to try to create a mental image of the item associated with the foreign language word in order to keep memorization strategies consistent between participants.

The words appeared individually for 8 seconds each. The set of 72 word pairs was shown twice per study session for repetition and were broken up randomly into four groups in order to prevent participants from feeling overwhelmed by the amount of content. The tDCS cap remained on the participants head through the entire session and was removed after the participant finished the study portion of the session. Part 2 was conducted in the same way 24 hours after Part 1, however participants completed questionnaires that were different from those on the first day.

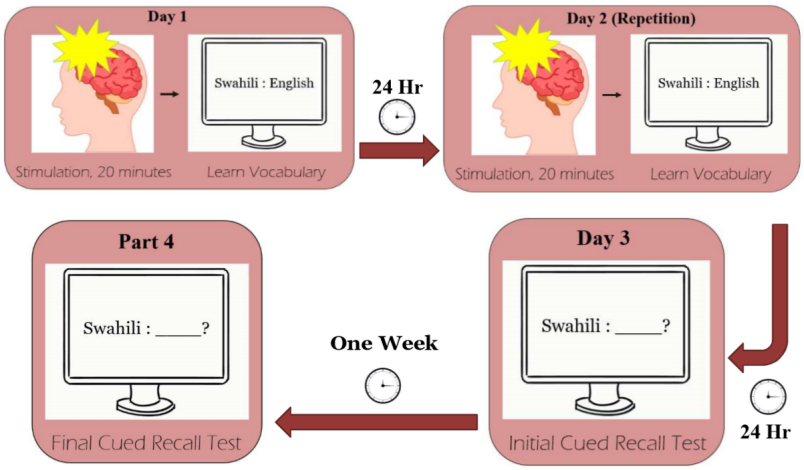

Figure 1.

Four Parts: Day 1. Study phase: participants received 20 minutes of tDCS while answering questionnaires, then studied a set of English-Swahili word pairs for 20 minutes. Day 2. Study phase: identical to day one for repetition. Day 3. Testing phase: subjects were given a cued-recall test where the Swahili word was provided, and participants typed the English equivalent. Part 4. Testing phase: Participants took the same test from Day 3 to determine long-term effects.
3 Conditions: Participants received anodal tDCS at 1 mA (n=20), 1.5 mA (n=15), or sham (a brief 30 second stimulation that causes a placebo; n=16)

For Part 3, participants returned to the lab 24 hours after Part 2 for the immediate recall task. They were shown the Swahili word and asked to type the English word equivalent. They were instructed to press an "I have an answer" button as soon as they recalled the English word in order to collect data on response time (analysis not included in this publication). If they did not know the word, they were instructed to leave it blank and move to the next one. They were given one opportunity for each word. Part 4 of the experiment was conducted 1 week after Part 3. The participants were emailed a link to access the delayed recall test (same format as the immediate test) from their personal computer and were instructed to complete the task at any time during that day.

Analysis

For the analysis of the main effect (stimulation group vs. immediate and delayed recall score), two separate one-way Analysis of Variance tests were conducted in SPSS.

For the forgetting score analysis, a one-way ANOVA, Pearson correlation, and ANCOVA were all conducted using SPSS. The forgetting score was calculated by subtracting the delayed recall score from the immediate recall score to demonstrate the amount forgotten over time by each participant.

For each analysis, participants who were identified to have possibly cheated on the delayed test were excluded from the analysis. Those individuals were identified because they had a higher score on the delayed test than the immediate test, suggesting they may have used outside resources on the delayed portion.

Recall scores were calculated by dividing the number of correct words by the number of total words. If the answer provided did not exactly match the given Swahili word, it was reviewed by undergraduate research assistants to decide whether the word would be counted as correct or not. For example, if the expected answer was "phone," but the participant typed "telephone," it would be counted correct for this analysis. Similarly, answers that had similar meanings to the expected word were given credit. For example, if the target word was "ship", but the participant

typed "boat" or "mail" then credit was given. Credit was also given for misspelled words or typos.

Results

Based on our initial analyses, we found that numerically, people with more stimulation did better on the immediate and delayed recall tests. This difference was not significant for the immediate score $F(2, 48) = 0.878$, $p = 0.422$ or the delayed score $F(2, 46) = 0.65$, $p = 0.53$, shown in Figure 2. This indicates that tDCS, administered to the DLPFC before encoding and using the parameters in this study, does not have a strong, beneficial effect on language learning in young adults.

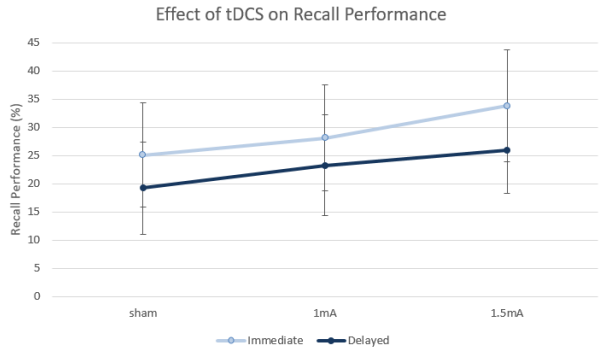

Figure 2. This graph displays the effects of tDCS on recall performance in the immediate and delayed tests. This figure shows that numerically, there was about a 4% and 9% increase on average between sham and the 1mA and 1.5mA control groups during the immediate recall test. These differences, however, did not meet traditional levels of statistical significance. Error bars indicate the 95% confidence interval.

We also calculated a forgetting score to capture the net effects of the immediate and delayed tests. In this analysis, we found that those in the 1.5mA stimulation group (M = .0787, SD = .0524) forgot significantly more than those in the 1mA group (M = .0344, SD = .0312, $t(32) = 3.145$, $p < 0.05$), using Fisher's least significant difference (LSD) for the post hoc restrictions (Figure 3 shown below).

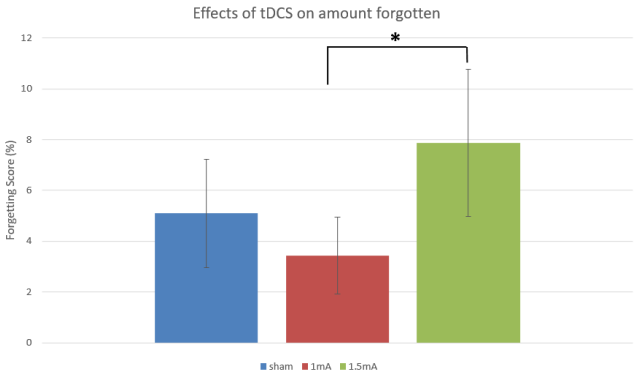

Figure 3. This graph displays the average of how much participants forgot between the immediate and delayed recall test. The forgetting score was calculated by subtracting the delayed score from the immediate score. This analysis shows that the 1.5mA group significantly forgot more than the 1mA group ($p = 0.011$). This test was done prior to the correction for the immediate score. The error bars represent the 95% confidence interval.

However, we also found a correlation between immediate recall performance and the degree of forgetting $r(47) = .633$, $p < 0.001$ (Figure 4), which could indicate that this increase in forgetting is simply due to the fact that a higher initial recall lends more opportunity to forget a greater amount of words. As a follow-up to the correlation, an ANCOVA was conducted on the forgetting score data to control for the immediate score as a covariate. The results of the pairwise comparisons indicated that there was still a significant difference between the 1.5mA (M = 0.071, SD = 0.008) and 1mA (M = 0.036, SD = 0.007) groups on forgetting score $t(32) = 3.091$, $p = 0.004$, but not due to an increase in the immediate score. This finding suggests that our initial interpretation from the correlation does not fully explain the finding that the 1.5mA group forgot significantly more than the 1mA group.

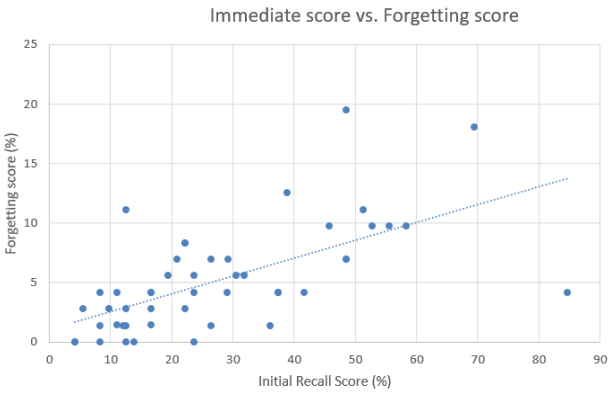

Figure 4. This graph shows a positive correlation between the immediate recall score and the forgetting score ($r = 0.633$, $p < 0.001$).

Discussion

The aims of this study were to determine the effects of tDCS on foreign language learning and memory. We tested whether anodal tDCS stimulation of the left DLPFC led to better language retention compared to the sham stimulation (control). We hypothesized that greater tDCS stimulation would increase the amount of words recalled in both the immediate and delayed cued-recall tasks. Additionally, we hypothesized that higher stimulation would lead to less forgetting in the delayed cued-recall task.

Based on our results, we can not support the hypothesis that administering tDCS to the DLPFC before encoding increases language acquisition. While there seems to be a general trend in which tDCS increased immediate recall, we can not confidently report those findings, as they were not statistically significant. However, we did find that higher stimulation led to more forgetting on the delayed recall task. Further analyses revealed that this effect was mostly because having higher initial scores led to more opportunity to forget. Yet, even when controlling for this factor, we still see higher forgetting scores in the 1.5mA group.

We speculate a number of possible reasons for this effect. First, we may have too few participants to lead to significant immediate and delayed scores. In addition, more participants may eliminate the significance in the forgetting scores. In terms of the forgetting scores, however, we propose several explanations of our significant findings. First, stimulating brain activity via tDCS may have interference effects that impedes ability to retain new information. Second, we propose the possibility that stimulating the left DLPFC may have a beneficial effect of native language organization (for example, a participant might be better able to recall just the English words that were presented rather than the exact word pair) at the expense of foreign language acquisition.

Limitations and Further Directions

The present study analyzed the effects of 20 minute tDCS stimulation on the left DLPFC before encoding. Future studies should take into consideration the amount of time tDCS is administered, to what region of the brain it is being administered (another brain region could include Wernicke's area due to its role in language comprehension), as well as whether administering tDCS after encoding or before retrieval has significant effects on the results.

Based on the results of this study, tDCS may have limited effects on language learning ability. We see very small, yet not significant, effects on tDCS stimulation of the left DLPFC. In terms of practice, tDCS to the left DLPFC may not be a useful tool in language learning in terms of long-term recall. If the findings remain consistent with further research, it might suggest that the left DLPFC is not causally involved in language learning, specifically in the aspect of verbal declarative memory.

Appendix

gozi	FOOTBALL	biri	CIGAR	reli	TRAIN	tundu	NEST	mashini	RADIO	waridi	ROSE
nyoka	SNAKE	mani	GRASS	kalamu	PENCIL	uzio	FENCE	chupa	BOTTLE	pombe	BEER
sindano	NEEDLE	ndege	PLANE	deski	DESK	mkono	HAND	kiazi	POTATO	majira	CLOCK
mkate	BREAD	mlango	DOOR	mahindi	CORN	ndimu	LIME	kiti	CHAIR	shingo	NECK
meli	SHIP	foni	PHONE	daraja	BRIDGE	kuku	CHICKEN	gurudumu	WHEEL	kichwa	HEAD
farasi	HORSE	kisu	KNIFE	samaki	FISH	boti	BOAT	wali	RICE	sahani	PLATE
kisiwa	ISLAND	kitabu	BOOK	ubao	BENCH	mshipi	BELT	miguu	FEET	maziwa	MILK
kondoo	SHEEP	kifungo	BUTTON	wingu	CLOUD	sungura	RABBIT	pua	NOSE	ulimi	TONGUE
dirisha	WINDOW	bahasa	ENVELOPE	tofali	BRICK	hema	TENT	jani	LEAF	uma	FORK
kifaranga	BIRD	mlima	MOUNTAIN	chungwa	ORANGE	sabuni	SOAP	karatasi	PAPER	kahawa	COFFEE
keki	CAKE	jino	TOOTH	kioo	MIRROR	mchanga	BABY	mpira	BALL	tungi	LAMP
kitunguu	ONION	kibanda	CABIN	jiwe	ROCK	moto	FIRE	limau	LEMON	nyumba	HOUSE

Table 1. The list of 72 common nouns in Swahili and their English word pairs that we used in this study.

References

[1] Cabeza R & Nyberg L. (2000). Neural basis of learning and memory: functional neuroimaging evidence. Curr Opin Neurol 2000; 13(4):415.

[2] Javadi AH & Walsh V. (2012). Transcranial direct current stimulation (tDCS) of the left

dorsolateral prefrontal cortex modulates declarative memory. Brain stimulation, 5(3), 231-241.
[3] Martin A. (2001). Functional neuroimaging of semantic memory. In: Handbook of functional neuroimaging of cognition. Cambridge (MA): MIT, 153-186.
[4] McDonough IM, Bui DC, Friedman MC, & Castel AD. (2015). Retrieval monitoring is influenced by information value: The interplay between importance and confidence on false memory. Acta Psychologica, 161, 7-17.
[5] Nitsche MA & Paulus W. (2001). Sustained excitability elevations induced by transcranial DC motor cortex stimulation in humans. Neurology, 57(10):1899-901.
[6] Reis J, Schambra HM, Cohen LG, Buch ER, Fritsch B, Zarahn E, Celnik PA & Krakauer JW. (2009). Noninvasive cortical stimulation enhances motor skill acquisition over multiple days through an effect on consolidation. Proc Natl Acad Sci U S A. 106(5):1590-5. doi: 10.1073/pnas.0805413106.
[7] Sanz C. (2005). Mind and Context in Adult Second Language Acquisition: Methods, Theory, and Practice. 150.
[8] Stagg CJ & Nitsche MA. (2011). Physiological Basis of Transcranial Direct Current Stimulation. The Neuroscientist, 17(1):37-53.

Inhibitory Effect of Ascorbic Acid on In Vitro Enzymatic Digestion of Raw and Cooked Starch

Alyssa Gutierrez[1], Jiayue Guo[2], Libo Tan[2], Lingyan Kong[2],*

Faculty Mentor: Lingyan Kong
[1]*Department of Biological Sciences, The University of Alabama, Tuscaloosa, AL 35487*
[2]*Department of Human Nutrition and Hospitality Management, The University of Alabama, Tuscaloosa, AL 35487*
** Corresponding author*

Ascorbic acid, also known as vitamin C, has previously been reported to inhibit the activity of pancreatic α-amylase, a digestive enzyme for starch. A major implication of such inhibition is a decreased rate of starch digestion into glucose, which thereby reduces postprandial hyperglycemia. Accordingly, this study explored the inhibitory effects of ascorbic acid on the digestion of a high amylose maize starch that was either raw, cooked without storage, or cooked and stored for 24 hours at freezing (-20°C), refrigeration (4°C), or room temperature (23°C). Defined as the starch remaining after 4 hours of simulated in vitro enzymatic digestion, resistant starch (RS) content was measured for the starch samples. First, the inhibitory effect of ascorbic acid on the digestion of raw starch increased with its concentration until it reached a plateau of effectiveness. An ascorbic acid concentration of 6.25 mg/mL increased the RS content to 78.59%, as compared to the 52.24% RS content in the raw starch without ascorbic acid. Cooked starch contained significantly less RS than raw starch ($p<0.05$). Additionally, one day of storage at freezing and refrigeration only slightly increased the RS content compared with freshly cooked starch, while storage at room temperature did not exhibit such an effect. Under all tested processing and storage conditions, the addition of ascorbic acid resulted in a significantly increased RS content ($p<0.05$). The combined effect of ascorbic acid with certain storage conditions more potently augmented RS than either ascorbic acid or cold storage alone. Overall, our results strongly indicate that ascorbic acid may function as a glycemic modulatory agent and that its effects persist under a variety of processing conditions.

Keywords: *starch; digestion; storage; ascorbic acid*

Introduction

As developed nations experience marked rises in caloric intake, obesity has become more prevalent. Considering that starch is a major source of energy in the human diet, excessive consumption of starch could contribute to obesity and related metabolic diseases. Accordingly, some metabolic treatments aim to reduce the extent of starch digestion and glucose absorption. For example, acarbose is a drug that inhibits starch digestive enzymes [8]. Besides the available pharmaceutical options, food-based strategies are also promising. One such alternative is ascorbic acid, which has demonstrated the ability to inhibit starch digestive enzymes [1,2] and therefore may function as a glycemic modulatory agent.

Ascorbic acid, commonly known as vitamin C, is a water-soluble micronutrient necessary for the proper functioning of the body. It is required for the formation and maintenance of connective tissues and serves as a potent antioxidant that protects the body from harmful free radicals [9]. Because it is water-soluble, excess ascorbic acid is easily excreted in urine and rarely accumulates to toxic levels, which makes the utilization of ascorbic acid advantageous over medications that may cause adverse symptoms at high doses. Aside from the aforementioned essential metabolic activities, ascorbic acid has also been shown to inhibit the activity of pancreatic α-amylase, a digestive enzyme that breaks down starch into glucose, via non-competitive antagonism [2]. Although the mechanism of such enzymatic inhibition was

well investigated, the effect of ascorbic acid was only examined in an α-amylase assay over the brief course of 30 min, which is only a fraction of the several hours that starch spends in the small intestinal tract. Moreover, only one concentration of ascorbic acid was considered, and few studies have evaluated its effects by using simulated in vitro digestion assays, therefore raising concern for the effect of concentration and how this may translate to real-life applications.

The objective of this study was to further investigate the inhibitory effect of ascorbic acid on starch digestion as well as to explore its general applicability as a glycemic modulatory agent. To simulate the digestion process in the small intestine, mixtures of starch and ascorbic acid were subjected to 4 hours of *in vitro* digestion. The amount of starch that remained undigested after the 4 hour period was defined as the resistant starch (RS) content. Different concentrations of ascorbic acid were used to determine whether the inhibition effect is dose-dependent. In addition, starches were subjected to various cooking and storage conditions prior to digestion in order to investigate the practicality of ascorbic acid as a potential glycemic modulatory agent.

Materials and methods

2.1. Materials

High amylose maize starch (HAMS, Hylon VII) was provided by Ingredion (Bridgewater, NJ, USA). Ascorbic acid was purchased from Sigma-Aldrich Inc. (St. Louis, MO, USA). Digestible starch and a resistant starch assay kit (K-DSTRS) were obtained from Megazyme (Wicklow, Ireland). Ethanol was purchased from VWR International (Radnor, PA, USA).

2.2. In vitro digestion

The in vitro starch digestion was conducted according to the method provided by the Megazyme resistant starch assay kit with slight modifications. The enzyme solution, containing pancreatic α-amylase and α-amyloglucosidase (0.8 KU/mL and 0.34 KU/mL, respectively), was prepared immediately before use. Cooked starch was prepared by boiling starch in a 100°C water bath for 20 minutes and allowed to cool to room temperature (20°C) before in vitro digestion. Starch (100 mg) alone and starch mixed with 12.5, 25, 50, or 75 mg of ascorbic acid were weighed into 20-mL round-bottom test tubes. A test tube with neither starch nor inhibitors was used as the blank. 3.5 mL of 50 mM sodium maleate buffer were added into each tube, and the reaction suspensions were mixed and placed in a water bath at 37°C for 5 min to equilibrate. Enzyme solution (0.5 mL) was added into each tube, and then the test tubes were capped and placed into a shaking water bath at 37°C and 170 strokes per minute. After incubating the tubes for 4 hours, 4.0 mL of 95% (v/v) ethanol was added to each tube and mixed vigorously. The samples were centrifuged (3600 g, 10 min), and the supernatant was decanted. The pellet was resuspended in 2 mL of 50% (v/v) ethanol and vigorously mixed, then 6 mL of 50% (v/v) ethanol were added, and the solution was thoroughly mixed again. The centrifugation, washing, and decanting steps were then repeated twice, and the remaining pellet was used for the resistant starch measurements.

2.3. Resistant starch content

The resistant starch content in starch samples was determined following the resistant starch assay procedure using the digestible starch and resistant starch assay kit (K-DSTRS) [6], with slight modifications. The remaining pellet obtained from the last step was resuspended in 2 mL of cold 1.7 M NaOH by stirring for 20 min in an ice bath, and then added with 8 mL of 1.0 M sodium acetate buffer and 0.1 mL of α-amyloglucosidase (3,300 U/mL). The tubes were mixed well and placed into a 50°C water bath for 30 min. The contents of the tubes were transferred and volumes adjusted to 100 mL in volumetric flasks using water. Aliquots of the diluted solutions were centrifuged (13,000 rpm, 5 min). In duplicates, aliquots of 30 μL from the diluted supernatants were measured for the glucose concentrations using the glucose oxidase-peroxidase (GOPOD)

method. The reagent blank was prepared using 30 µL of 100 mM sodium acetate buffer, and the glucose standard was prepared in duplicates using 30 µL of D-glucose (1 mg/mL). The absorbance was measured at 510 nm against the reagent blank.

2.4. Statistical Analysis

All experiments were conducted in duplicates. Data were analyzed by one-way analysis of variance (one-way ANOVA) followed by Tukey multiple comparison test using the OriginPro software (OriginLab, Northampton, MA, USA). The letters a, b, and c indicate statistically significant differences, $p < 0.05$ (a > b > c).

Results and discussion

3.1. Dose-dependent effect of ascorbic acid on inhibiting starch digestion

In order to better understand the applicability of ascorbic acid as an inhibitor of starch digestion, it is necessary to determine its most effective concentration. The effects of four concentrations of ascorbic acid on the RS content of raw starch were examined. The results showed that as the concentration of ascorbic acid increased up to 6.25 mg/mL, the RS content was significantly increased, showing a dose-dependent effect of ascorbic acid. However, increase of the ascorbic acid concentration beyond 6.25 mg/mL did not result in further increases in the RS content. (**Figure 1**). The RS content of raw HAMS was 52.24%, which is close to previous findings in high amylose maize starches, e.g., the Hi-Maize 260 starch, and the reference value, 47.4% in HAMS Hylon VII, provided by Megazyme [6]. All tested concentrations of ascorbic acid resulted in significantly increased RS compared to the control group containing no ascorbic acid. The highest RS contents of starch were obtained with the addition of ascorbic acid at concentrations of 6.25, 12.50, and 18.75 mg/mL but were not statistically different, thereby demonstrating a saturation effect. Accordingly, ascorbic acid at a concentration of 6.25 mg/mL was used for the rest of the experimental protocol.

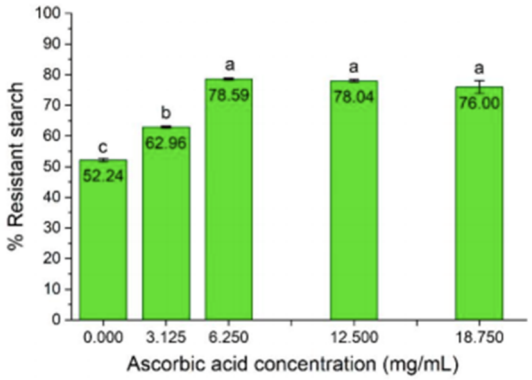

Figure 1. Resistant starch contents, presented as a proportion of total starch, with the presence of ascorbic acid. Error bars show standard deviation; n=2. Significant differences among treatments of differing ascorbic acid concentrations are denoted by different letters (a>b>c, $p< 0.05$).

The absorption of ascorbic acid in the small intestines is tightly regulated and peaks at approximately 162 mg/day [9]. Since ascorbic acid is water-soluble and is easily excreted in urine, it rarely accumulates to toxic levels in tissue and plasma. At high intakes, the most common symptoms are gastrointestinal issues resulting from the osmotic effect of high concentrations of unabsorbed ascorbic acid, such as diarrhea and nausea [9]. In the small intestinal tract, the total fluid volume reaches a maximum of approximately 94 mL [7]. Using the concentration of ascorbic acid at 6.25 mg/mL, the amount of ascorbic acid required to saturate the peak fluid volume is still substantially below the tolerable upper intake level of ascorbic acid for adults at 2,000 mg/day [9]. Even after compensating for the amount of ascorbic acid that is ultimately absorbed in the small intestines, the amount of ascorbic acid required to reach maximum inhibitory activity is unlikely to be toxic in human applications.

3.2. Effect of cooking and storage

Starch digestibility is dependent on the activity of digestive enzymes as well as the characteristics of the starch itself, such as the botanical source and degree of gelatinization [11]. Although the results have confirmed the inhibitory effect of ascorbic acid on the in vitro

digestion of raw starch samples, it is important to verify that such an effect is present in forms of starch that would realistically be consumed in the human diet, i.e., subjected to cooking and storage conditions. Accordingly, we further studied the effects of ascorbic acid (6.25 mg/mL) on the digestion of starch that was cooked without storage, or cooked and stored for 24 hours at freezing (-20°C), refrigeration (4°C), or room temperature (23°C) (**Figure 2**).

Heating starch in the presence of water, i.e., cooking, results in the gelatinization of starch. This process causes the disruption and swelling of starch granules, leaching of amylose into the water, and the loss of molecular order in amylopectin. Consequently, the starch is more readily accessible and susceptible to enzymatic digestion [10]. This outcome is reflected by the relatively low RS contents for the cooked starches, ranging from 23.05% to 25.02%, compared to 52.24% in the raw starch sample. This result is consistent with other reports that the gelatinization of starch results in significant reductions of RS contents in canna, rice, and potato starches [3,4,5].

The inhibitory effect of ascorbic acid was most substantial in the raw starch, in which RS increased from 52.24% to 78.59% with the addition of ascorbic acid at a level of 6.25 mg/mL. In all cooking and storage treatment groups, ascorbic acid also resulted in significant increases in RS, but the effects were rather modest, which could be attributed to the high moisture content of the cooking condition. After gelatinization, starch may undergo a process called retrogradation, in which the disordered amylose and amylopectin molecules re-associate into crystallized structures. Retrograded starch contributes to increased RS contents because the more ordered arrangement results in slower enzymatic digestion [12]. The storage of gelatinized starch facilitates this process, but the water content plays a major role in the extent to which the starch retrogrades. More specifically, retrogradation for maize starch only occurs when the water content is between 20% and 90% [12]. In our study, the moisture content of the gelatinized starch was approximately 97%, as the starches were suspended in the buffer solutions while being cooked, thereby rendering retrogradation unlikely. This could also explain the lack of differences in the RS contents among cooked and stored starches. Considering that ascorbic acid could still significantly increase the RS contents of the starches under various storage treatments, future studies are warranted to examine the RS contents and the inhibitory effects of ascorbic acid in retrograded starches.

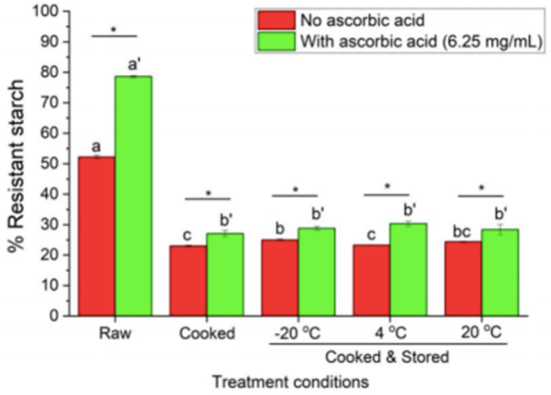

Figure 2. Resistant starch contents, presented as a proportion of total starch, with the presence of 6.25 mg/mL ascorbic acid under various processing treatments. Error bars show standard deviation; n=2. Significant differences among treatments are denoted by different letters (a>b>c, $p<0.05$). Significant differences within treatments between samples with and without ascorbic acid are denoted by an asterisk ($p<0.05$).

Conclusion

This study investigated the inhibitory effect of ascorbic acid on simulated in vitro starch digestion, as evidenced by the increased amounts of RS. Our results demonstrated the dose-dependent response of the inhibitory effect and that the optimal level of ascorbic acid was unlikely to result in toxicity in the human body. Furthermore, in all tested cooking and storage conditions, the RS contents were significantly increased in the presence of ascorbic acid. This evidence suggests that ascorbic acid can be broadly applied to realistic starch systems. Its inhibitory ability was most potent in raw starch, and the slighter impacts on cooked starch are likely the result of starch gelatinization with a high water content. Thus, future studies illustrating the inhibitory effect of ascorbic acid

on starch cooked in relatively drier conditions are warranted to study the effects of retrogradation on starch digestibility. Given that ascorbic acid has already been established as an essential nutrient, this study supports its further utilization as a promising agent in glycemic modulation.

Acknowledgments

This project is funded by the USDA National Institute for Food and Agriculture, Agriculture and Food Research Initiative Program, and the Competitive Grants Program award from the Improving Food Quality (A1361) program FY 2018 as grant # 2018-67017-27558. The Emerging Scholars Program of the University of Alabama is acknowledged for sponsoring A. Gutierrez as an undergraduate researcher.

References

[1] Abell, A. D., Ratcliffe, M. J., & Gerrard, J. (1998a). Ascorbic acid-based inhibitors of α-amylases. *Bioorganic and Medicinal Chemistry Letters*, *8*(13), 1703–1706. https://doi.org/10.1016/S0960-894X(98)00298-4

[2] Borah, P. K., Sarkar, A., & Duary, R. K. (2019b). Water-soluble vitamins for controlling starch digestion: Conformational scrambling and inhibition mechanism of human pancreatic α-amylase by ascorbic acid and folic acid. *Food Chemistry*. https://doi.org/10.1016/j.foodchem.2019.03.022

[3] Gutierrez, A. S. A., Guo, J., Feng, J., Tan, L., & Kong, L. (2020c). Inhibition of starch digestion by gallic acid and alkyl gallates. *Food Hydrocolloids*, *102* (December 2019), 105603. https://doi.org/10.1016/j.foodhyd.2019.105603

[4] Inan Eroglu, E., & Buyuktuncer, Z. (2017d). The effect of various cooking methods on resistant starch content of foods. *Nutrition and Food Science*, *47*(4), 522–533. https://doi.org/10.1108/NFS-10-2016-0154

[5] Juansang, J., Puttanlek, C., Rungsardthong, V., Puncha-Arnon, S., & Uttapap, D. (2012e). Effect of gelatinisation on slowly digestible starch and resistant starch of heat-moisture treated and chemically modified canna starches. *Food Chemistry*, *131*(2), 500–507. https://doi.org/10.1016/j.foodchem.2011.09.013

[6] Megazyme. (2019f). *Resistant Starch Assay Procedure K-RAPRS*.

[7] Mudie, D. M., Murray, K., Hoad, C. L., Pritchard, S. E., Garnett, M. C., Amidon, G. L., Gowland, P. A., Spiller, R. C., Amidon, G. E., & Marciani, L. (2014g). Quantification of gastrointestinal liquid volumes and distribution following a 240 mL dose of water in the fasted state. *Molecular Pharmaceutics*, *11*(9), 3039–3047. https://doi.org/10.1021/mp500210c

[8] National Center for Biotechnology Information. (2020h). *Acarbose*. PubChem. https://pubchem.ncbi.nlm.nih.gov/compound/Acarbose

[9] National Institutes of Health. (2019i). *Vitamin C Fact Sheet for Health Professionals*. https://ods.od.nih.gov/factsheets/VitaminC-HealthProfessional/#h8

[10] Ratnayake, W. S., & Jackson, D. S. (2008j). Chapter 5 Starch Gelatinization. *Advances in Food and Nutrition Research*, *55*(113), 221–268. https://doi.org/10.1016/S1043-4526(08)00405-1

[11] Rooney, L. W., & Pflugfelder, R. L. (1986k). Factors affecting starch digestibility with special emphasis on sorghum and corn. *Journal of Animal Science*, *63*(5), 1607–1623. https://doi.org/10.2527/jas1986.6351607x

[12] Wang, S., Li, C., Copeland, L., Niu, Q., & Wang, S. (2015l). Starch Retrogradation: A Comprehensive Review. *Comprehensive Reviews in Food Science and Food Safety*, *14*(5), 568–585. https://doi.org/10.1111/1541-4337.12143

The Role of Cytokines in Memory and Neurodegenerative Disease

Rebecca Burns

Faculty Mentor: Dr. Sergio Marini
Department of psychology, Cape Cod Community College, West Barnstable, MA 02668

This review introduces the role of cytokines and associated neuroinflammation in memory and neurodegenerative disease. Cytokines appear to function in networks involving other cytokines and molecules in the context of larger bodily systems. Research from the past decade has found that cytokines enhance memory in the healthy brain, and impair memory in individuals with neurodegenerative disease. The mechanism by which cytokine signaling networks cease to promote health and begin to promote disease is unclear, although researchers have many hypotheses. Understanding this mechanism may be key in the development of effective treatments for neurodegenerative diseases.

Introduction

Ancient Egyptian scrolls from almost five thousand years ago documented symptoms of inflammation (e.g., of the joints). Nonetheless, scientists did not isolate inflammatory biological molecules until the nineteenth century, when immunology emerged as a scientific discipline (Libby, 2012). In the twentieth century, scientists discovered that cytokines, small proteins, produce the inflammatory phenomenon known as "innate immunity." Within hours of infection, an army of cytokines are directed to the site of infection in order to protect the body (Dinarello, 2007). In the past forty years, medical research on cytokines has exploded. Investigations into the effects of cytokines have yielded results relevant to almost every field of medicine, and cytokines have been implicated in conditions as different as cancer and obesity (Dinarello, 2007).

This paper will examine the role of cytokines in memory. Experimental research has demonstrated that cytokines enhance memory processes in individuals with healthy brains (without neurological disease) (Yirmiya & Goshen, 2010). At the same time, cytokines have consistently been linked to excessive and harmful neuroinflammation in neurodegenerative diseases that involve memory deficits, including Parkinson's disease, Alzheimer's disease, and multiple sclerosis (Kempurai et. al, 2017; Ramesh et. al, 2013). The mechanism by which cytokine signaling networks cease to promote health and begin to promote disease is unclear, although researchers have many hypotheses. These hypotheses include defects in the blood-brain barrier (i.e., the semipermeable membrane that separates circulating blood from the brain and spinal cord), neuronal hyper-excitability (i.e., out-of-control neuronal firing), changes in neurogenesis (i.e., the birth of new neurons from neural stem cells), and epigenetic modifications (i.e. activation or deactivation of genes caused by environmental factors) (Donzis & Tronson, 2014; Kempuraj et. al, 2016; McAfoose & Baune, 2009; Yirmiya & Goshen, 2010).

Many researchers cite limited knowledge about neuroinflammation and its associated processes as obstacles in creating effective treatments for neurodegenerative disease (Donzis & Tronson, 2014; Ramesh, MacLean, & Philipp, 2013; Yirmiya & Goshen, 2010). Understanding the functions of cytokines in healthy brains as well as in diseased brains could lay the foundation for the development of therapeutic options for treating and preventing devastating neurodegenerative diseases.

This paper provides a summary and synthesis of seven articles, which elucidate the role of cytokines and neuroinflammation in memory and neurodegenerative disease, and discusses future research needed in this area.

Literature Review

Donzis & Tronson (2014) referred to both experimental data from animal studies as well as correlational data from human studies in

order to analyze the relationships between cytokine signaling, learning, and memory. Experimental data in animal studies was obtained through measuring the effects of lipopolysaccharide injections on cytokine signaling and associated changes in learning and memory. Cytokines are used by the body in many processes, including immune and cognitive functions. Even within a single function, many cytokines are involved. According to the authors, it may not be possible to isolate the effects of a single cytokine within a biological system, because affecting one cytokine triggers changes in a wide range of cytokines. Authors of this article theorize that much of the research may be synthesized through acknowledging the complex signaling that occurs among cytokine molecules. For example, IL-4, IL-10 and CCL2 interact with IL-1β, IL-6, TNFα to affect memory. Specifically, IL-1$\boldsymbol{\beta}$ appears to affect memory, but site of injection, timing, and dose all strongly influence these effects.

Furthermore, although IL-1β and IL-1ra appear to each individually impair long-term potentiation (the process by which patterns of activity strengthen synapses), they actually appear to maintain normal long-term potentiation when they work together. Yirmiya & Goshen (2010) synthesized data elucidating the role of immune cells in the brain (e.g., microglia and astrocytes) and peripheral immune cells (e.g., T cells and macrophages) for both healthy subjects and subjects with neurological impairments in the following processes: learning, memory, neural plasticity (the capacity of the brain to change), and neurogenesis (the birth of new neurons from neural stem cells).

Neuroimmune cells communicate with peripheral immune cells via the hypothalamic-pituitary-adrenal axis. It appears that peripheral immune cell activity activates neuroimmune cells through hormonal processes. Under normal conditions, an immune response is activated in the brain in response to low-level environmental and psychological stimuli in order to enable learning. Specifically, the levels of many cytokines and their receptors are elevated following learning and memory tasks. Cytokines appear to be involved in many normal neurological functions, including sleep.

An accumulation of evidence suggests that neurogenesis plays a significant role in learning, memory, and neuroplasticity. The authors hypothesized that newly generated neurons may facilitate synaptic plasticity through unique mechanisms. In normal subjects, microglia aid neurogenesis. Peripheral immune cells, especially T cells, also appear to support neurogenesis. Removal of T cells in mice causes difficulties with hippocampal memory. However, in neurodegenerative conditions, this immune response creates hyper-excitability and excessive inflammation. The authors proposed that memory deficits may occur not only due to the hyper-excitability itself, but also as a side effect of physiological changes intended to counteract this hyper-excitability.

McAfoose & Baune (2009) reported that high levels of cytokines are associated with states in both the central and peripheral nervous system including infection (viral, bacterial and fungal), autoimmune disease (e.g., multiple sclerosis), stroke, trauma, neurodegenerative disease (e.g., Alzheimer's disease) and neuropsychiatric disorders. Cytokines are especially implicated in hippocampal-dependent learning and memory (i.e. spatial memory, object recognition, and contextual fear conditioning).

These processes are also associated with memory consolidation, a category of processes that allow memories to be stored in long-term memory. According to Hebbian synaptic plasticity, synapses become stronger when a presynaptic neuron is active while the postsynaptic neuron is firing (i.e. long-term potentiation). Neurogenesis also appears to affect memory consolidation. Most research has focused on hippocampal-dependent learning and memory, because it is less complex than higher cognitive processes, and because higher cognitive processes appear to depend on hippocampal-dependent learning and memory. Cytokines appear to affect cognitive functions through affecting long-term potentiation, neurogenesis, and synaptic plasticity. Specifically, Il-1 appears to affect long-term potentiation and neurogenesis; IL-6 appears to

affect neurogenesis and synaptic plasticity; and TNFα and TNFβ appear to directly affect long-term potentiation and pruning (a developmental process involving the destruction of neurons in order to improve the functioning of neural circuits).

The authors proposed that further research is needed in therapeutic agents that can repair damaged neurons and regenerate new neurons. Kempuraj et. al (2016) reported that acute low-grade inflammatory responses promote nervous system health through removing pathogens, toxins, and injured and dead cells from the brain. Sustained neuroinflammation, however, appears to be implicated in many diseases of the nervous system.

Kempuraj et. al (2017) presented findings that implicated "excessive and chronic" neuroinflammation in the pathogenesis of neurodegenerative diseases such as Parkinson's disease, Alzheimer's disease, and multiple sclerosis through activating immune cells, brain cells, and signaling molecules. According to the authors, bidirectional communication clearly exists between the brain and the peripheral immune system. Neuroinflammation can intensify when inflammatory molecules from the brain leave the brain through the defective blood-brain barrier and mobilize peripheral immune cells to enter the brain. Furthermore, activation of the peripheral immune system is strongly associated with the severity of neurodegenerative disease. Cells in the brain and peripheral immune system that are involved in inflammation include glial cells and mast cells. Glial cells release a pro-inflammatory protein called glia maturation factor, which impels mast cells to release inflammatory cytokines and powerful immune modulators. Some of these factors—like nerve growth factor—are necessary for the brain to survive and also help the processes of neurotransmission and neuronal growth.

However, the mobilization of excessive numbers of mast cells can increase neuro-inflammation and cause harm by increasing blood-brain barrier permeability and by activating astrocytes, oligodendrocytes, microglia and T cells. Since mast cells are very powerful, even a small excess of mast cells in the brain may cause harmful neuro-inflammation. Ramesh, MacLean, & Philipp (2013) analyzed the roles of cytokines in infectious diseases (bacterial meningitis, Lyme neuroborreliosis, and human immunodeficiency virus encephalitis) that frequently involve memory difficulties and even dementia. Finally, Martens, Bronckaers, Politis, Jacobs, & Labrichts (2013) reviewed the promising role of dental stem cells in neurogenesis. Because neural stem cells can regenerate and differentiate in the brain, their use in the treatment of neurodegenerative disorders has catalyzed much recent research.

Discussion

Interactions Among Cytokines and Other Molecules

Recent research has approached the role of cytokines in memory from the perspective that cytokines do not act in isolation, but rather in networks that also involve other molecules. When cytokines were first discovered, it was thought that they were specific to innate immunity (Dinarello, 2007). However, further research has demonstrated that cytokines are involved in many other essential functions, including tissue healing, formation of new blood vessels, and healthy nervous system development (Kempuraj et. al, 2016). Consequently, many researchers now view the functions of cytokines in the context of larger bodily systems. Cytokines not only circulate throughout the blood and tissues, but also throughout the nervous system (Donzis & Tronson, 2014; McAfoose & Baune, 2009; Ramesh, MacLean, & Philipp, 2013; Yirmiya & Goshen, 2010). The ability of cytokines to travel throughout the body may be related to the fact that the blood-brain barrier is more permeable than previously believed (Kempuraj et. al, 2017). In fact, many cells and molecules in the brain appear to communicate with cells and molecules outside the brain, most likely through hormonal processes involving the hypothalamic-pituitary-adrenal axis (Kempuraj et. al, 2017; Yirmiya & Goshen, 2010). Cytokines appear to interact with other molecules, but also with each other, forming complex signaling mechanisms.

Donzis & Tronson (2014) theorized that it is not possible to isolate the effects of a single cytokine within a biological system; affecting one cytokine signals changes in a wide range of cytokines.

Cytokines' Role in Memory in the Healthy Brain

Significant evidence has accumulated that cytokines are critical to the healthy functioning of the brain (Donzis & Tronson, 2014; McAfoose & Baune, 2009; Yirmiya & Goshen, 2010). Acute low-grade inflammatory responses promote health through removing pathogens, toxins, and injured and dead cells from the brain (Ramesh, MacLean, & Philipp, 2013).

Individual cytokines may affect cognition by specific pathways. Research has found that IL-1 appears to affect long-term potentiation and neurogenesis, IL-6 appears to affect neurogenesis and synaptic plasticity, and TNFα appears to directly affect long-term potentiation and pruning (McAfoose & Baune, 2009).

Even so, researchers have found very contradictory results for the functions of cytokines in memory and cognition. For example, some cytokines, like IL-6, appear to play both neuroprotective and neurodegenerative roles (Ramesh, MacLean, & Philipp, 2013). These discrepancies led Donzis & Tronson (2014) to theorize that many of the diverse findings may be synthesized through recognition of the complex signaling that occurs among cytokine molecules. For example, IL-4, IL-10, and CCL2 interact with IL-1β, IL-6, TNFα to affect memory, demonstrating this difficulty.

Transition from Beneficial Immune Processes to Detrimental Immune Processes

Cytokines help to mobilize peripheral immune cells to the central nervous system, which appears to help the body fight nervous system infection through creating inflammation (Ramesh, MacLean, & Philipp, 2013). Sustained neuroinflammation, however, can induce and accelerate the pathogenesis of neurodegenerative diseases, including Alzheimer's Disease, Parkinson's Disease, and multiple sclerosis, through activating immune cells in the brain (especially microglia and astrocytes), peripheral immune cells (especially T cells and macrophages), and signaling molecules (Kempuraj et. al, 2016; Kempuraj et. al, 2017).

In general, researchers have found that inflammatory events have long-lasting effects on memory and learning (Donzis & Tronson, 2014; Ramesh, MacLean, & Philipp, 2013). Although there is currently no consensus about the cause of transition from beneficial immune processes to detrimental immune processes in people suffering from neurodegenerative diseases, researchers have many hypotheses. For example, Yirmiya & Goshen (2010) hypothesized that changes in neurogenesis (i.e., the birth of new neurons from neural stem cells) play a role in memory deficits. The same immune response that recruits cytokines to the brain and enhances memory (possibly through neurogenesis) in healthy subjects could in fact cause neuronal hyper-excitability (i.e. out-of-control neuronal firing) and excessive inflammation in individuals with neurodegenerative diseases. Thus, memory deficits could occur not only due to the hyper-excitability itself, but also as a side effect of physiological changes intended to counteract this hyper-excitability.

Because neurogenesis appears to be modulated by cytokine signaling, Donzis & Tronson (2014) hypothesized that changes in cytokine signaling could inhibit neurogenesis. Donzis & Tronson (2016) also hypothesized that epigenetic modifications (i.e. activation or deactivation of genes caused by environmental factors) may also affect long-term memory difficulties, since histone methylation and demethylation are correlated with cognitive disabilities. Kempuraj et. al (2016) hypothesized that neurodegeneration, which can increase the permeability of the blood-brain barrier, may further increase neuroinflammation (through enabling immune and inflammatory cells to cross the blood-brain barrier), perpetuating a harmful feedback loop.

Therapeutic Options for Decreasing Inflammation

Currently, effective therapeutic options for decreasing neuroinflammation are limited. Neurons and other cells may secrete anti-inflammatory cytokines that protect neurons against neuro-inflammation. However, therapeutic options for decreasing inflammation have not been successful due to difficulties in transporting drugs such as NSAIDs across the blood-brain barrier and limited knowledge of the mechanisms of neurodegeneration (Kempuraj et. al, 2017).

Since cytokines are implicated in many inflammatory processes, it is possible that cytokines could be a target of future treatments for neurodegenerative diseases that involve neuroinflammation. Supplementing a diet with the anti-inflammatory compound omega-3 fatty acid ethyl-eicosapentaenoic acid (E-EPA) reduced memory impairment and blocked detrimental IL-1 hormonal activity in rats (Song & Horrobin, 2004).

A promising new treatment for neurodegenerative disorders is the use of dental stem cells. Although neural stem cells are difficult to harvest from the adult human brain, dental stem cells may have similar mechanisms of action in regeneration and differentiation. Like neural stem cells, dental stem cells express neural markers and produce and excrete neurotrophic factors. Mesenchymal stem cells, a cell population thought to have promise for stem cell-based regenerative therapies appear to have immunomodulatory and anti-inflammatory capacities. Stem cells from human exfoliated deciduous teeth have been found to reduce levels of inflammatory cytokines, both in vitro and in mice with systemic lupus erythematosus. (Martens, Bronckaers, Politis, Jacobs, & Lambrichts, 2013). If changes in cytokine signaling impair memory by inhibiting neurogenesis in individuals with neurodegenerative disorders (Donzis & Tronson, 2014), then it is possible that treatment with dental stem cells or related therapies (which enhance neurogenesis) could reduce these impairments.

Future Research Needed

Many reviews of neurological diseases, such as that of Ramesh, MacLean, & Philipp (2013), and that of Kempuraj et. al (2016), may be limited by their scope and non-specificity. For example, further research is needed to measure the associations between specific symptoms of neurodegenerative disorders with specific mechanisms of actionbecause not every person with a neurodegenerative disease will experience every symptom of the disease, and certainly not to an equal extent. Furthermore, some researchers have drawn correlations among cytokines, neuroinflammation, and memory. However, causation is not always clear, or relies mostly on data from animal studies. According to McAfoose & Baune (2009), further analysis must be performed on humans to understand how human neuroimmunity differs from those of other animals, such as mice, before effective treatments can be conceptualized.

Finally, limited knowledge about the mechanisms of neuroinflammation and neurodegeneration hinder the development of effective treatments for neurodegenerative diseases (Donzis & Tronson, 2014; Ramesh, MacLean, & Philipp, 2013; Yirmiya & Goshen, 2010). Further research is also needed on the factors that might cause prolonged inflammation in excess of a healthy immune response, so that effective therapies may be developed to prevent, halt, and reverse this inflammation in individuals suffering from neurodegenerative diseases.

References

[1] Dinarello, C. A. (2007). Historical Review of Cytokines. *European Journal of Immunology*, 37(1), S34–S45.

[2] Donzis, E.J. & Tronson, N.C. (2014). Modulation of learning and memory by cytokines: Signaling mechanisms and long term consequences. *Neurobiology of Learning and Memory*, 115, 68-77.

[3] Kempuraj, D., Thangavel, R., Natteru, P.A., Selvakumar, G.P., Saeed, D., Zahoor, H.,...Zaheer, A. (2016). Neuroinflammation induces neurodegeneration. *Journal of Neurology, Neurosurgery and Spine*, 1(1), 1003.

[4] Kempuraj, D., Thangavel, R., Selvakumar, G.P., Zaheer, S., Ahmed, M.E, Raikwar, S.P.,...Zaheer, A. (2017). Brain and peripheral atypical inflammatory mediators potentiate neuroinflammation and neurodegeneration. *Frontiers in Cellular Neuroscience*, 11, 216.
[5] Libby, P. (2012). History of Discovery: Inflammation in Atherosclerosis. *Arteriosclerosis, Thrombosis, and Vascular Biology*, 32(9), 2045–2051.
[6] Martens, W., Bronckaers, A., Politis, C., Jacobs, R. & Lambrichts, I. (2013). Dental stem cells and their promising role in neural regeneration: an update. *Clinical Oral Investigations*, 17, 1969-1983.
[7] McAfoose, J. & Baune, B.T. (2009). Evidence for a cytokine model of cognitive function. *Neuroscience and Biobehavioral Reviews*, 33, 355-366.
[8] Ramesh, G., MacLean, A.G., & Philipp, M.T. (2013). Cytokines and chemokines at the crossroads of neuroinflammation, neurodegeneration, and neuropathic pain. *Mediators of Inflammation*, 2013, 480739-48059.
[9] Song, C. & Horrobin, D. (2004). Omega-3 fatty acid ethyl-eicosapentaenoate, but not soybean oil, attenuates memory impairment induced by central IL-1β administration. *Journal of Lipid Research*, 45, 1112-1121.
[10] Yirmiya, R. & Goshen, I. (2010). Immune modulation of learning, memory, neural plasticity and neurogenesis. *Brain, Behavior, and Immunity*, 25, 181-213.

Herbicide Induced Reproductive Dysfunction in Fruit Fly *Drosophila melanogaster*

Jacob Smith[1], Kim Lackey[2], Laura Reed[3] and Andy Chaudhuri[4]

Faculty Mentor: Andy Chaudhuri
Department of Biological Sciences, University of Alabama, Tuscaloosa, AL 35401

Spectracide is a commonly used herbicide that contains four harmful ingredients (atrazine, diquat dibromide, fluazifop-p-butyle and dicamba) that are banned in various European countries due to their significant health hazards [3]. This experiment is designed to find out the effects of Spectracide on reproductive behavior and performances using the fruit fly, Drosophila melanogaster.

Young adult male and female flies (5-7 days old) were fed with 10% Spectracide mixed with 5% sucrose for 6hrs and 24hrs. The flies were allowed to mate immediately after being fed with the herbicide. The control flies were fed with only 5% sucrose solution. We observed that male grooming behavior in the presence of females is severely affected by Spectracide when adult flies fed for a period of 6hrs. Also, Spectracide significantly delayed the larval development in the subsequent generation. However, we did not find any significant differences in pupa and adult count upon immediate exposure to Spectracide.

In another set of experiments, the flies were fed with 10% Spectracide for 6 hours then fed 5% sucrose for three days prior to mating. During this time, we cultured the male and female flies in 5% sucrose separately. We recorded a significant decline in the production of offspring (pupal and adult count) by Spectracide fed parents. Interestingly, we observed that ovarian and ovum length are significantly reduced in Spectracide fed flies. Taken together, these results suggest that Spectracide has a negative effect on reproductive behavior and outcome in Drosophila which could also be harmful to humans. Histopathology of the adult reproductive system and the sperm motility will help in better understanding the actual deleterious effect of Spectracide which is under progress.

Introduction

The purpose of this research is to focus the reproductive dysfunction caused by commonly used herbicides, particularly Spectracide. Pesticide vulnerability is a growing global health concern according to a report from the United States Environmental Protection Agency (EPA). The United States alone uses an average of 5.2 billion pounds of pesticide per year. [1] Occupational exposure to pesticides can cause serious health risks. This includes cancer and reproductive dysfunction. [2, 4] The possible health hazards to humans exposed to such herbicides/pesticides demand intensive investigation. Present study reports the effect of Spectracide on reproduction using fruit fly as a model system to study the human diseases.

Since Spectracide is used commonly among American farmers and consumers, it is of great interest to investigate the repercussions of this herbicide on the Drosophila reproductive system. This will serve as a model to show possible effects on the human reproductive functions.

It is hypothesized that exposure to Spectracide will have negative effects on the reproductive system which may include delayed embryonic development, reduced ovule size, and grooming behavior including disruption in neurological functions.

Materials and Methods

A total of ten groups of flies were used for the first data collection. In the first experiment, grooming behavior among male flies in the presence of females was measured. 10 male flies and 10 female flies were fed a solution made of 10% Spectracide and 5% sucrose for 6 hours. A separate group of 10 male flies and 10 female flies were fed the same solution for 12 hours. A third group of 10 male and 10 female flies were fed the same solution for 24 hours. To counter each of these groups, a control group was fed 5% sucrose solution for the same time periods. In

total, there were three control groups, each group had 10 males and 10 females.

At the end of each feeding time interval, one male and one female were placed in a glass tube with a radius of 0.5 inches and length of 2 inches. After five minutes of being together, the observation of grooming started. The amount of times that the male drosophila vibrated its wings or antennas was recorded for a period of 60 seconds. The flies that were fed for 24 hours only provided four living flies from both the experimental and control groups. The groups that were fed for 6 hours and 12 hours both provided 10 flies from both the experimental group and the control group. A standard t-test was applied to the measurements of this experiment.

The next experiment performed was made to measure the amount of progeny by larva count, negative geotaxis, and rate of emergence. Two groups of flies were divided by sex to make four groups. One male exclusive group and one female exclusive group were fed 10% Spectracide 5% sucrose solution for six hours. Another male exclusive group and female exclusive group were fed 5% sucrose solution for 6 hours. After the six hours of feeding, both sexes from the experimental group were integrated into five separate vials. Each vial had eight males and five females. Both sexes of the control group were separated in the same fashion. The control group was also grouped evenly into five vials, each having eight males and five females.

The five experimental groups could mate for seven days before being killed. The five control groups could mate for seven days before being killed. Through the time that the flies were mating, daily recordings of larva and pupa numbers were made.

After the adult flies were killed on the seventh day, daily recordings of new progeny were made. After the number of new progeny was recorded, all new progeny for that day were killed. The rate of larva emergence was compared to the number of larva to give a rate of emergence for both groups. Standard t-test was applied to this measurement.

Larval migration was measured on the progeny of the parent generation that was allowed to mate for seven days. Larval migration was recorded by making 0.5 inch intervals on each vial. Each segment that comprised of 0.5 inches contained a select amount of pupa. The amount of pupa in each section was counted to obtain the average migration distance of larvae (pupa was larva before pupation). This measurement on negative geotaxis was recorded in a graph. Standard t-tests were applied to this measurement.

15 female and 24 male adult drosophila 3-5 days old were fed 10% Spectracide solution for 6 hours, they were then put onto a 5% sucrose diet for 3 days. During all of this feeding time the sexes were kept separate. The control group also consisted of 15 female and 24 adult drosophila that were 3-5 days old. They were fed sucrose solution for 6 hours and 3 days. After the third day was complete, the experiment males and female were allowed to mate; each vile contained five females and eight males. The same proportion was for the control group.

Female reproductive morphology was also recorded by microscopy. Female flies from the 3-day experimental group as well as the control group were dissected. The ovaries and ovums were analyzed under a 5X magnification and were measured with microscope technologies.

Results & Discussion

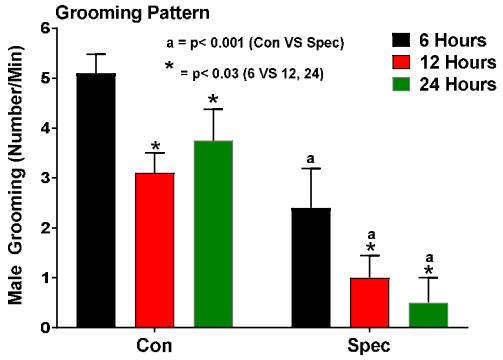

The graphic to the left displays the significant change of grooming behavior that Spectracide caused for the experimental male flies. The male grooming patterns significantly decrease in occurrence after exposure to the 10% Spectracide solution. The data shows that the decrease was present after 6, 12, and 24 hours of feeding.

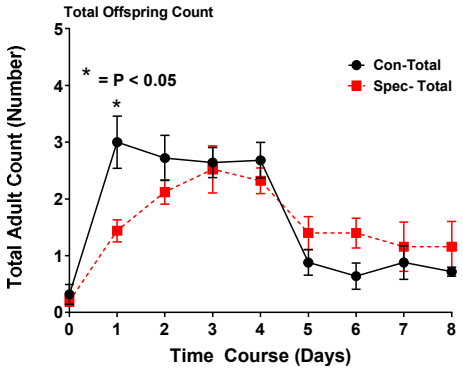

The graphic to the left displays the total offspring count per female of both experimental and control groups. The experimental group was fed 10% Spectracide for 6 hours and allowed to mate immediately for seven days. The control group was kept on a 5% sucrose diet for 6 hours and seven days. The data suggests a delay in offspring eclusion after parental exposure to Spectracide.

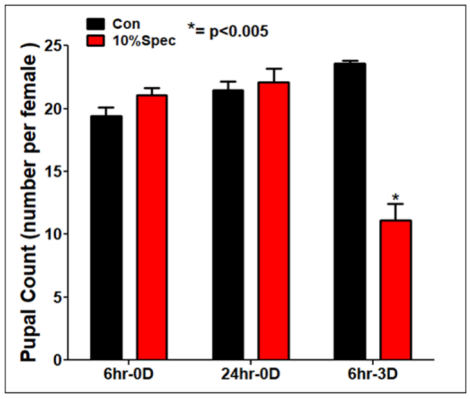

The graphic to the left displays three different dose-responses for 10% exposure with respective control groups. The data shows that there was a significant decrease in the number of pupa recorded after the parental generation was exposed to 10% Spectracide solution and then before mating, placed on a 5% sucrose diet for 3 days. The data suggests that Spectracide causes a significant decrease in progeny rates after 3 days for the drug to work into the physiology of the flies. Standard t-tests were applied for significance.

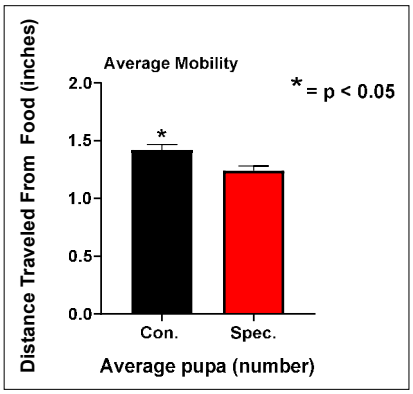

The graphic to the left illustrates the difference in negative geotaxis. The distances measured were the migration patterns of the larva. The larva were progeny of a set of flies fed 10% Spectracide for 6 hours; after a 7 day mating period, these measurements were taken of their progeny. There is a significant decrease in the length covered by larva who are the progeny of the experimental group. The control group was fed 5% sucrose for 6 hours. A standard t-test was conducted for significance.

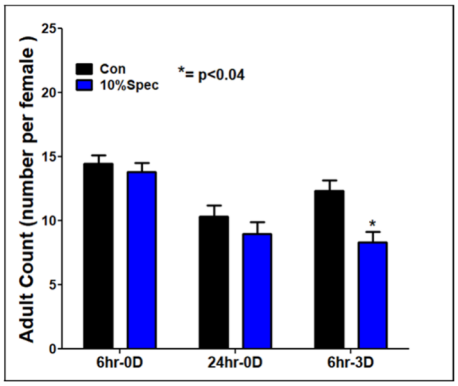

The graphic to the left shows that the adult count in both the 6 hour exposed and 24 hour exposed groups did not have significant decreases in total elosion of pupa. The 6hr-3D indicators show that the F1 generation of pupa had significantly less eclosion after the parental generation had exposure to 10% Spectracide for 6 hours and then remained

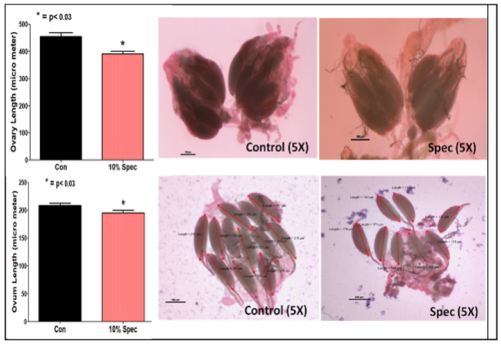

The graphic to the left shows the different morphology of the experimental (10% Spectracide solution exposure for 6 hours – 3 days of 5% sucrose after then integrated) group and the control group. The data shows a significant decrease in the average size of ovaries and ovums of the experimental group vs. the control group. Standard t-test was applied.

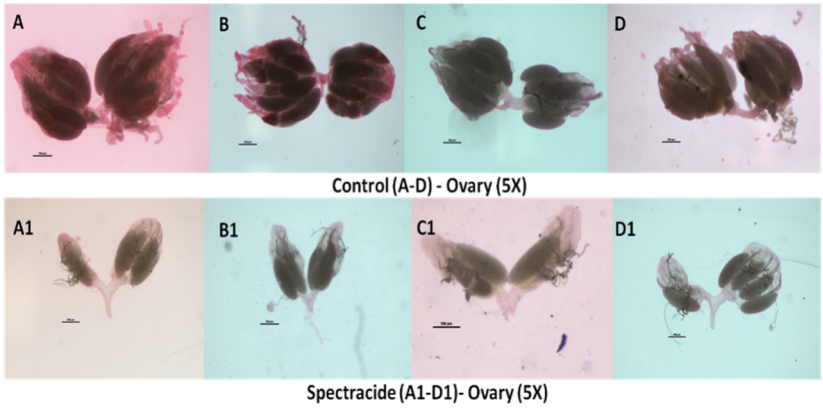

The graphic to the left shows a clear change in female reproductive morphology. The groups marked A,B,C and D are control flies fed a 5% sucrose diet for three days. The groups marked A2, B1, C1, and D1 were fed 10% Spectracide solution for 6 hours and then placed on a 5% sucrose diet for three days.

The data appears to show that different exposures to Spectracide can lead to not only negative effects of reproductive morphology, but also to changes to offspring counts. These data appear to show how Spectracide negatively affects grooming behavior among males, progeny count, larval development, as well as reproductive morphology among females.

Conclusion

As previously hypothesized, Spectracide appears to have negative consequences on the reproductive system of Drosophila melanogaster. It was found that the grooming behavior of males was significantly decreased. Surprisingly, there was no significant decrease in progeny count of the first experimental group (6 hours feeding, immediate mating); however, there was a decrease in progeny count for the second experimental group (6 hours feeding, 3-day sucrose diet, mating begins on day 3). The first experimental group, however, still yielded progeny that had significantly lower negative geotaxis. In addition to these findings, the morphology of the female reproductive system had significant decreased in size in the second experimental group compared to the control groups. This would lead one to believe that the 3-day waiting period is a crucial part of the integration of the Spectracide drug through the tissue. More research must be done to find out what portion of the cell cycle or tissue development is being changed by Spectracide.

References

[1] Grube A, Donaldson D, Kiely T, Wu L. 2011. Pesticides Industry Sales and Usage: 2006 and 2007 Market Estimates. Washington, DC:U.S. Environmental Protection Agency, Office of Chemical Safety and Pollution Prevention.
[2] Zuskin E, Mustajbegovic J, Schachter E.N, Kern J, Deckovic-Vukres V, Trosic I, Chiarelli A. 2008. Respiratory function in pesticide workers. J. Occup. Environ. Med. 50:1299–1305. doi: 10.1097/JOM.0b013e3181845f6c.
[3] Mathew P, Jose A, Alex R.G, Mohan V.R. 2015. Chronic pesticide exposure: Health effects among pesticide sprayers in Southern India. Indian J. Occup. Env. Med. 19:95–101.
[4] Mostafalou S, Abdollahi M. 2017. Pesticides: An update of human exposure and toxicity. Arch. Toxicol. 91:549–599. doi: 10.1007/s00204-016-1849-x.

Recent Developments in Electrospinning of Chitosan Nanofibers

Isabelle Berry [1], Hui Wang [2], Lingyan Kong [2,*]

[1] *Department of Chemical and Biological Engineering, The University of Alabama, Tuscaloosa, AL 35487, USA*
[2] *Department of Human Nutrition and Hospitality Management, The University of Alabama, Tuscaloosa, AL 35487, USA*
** Corresponding author*

Electrospinning is a technique used to fabricate micro- to nano-sized nonwoven fibers by stretching polymer melts or solutions in a high voltage electric field. Nowadays, electrospinning has become an attractive process due to its versatility and scalability in addition to the unique properties of nanofibers. Chitosan is a highly abundant biopolymer derived from the partial deacetylation of chitin, a polysaccharide found in the exoskeletons of insects and crustaceans, such as lobsters, shrimp, and crabs. Chitosan is a prime candidate for electrospinning into nanofibers due to its higher solubility than chitin, non-toxicity, biodegradability, abundance, and antimicrobial and chelating properties. The rigid structure of chitosan does present difficulties, as it is not soluble in water or most aqueous systems. Certain organic solvents or their mixtures with aqueous solvents are required to dissolve chitosan. Improving the electrospinnability of pure chitosan by modifying electrospinning parameters, altering solvent systems, blending with other polymers, and even hydrolyzing chitosan prior to spinning have all been attempted by various authors. To improve the mechanical and chemical stability of chitosan nanofibers, crosslinking agents which stabilize chitosan through the coupling and bonding of their functional groups, such as glutaraldehyde and genipin, were also employed. If successfully spun, chitosan nanofibers could be a useful material in wound dressing, bone tissue engineering, drug delivery, water and air filtration, solar panels, and food packaging. Hence, this article reviews recent reports on the preparation, characterization, and application of chitosan-based nanofibers.

Keywords: *electrospinning, chitosan, chitin, nanofibers*

Introduction

The basic theory that led to the development of the electrospinning process was documented by Rayleigh in 1882 and Formhals in 1934 [1]. During the 1990s, Doshi and Reneker further advanced the knowledge of this electrohydrodynamic phenomenon through detailed observations and mechanism discoveries [2]. Electrospinning has since become a more popular method to accurately and cheaply produce continuous fibers with unique properties. Unlike synthetic polymers, biopolymers started to obtain more attention in the past decade due to their advantages in biodegradability, biocompatibility, competitive cost, and wide availability from renewable resources [3].

Chitosan is a highly abundant biopolymer derived from partial deacetylation of chitin, a polysaccharide found in the shells of crustaceans. Treating chitin with an alkaline substance leads to the formation of the linear polysaccharide chitosan. Structurally, chitosan is a copolymer of 2-amino-2-deoxy-D-glucopyranose and N-acetyl-2-amino-2-deoxy-D-glucopyranose linked by β-D (1→4) bonds. Chitosan has ideal properties for electrospinning into nanofibers; however, its rigid structure and high molecular weight make choosing the best solvent system a challenge. Certain organic solvents, some of which are toxic or expensive, or their mixture with aqueous solvents are required. If successfully spun into nanofibers, chitosan could be a useful substance in a variety of applications and industries due to its

favorable properties [4]. Extensive research exists on the electrospinning of chitin and chitosan and their applications [3, 5-9]. The most recent advancements (1999-2019) in the field of electrospinning chitosan and the applications of chitosan nanofibers are summarized in the following review.

Literature search methods

The electronic database "Web of Science" was used to search for relevant studies with keywords including "electrospinning" and "chitosan." Articles published in English between January 2000 and January 2019 from peer-reviewed academic journals were screened for further review. Titles and abstracts were reviewed to eliminate reviews and irrelevant articles, and then a list of relevant studies was identified for full-text review. Finally, the 14 most informative and innovative articles on this topic were further analyzed and discussed in this review.

Electrospinning of chitosan

Pure chitosan

Chitosan nanofibers have the potential for numerous applications due to their excellent biocompatibility, biodegradability, antimicrobial activity, and the natural abundance of chitin. However, electrospinning of chitosan presents several challenges. It has poor solubility in many common aqueous and organic solvents due to its crystalline structure and strong hydrogen bonds. Therefore, many attempts have been made to improve the electrospinnability of pure chitosan by changing solvent systems or hydrolyzing chitosan prior to spinning. Recent studies on electrospinning pure chitosan are summarized in Table 1, and detailed discussion follows.

To dissolve chitosan for electrospinning, the most commonly used solvent systems include acetic acid, trifluoroacetic acid (TFA), and TFA/dichloromethane (DCM) solutions. Chitosan dissolved in each solvent system will demonstrate different properties, especially rheological properties, which further affect the optimal electrospinning parameters to achieve fiber formation. For example, Mazoochi [10] dissolved chitosan with a degree of deacetylation (DD) of 85% in 99% (v/v) TFA and optimized the electrospinning parameters, including applied voltage and tip to collector distance. In general, fiber diameter decreased with higher applied voltage and shorter tip to collector distance. Applied voltage mainly affects the electric field strength (or Coulomb force on the jet) and thus the velocity of the polymer jet. Varying the tip to collector distance has a direct influence on both the flight time of the polymer solution and the electric field strength. For independent fibers to form, the electrospinning jet must be allowed enough time for most of the solvent to be evaporated. However, a tip to collector distance that is too long results in a weak electric field, which allows fiber diameter to increase [10]. Another study utilized a Box-Behnken three-factor design to investigate the effects of three parameters (electric field strength, solvent ratio, and chitosan concentration) on fiber formation [11]. With multiple regression analysis, main factors (including electric field strength and chitosan concentration) and their interactions (including electric field strength and solvent ratio, electric field strength and chitosan concentration) had the most significant effect on fiber diameter. The lowest average uniform fiber diameter of 176 nm was achieved at 0.75 kV/cm, TFA/DCM ratio of 80/20% (v/v), and 5.5% (w/v) chitosan in solution. This study showed that the interactions between parameters, not just the individual parameters, significantly affect the resulting nanofiber diameter.

Chitosan can also be partially hydrolyzed to facilitate the dissolution of chitosan and reduce its viscosity for electrospinning. In a study by Homayoni et al. [12], chitosan chains were hydrolyzed by an alkali treatment. The hydrolyzed chitosan in acetic acid solutions showed reduced viscosity and improved electrospinnability. Similar to most other studies, the researchers found that electrospinning parameters, including applied voltage, tip to collector distance, and solvent composition, all strongly influence the fiber diameter. The finest average fiber diameter achieved was 140 nm.

Traditionally, electrospinning only produces randomly oriented fibers as a non-

woven mat. Highly aligned fibers may be desirable in certain applications requiring anisotropic properties, such as tissue engineering, where aligned fibers can mimic the extracellular matrix to direct cell responses. Highly aligned chitosan nanofibers were successfully prepared by Haider et al. [13]. This study focused on the optimization of chitosan concentration and rotation speed of the rotating drum collector, while keeping other parameters constant. Fiber formation required a concentration of 6% (w/v) chitosan in solution to achieve sufficient molecular chain entanglements and avoid bead formation. To improve the degree of alignment, polymer jet velocity had to match well with the rotation speed of the drum collector. At low rotation speeds (2.09 m/s, 5.20 m/s), fibers were deposited randomly. As rotation increased to 21.98 m/s, fiber alignment increased to 94.4% nanofibers aligned with a reference (zero) angle. Increasing collector rotation speed also showed a steady decrease in average fiber diameter due to the mechanical stretching force of the collection cylinder on the incoming fibers.

The electrospun chitosan nanofibers may be used for numerous applications in the future, yet most researchers over the past decade focused on its application in water purification. For instance, Horzum et al. fabricated chitosan nanofibers (mean diameter = 42 ± 15 nm) from its 1,1,1,3,3,3-hexafluoroisopropanol (HFIP) solution and tested the chitosan nanofiber mat for its efficiency as an adsorbent of metal ions, including Fe (III), Cu (II), Ag (I), and Cd (II), from water [14]. This study indicated chitosan in the nanofiber form is much more effective at absorbing metal ions from water than chitosan in powder form. This increase in efficiency was due to the increased surface area of the nano-sized fibrous structure. The nanofiber mat has an additional advantage over powder chitosan in that powder absorbents need a carrier; otherwise, the powders will be flushed away during water treatment.

Crosslinking of chitosan-based nanofibers

To improve the mechanical and chemical stability of chitosan nanofibers, many researchers experimented with crosslinking of chitosan nanofibers. Crosslinkers, such as glutaraldehyde and genipin, stabilize polymers (chitosan) through the coupling and bonding of their functional groups. When the polymer molecules are crosslinked, the fibers may show increased mechanical strength, lower susceptibility to water, and less weight loss after multiple uses, allowing the nanofibers to be more easily reused for various applications, especially in water treatment.

Several groups evaluated various crosslinkers and different methods of crosslinking, for instance, mixing crosslinkers prior to spinning and applying post-spinning crosslinking treatment. Kiechel and Schauer [15] evaluated the combination of glycerol phosphate (GP), tripolyphosphate (TPP), and tannic acid (TA) to crosslink electrospun chitosan fibers, using both prior to spinning and post-spinning crosslinking methods. A wide range of fiber morphologies and characteristics were obtained. The prior to spinning method created mostly unbranched, partially crosslinked chitosan fibers, while the post spinning method created more branched and web-like crosslinked nanofiber mats. In another study, Austero et al. [16] evaluated the use of crosslinkers, including genipin, hexamethylene-1,6-diaminocarboxysulphonate (HDACS), and epichlorohydrin (ECH), on the electrospinning of chitosan nanofibers. None of the three crosslinkers inhibited electrospinning, but they all increased the fiber diameter. It was found that the degree of crosslinking using genipin is pH dependent; at a higher pH, higher self-polymerization of genipin leads to a lower degree of crosslinking. Heat or base activation of the chitosan-HDACS and chitosan-ECH mats improved the degree of crosslinking and decreased the average fiber diameters. In addition, glutaraldehyde is another commonly used crosslinker, and fibers can be crosslinked using its vapor. Crosslinking with glutaraldehyde vapor does not usually affect fiber morphology, but it does usually increase fiber diameter, as reported by several researchers [17, 18]. Crosslinked chitosan nanofibers may swell in water but can remain insoluble and maintain fibrous structure as expected [18, 19].

In addition to process optimization and crosslinking, researchers explored potential applications of chitosan nanofibers, including water purification [17], tissue engineering [19], and cancer treatment [18]. For instance, Cao et al. [17] tested chitosan nanofibers crosslinked with glutaraldehyde vapor for adsorption of metal ions and subsequent regeneration. Crosslinking was found to increase the fiber diameter as well as the regeneration ability. The crosslinked chitosan nanofibers were able to be regenerated and reused five times, although absorption capacity of Cu (II) gradually decreased after each use. For biomedical applications, such as tissue engineering and cancer treatment, although pure chitosan is an ideal material due to its biocompatibility, there was some concern that the crosslinker, glutaraldehyde, would result in cytotoxicity. However, both Sencadas et al. [19] and Lin et al. [18] found chitosan nanofibers crosslinked with glutaraldehyde to be non-cytotoxic. Furthermore, preliminary cell culture results of Sencadas et al. [19] showed good adhesion and proliferation of MC-3T3-E1 osteoblast cells, therefore showing the viability of glutaraldehyde-crosslinked chitosan nanofibers as scaffold applications. In the study of Lin et al. [18], Fe_3O_4 magnetite nanoparticles were incorporated into chitosan nanofibers crosslinked with glutaraldehyde vapor as a potential hyperthermia treatment for cancer cells. These magnetic electrospun nanofibers are non-cytotoxic and can be used for endoscopic or surgical delivery for hyperthermia cancer therapy to effectively reduce tumor cell proliferation. Many applications of chitosan nanofibers are still in their preliminary evaluation phase, yet these results are promising and encourage increasingly more investment in this area of research.

Table 1. Electrospinning of pure chitosan

Polymer	Solvent	Degree of deacetylation	Intended applications	Reference
Chitosan	TFA/DCM (2:1)	≥95	Water purification	Li, Lou [20]
Chitosan	TFA	varied	Water purification	Cao, Li [17]
Chitosan	Acetic acid	90	Water purification	Li, Li [21]
Chitosan	TFA	77		Kiechel and Schauer [15]
Chitosan	TFA	N/A		Haider, Al-Zeghayer [13]
Chitosan	TFA/DCM (70:30 % v/v)	86	Tissue engineering	Sencadas, Correia [19]
Chitosan	TFA	75		Austero, Donius [16]
Chitosan	TFA/DCM (7:3)	N/A	Cancer treatment	Lin, Lin [18]
Chitosan	Acetic Acid (0.5M)	>75		Pati, Adhikari [22]
Chitosan	TFA/DCM	85		Jacobs, Patanaik [11]
Chitosan	TFA	85		Mazoochi[10]
Chitosan	HFIP	70-75	Water purification	Horzum, Boyacı [14]
Chitosan	Acetic acid	75-85		Homayoni, Ravandi [12]
Chitosan	Acetic acid	54, 56, 65		Geng, Kwon [23]

TFA = trifluoroacetic acid, DCM = dichloromethane, HFIP = 1,1,1,3,3,3-hexafluoroisopropanol

Conclusion

This review summarized the preparation and characterization of chitosan nanofibers produced by electrospinning. Chitosan is a promising potential material for electrospinning due to its advantages in biodegradability, biocompatibility, competitive cost, and the abundance of its parent polymer, chitin. Nanofibers produced via electrospinning have the advantages of high surface area in addition to cost-effectiveness. Chitosan nanofibers have been shown to possess a wide variety of properties and potential applications. However, the high molecular weight and rigid backbone structure makes it difficult to dissolve and electrospin unless certain solvents are used, such as trifluoroacetic acid, acetic acid, and dichloromethane. Nanofibers crosslinked with agents such as glutaraldehyde or genipin have also been produced. Crosslinked chitosan nanofibers have improved mechanical and chemical stability due to the coupling and bonding of functional groups between the crosslinking agent and chitosan. Crosslinked nanofibers show an improved stability after electrospinning, which makes the nanofibrous mats more easily reused for application purposes. The chitosan or chitosan-based nanofibers produced in these different conditions have shown great potential for future applications in water or air purification, drug delivery, tissue engineering, antimicrobial wound dressing, and food packaging.

References

[1] Khan, W.S., et al., Recent progress on conventional and non-conventional electrospinning processes. Fibers and Polymers, 2013. 14(8): p. 1235-1247.
[2] Doshi, J. and D.H. Reneker, Electrospinning process and applications of electrospun fibers. Journal of Electrostatics, 1995. 35(2): p. 151-160.
[3] Kong, L., G.R. Ziegler, and R. Bhosale, Fibers spun from polysaccharides, in Handbook of carbohydrate polymers: Development, properties and applications. 2011, Nova Science Publishers, Inc. p. 1-43.
[4] Sun, K. and Z. Li, Preparations, properties and applications of chitosan based nanofibers fabricated by electrospinning. Express Polymer Letters, 2011. 5(4): p. 342-361.
[5] Kalantari, K., et al., Biomedical applications of chitosan electrospun nanofibers as a green polymer–Review. Carbohydrate polymers, 2018. 207: p. 588-600.
[6] Schiffman, J.D. and C.L. Schauer, A review: electrospinning of biopolymer nanofibers and their applications. Polymer Reviews, 2008. 48(2): p. 317-352.
[7] Elsabee, M.Z., H.F. Naguib, and R.E. Morsi, Chitosan based nanofibers, review. Materials Science and Engineering: C, 2012. 32(7): p. 1711-1726.
[8] Lim, L.-T., A.C. Mendes, and I.S. Chronakis, Chapter Five - Electrospinning and electrospraying technologies for food applications, in Advances in Food and Nutrition Research, L.-T. Lim and M. Rogers, Editors. 2019, Academic Press. p. 167-234.
[9] Mendes, A.C., K. Stephansen, and I. Chronakis, Electrospinning of food proteins and polysaccharides. Food Hydrocolloids, 2017. 68: p. 53-68.
[10] Mazoochi, T. and V. Jabbari, Chitosan Nanofibrous Scaffold Fabricated via Electrospinning: the Effect of Processing Parameters on the Nanofiber Morphology. International Journal of Polymer Analysis and Characterization, 2011. 16(5): p. 277-289.
[11] Jacobs, V., et al., Optimization of electrospinning parameters for chitosan nanofibres. Current Nanoscience, 2011. 7(3): p. 396-401.
[12] Homayoni, H., S.A.H. Ravandi, and M. Valizadeh, Electrospinning of chitosan nanofibers: Processing optimization. Carbohydrate Polymers, 2009. 77(3): p. 656-661.
[13] Haider, S., et al., Highly aligned narrow diameter chitosan electrospun nanofibers. Journal of Polymer Research, 2013. 20(4): p. 105.
[14] Horzum, N., et al., Sorption Efficiency of Chitosan Nanofibers toward Metal Ions at Low Concentrations. Biomacromolecules, 2010. 11(12): p. 3301-3308.
[15] Kiechel, M.A. and C.L. Schauer, Non-covalent crosslinkers for electrospun chitosan

fibers. Carbohydrate Polymers, 2013. 95(1): p. 123-133.
[16] Austero, M.S., et al., New crosslinkers for electrospun chitosan fibre mats. I. Chemical analysis. Journal of The Royal Society Interface, 2012. 9(75): p. 2551-2562.
[17] Cao, J., et al., Glutaraldehyde cross-linked chitosan nanofibers: preparation, characterization and application in adsorption of Cu (II). Journal of Nanoscience, 2016. 16(3): p. 2922-2928.
[18] Lin, T.-C., F.-H. Lin, and J.-C. Lin, In vitro feasibility study of the use of a magnetic electrospun chitosan nanofiber composite for hyperthermia treatment of tumor cells. Acta Biomaterialia, 2012. 8(7): p. 2704-2711.
[19] Sencadas, V., et al., Physical-chemical properties of cross-linked chitosan electrospun fiber mats. Polymer Testing, 2012. 31(8): p. 1062-1069.
[20] Li, C., et al., Fabrication of pure chitosan nanofibrous membranes as effective absorbent for dye removal. International Journal of Biological Macromolecules, 2018. 106: p. 768-774.
[21] Li, L., et al., Enhanced chromium (VI) adsorption using nanosized chitosan fibers tailored by electrospinning. Carbohydrate polymers, 2015. 125: p. 206-213.
[22] Pati, F., B. Adhikari, and S. Dhara, Development of ultrafine chitosan fibers through modified wetspinning technique. Journal of Applied Polymer Science, 2011. 121(3): p. 1550-1557.
[23] Geng, X., O.-H. Kwon, and J. Jang, Electrospinning of chitosan dissolved in concentrated acetic acid solution. Biomaterials, 2005. 26(27): p. 5427-5432.

Interview with Dr. Laura Reed

Laura Reed, PhD
Associate Professor
University of Alabama Department of Biological Sciences

JOSHUA Staff: *Regarding your background, what eventually led you to become a professor at the University of Alabama? Where are you from, where did you go to college, and what did you do prior to taking on this role?*

Dr. Reed: I grew up in Eugene, Oregon. Eugene at the time was the second-largest city in Oregon, and it is where the University of Oregon is based. My father is a geologist and taught geology [at the University of Oregon], so that's how we ended up there. I grew up with graduate students coming over to the house for dinner, so I grew up in an academic, scientific environment from the very beginning. My mother was a biology major. She didn't go on to do any upper-level degrees, but she was always doing her at-home biology experiments. I knew going into college that I wanted science to be a part of whatever I ended up doing, but I wasn't sure if I wanted to be a scientist or use science to help the world in some way, such as for environmental issues. My sophomore year, I got started doing undergraduate research. I knew that ecology and evolution were things that I was very excited about, so I started in a lab that did research in ecology and evolution. I did a very evolution-heavy undergraduate research project and wrote a thesis based on that project, which got me into quantitative genetics, and I never got back out of it. Quantitative genetics has been my passion ever since. Quantitative genetics is using general rules about how traits are inherited to make predictions about how they might respond to selection or how selection may have shaped them. I knew coming out of my undergraduate degree that I wanted to go straight into a PhD, and I knew I wanted to do evolutionary biology. I wasn't sure exactly within evolutionary biology specifically what I wanted to do, so I applied to programs that had strong ecology and evolution departments and decided to go to the University of Arizona's Ecology and Evolution Department. Going into it, I wasn't committed to any specific organism or any specific question yet. Part of the reason I chose that program was because they had rotations, which meant that during the first year, I spent nine or so weeks progressively in different research labs so I could experience what they did in their lab and figure out what kinds of questions I might answer if I did my PhD in that lab. Through that process, I ended up joining a lab that studied speciation in cactophilic fruit flies, flies that use rotting cactus as their host as opposed to rotting fruit. Because of that, my advisor was very involved in the early era of genomics. I got into doing *Drosophila* genomics in her lab, and actually one of my lines was the one that was sequenced for one of the early genomes of *Drosophila*. Leaving graduate school, I wanted to further develop my skills in genomics, so I did a post-doc at North Carolina State University still working on fruit flies, this time *Drosophila melanogaster*, which is the species that most people do research on because it has more tools for genomics since it is so heavily studied. During my post-doc, I established what is the kernel of my current research program, which is using *Drosophila melanogaster* to study the genotype by environment interactions that affect traits, especially metabolic traits. After four years of my post-doc, I applied for faculty positions and came here to the University of Alabama.

JS: *How did you become aware of the Genomics Education Partnership, and what were the steps that led you to become the*

director of this nation-wide effort? What are your roles as the director?

R: When I started [at the University of Alabama], one of the classes I was hired to teach was called "Integrated Genomics." It was a course that I had the opportunity to shape into what I thought it should be. It was already on the books and was taught from a much more molecular perspective prior to my joining, and I was able to reshape it from a more evolutionary perspective. In the course of doing that, I wanted to involve active learning and research as part of the course because I was already aware that active learning involving research by undergraduate students led to better pedagogical outcomes than just me telling them stuff and expecting them to regurgitate information on exams. Also, I attended an annual fly meeting, and at that fly meeting, the members of the Genomic Education Partnership (GEP) were there presenting. I talked to them and got a sense of what the GEP was, so I went through their training, so that I could integrate that curriculum into my Integrated Genomics class. That's how I got started in around 2010-2011, and I became more and more involved in it. The GEP is a group of very collaborative faculty who are passionate about being effective educators. Many of the faculty are from smaller schools, so they may not have access to the resources for highly-involved student research projects or the faculty themselves may not have time to run complex research projects. [Therefore], the GEP is a way to make research accessible to students and faculty at schools that may not have as many resources. The project was started in 2006 by Dr. Sarah Elgin at Washington University in St. Louis. She is an amazing leader and is now in the National Academy of Science. She was getting to the point around 2016 to start thinking about retirement, so she started probing about what was going to happen with the GEP, and if it were going to continue, what it would look like and what the leadership would look like. I started talking to her about it around that time because I was close to getting tenure, an important step in career development for somebody who is a researcher. It's dangerous to take on major tasks before you've gotten tenure, but I knew I was close to getting tenure when I started this conversation. It was a productive conversation, and I got comfortable with the idea that I could take over the group with heavy support from the other GEP members. I oversee the whole business and try to get everyone headed in the right direction. That strategy has worked out well thus far. As the director, there is a lot of administration, which is writing the grants and dealing with the paperwork and budgeting. My other roles are to oversee the scientific goals of the projects. Part of why the GEP works is that people are doing real research and have real scientific goals. There has to be somebody who is thinking about what those scientific goals are and turning the data into publications and so on. We have now expanded to three total projects. The original one that Dr. Elgin led has been partially handed off to another GEP faculty member. There is another project based on parasitoid wasps, and I'm leading one on the evolution of pathways across *Drosophila*, which fits into my research interests in the genetic architecture and evolution of metabolic traits in *Drosophila*.

JS: *How has UA taken steps to lead the way in undergraduate research, and how do you think the GEP will affect research at UA in the future?*

R: Something that I've found very refreshing at UA is the extent to which undergraduate research is a priority in the College of Arts and Sciences and at the university as a whole. Having come out of undergraduate research myself, which was a formative experience for me, it's clear to me that that is something that should be available as much as possible to current students. It has always been strongly encouraged at UA, and I've always had people in my research lab working on their own projects as well. Part of the philosophy of the GEP involves something called "CUREs," which are Course-based Undergraduate Research Experiences. CUREs are the current way to try to get as many students as possible to have some sort of research experience. It's not practical for all biology majors to spend time in an actual research lab. There's not physically enough space for that. But if you can figure out

some way to package research projects into something that can fit into a classroom, then in principle, you could reach everybody. That's what the GEP is shooting for: coming up with these packaged projects that are genuine research projects that can teach the research process and generate real scientific results that are useful. I've been doing it in my classroom since I started in 2011. Going forward, we're thinking about adapting the GEP curriculum in our introductory labs. Exactly what that will look like, we're not completely sure yet, but one of my goals is to try to incorporate that into our intro labs. Not everybody is going to take my 400-level Integrated Genomics class, so as a department, we have to think about how to provide that experience more broadly.

JS: *We understand your current research involves projects that revolve around investigating how genetic differences between individuals can cause predispositions to metabolic diseases such as diabetes and obesity. What led you to this field? Did you have any personal or professional experiences that drew you to this career path?*

R: My passion is evolutionary and quantitative genetics. I want to know how phenotypes are built both from an evolutionary perspective and a mechanical, genetic perspective. When I was a PhD student, the phenotype I was focused on was speciation, specifically hybrid male sterility. It's absolutely fascinating, but it's difficult to make the average person appreciate why it's a worthwhile focus. Part of what I was hoping for when I transitioned toward looking at metabolic phenotypes was that I could still answer the same types of questions, but I could do it with a phenotype that people could relate to. I ended up studying metabolic syndromes and type 2 diabetes specifically because it dovetailed well with another thing that emerged when I was doing my post-doc, metabolomics. Partly to try to catch that wave, my post-doc advisor suggested that I try to incorporate that into my project in some way. Metabolic syndrome makes sense as a phenotype to focus on, especially because metabolomics fits right into that as a tool to help understand that trait. It's easy to explain to others why those traits are important, and I could still answer the questions I was initially motivated by.

JS: *What does a typical day in your lab look like?*

R: My goal is to have everybody in the lab have ownership of some aspect of the research that we are doing. Currently, I'm structuring it so that there is a graduate student or a post-doc who leads a team, and within that team, there are a group of undergraduates who are working to accomplish the experimental goals of the team. Each undergraduate has a certain responsibility within the team that becomes their thing, so they have a big role in designing the experiments and analyzing the data. All that collectively becomes a scientific publication. There have been a few times when an undergraduate has come up with a novel idea of their own that they want to pursue, and when that is financially feasible, I try to encourage that. One of those ideas is actually a centerpiece of what my lab does. It came from a conversation I had with a student where we were discussing ways to exercise the flies. We already manipulated their diet, but one of the other major components of obesity and diabetes is exercise. Flies exhibit negative geotaxis, which means if they're at the bottom of something, they find a way to get to the top. We came up with the idea of rotating the vials; if "up" kept changing, maybe they'd keep moving to get to the top. He built a prototype of a contraption that would do this, and it worked in the sense that the flies walked more than they would have if they were just holding still in their vial. From the prototype, we built a more official-looking version in a collaboration with UAB, and we now call it the TreadWheel. We have several projects that depend on the TreadWheel now where we look at the relationship between exercise and diet and genotype in producing the phenotypes of obesity and diabetes in the flies. So that's an example of when an undergraduate project became a centerpiece of the lab.

JS: *What has been the most exciting advancement in your research since you started at the University of Alabama?*

R: The thing I'm most excited about right now is looking at how the natural gut microbiota interacts with other factors like diet to influence phenotype. One of my goals is to understand the relative contribution of different environmental factors that contribute to obesity and diabetes. In humans, we know that there are four major factors: diet, exercise, sleep, and gut microbiome. My goal is to get to the point where we can model all four and then start modifying them in combinations so we can see how the environmental factors interact with each other to produce phenotypes. We've got diet and exercise down. I'm leading the research team to begin to study sleep. In humans, if people have poor quality sleep or not enough sleep, they're at a much higher risk of developing obesity and diabetes. We're looking to see if we can replicate that in the flies. And lastly, for the gut microbiome, it's a hot topic, in general, in biology right now. It's been modeled in fruit flies before, but those models have all been a lab-based model in that they feed the flies whatever we would feed them normally in the lab and not necessarily what the fly would be experiencing out in the wild. These flies didn't evolve to be in labs; they evolved to be out in the wild. We would expect them to have a different relationship with microbes they experience out in the wild than what we might perceive in the lab. so we've figured out a way to model the wild gut microbiome for flies that are in the lab. Having the realistic gut microbes available for the flies makes a big difference in how they handle the nutrients in their diet.

JS: *What unique opportunities has being affiliated with the University of Alabama, and now the Genomics Education Partnership brought to your research?*

R: The University of Alabama has been incredibly supportive of my research program. Early on, undergraduates were the primary researchers in my lab, and they're still the bulk of the researchers in my lab. Having a culture that valued and supported undergraduate research was very important for me being able to establish my program here. Giving me the freedom to develop this Integrated Genomics class in the way that I felt it should be was also very important to my development and success here. The Genomics Education Partnership brings in both pedagogical experience and training that I otherwise might not have gotten, but it also keeps me up to date on genomic technologies and the cutting-edge things that we should be teaching our students. If I didn't have that, I would probably fall behind.

JS: *What advice would you give a student interested in going into this field of research?*

R: I would recommend that anyone who wants to get into undergraduate research should do some soul-searching and figure out if they are genuinely interested in answering fundamental scientific questions or if they're just trying to go through the motions. The next step is to identify what types of questions you're passionate about. It's tedious and hard at times, so you don't want to be spending that effort on questions you're not excited to answer. If you're going to give years of your life to answering a question, which is how long it usually takes to answer a question properly, you want it to be a question you believe in on some fundamental level. Identifying a research lab that you might join that deals with ideas that you feel passionate about is an important step in being successful. But also know that various research labs can teach you things in the context of doing research that might not be obvious in the description of what the research does. At this point, virtually everything that happens in the biology department involves molecular techniques in some way. Even if you're not particularly thrilled with the question you end up working on, you may gather really valuable skills and understand concepts about molecular biology by working on that project, so keep an open mind.

This interview was conducted by Lainey Pickens, Abigail Giunta, and Richard Blankenberker, Assistant Editors on the JOSHUA staff. The text has been condensed and edited.

JOSHUA was made possible by the following organizations:

University of Alabama Office for Academic Affairs

University of Alabama Department of Biological Sciences

Tri-Beta National Honor Society Kappa Beta Chapter

Howard Hughes Medical Institute

Randall Research Scholars Program

And by the 2019-2020 JOSHUA Editing Staff

2021 Submission Guidelines

We accept articles from current undergraduate students at accredited universities. If you are a graduate student or recent alumnus of UA, we will consider your article if the majority of your work was conducted while you were an undergraduate at UA. Undergraduate students from other institutions may submit; however, priority will be given to those who conducted their research at UA.

1. Your name, e-mail address, and phone number must be included.
2. Your submission must relate to science or health.
3. Your work must be sponsored by a faculty member.
4. The length of your submission must be between 2000 and 4500 words. We will accept longer submissions if the author can limit the submission to the required length for the publication, and any extra material is able to be published online.
5. Figures, charts, and graphs are allowed but not required. (Note: The color will be mostly black and white.)
6. Your paper must contain an abstract.
7. Your citations must follow the guidelines listed on our website at: https://joshua.ua.edu/submissions-and-guidelines.html
8. The deadline for submission is February 28, 2021.
9. E-mail submissions to joshua.alabama@gmail.com

THE UNIVERSITY OF ALABAMA®